

**T.R.**  
**GEBZE TECHNICAL UNIVERSITY**  
**GRADUATE SCHOOL**

**DEVELOPMENT OF DECISION-MAKING MECHANISMS  
IN RESTORATION PROJECTS THROUGH STRUCTURAL  
HEALTH MONITORING METHODS**

**FIRAT AKTÜRK**

**A THESIS OF MASTER OF SCIENCE  
DEPARTMENT OF CIVIL ENGINEERING  
EARTHQUAKE AND STRUCTURAL ENGINEERING  
PROGRAM**

**ADVISOR: PROF. DR. FERİT ÇAKIR**

**JANUARY 2025**

**T.R.**  
**GEBZE TECHNICAL UNIVERSITY**  
**GRADUATE SCHOOL**

**DEVELOPMENT OF DECISION-MAKING MECHANISMS  
IN RESTORATION PROJECTS THROUGH STRUCTURAL  
HEALTH MONITORING METHODS**

**FIRAT AKTÜRK**

**A THESIS OF MASTER OF SCIENCE  
DEPARTMENT OF CIVIL ENGINEERING  
EARTHQUAKE AND STRUCTURAL ENGINEERING  
PROGRAM**

**ADVISOR: PROF. DR. FERİT ÇAKIR**

**Co-ADVISOR: ASSOC. PROF. DR. ABDULLAH CAN ZÜLFİKAR**

**JANUARY 2025**

**T.C.  
GEBZE TEKNİK ÜNİVERSİTESİ  
LİSANSÜSTÜ EĞİTİM ENSTİTÜSÜ**

**YAPI SAĞLIĞI İZLEME YOLUYLA RESTORASYON  
PROJELERİNDE KARAR VERME  
MEKANİZMALARININ GELİŞTİRİLMESİ**

**FIRAT AKTÜRK**

**YÜKSEK LİSANS TEZİ  
İNŞAAT MÜHENDİSLİĞİ ANA BİLİM DALI  
DEPREM VE YAPI MÜHENDİSLİĞİ PROGRAMI**

**DANIŞMAN: PROF. DR. FERİT ÇAKIR  
2. DANIŞMAN: DOÇ. DR. ABDULLAH CAN ZÜLFİKAR**

**OCAK 2025**



## MASTER of SCIENCE JURY APPROVAL FORM

A thesis submitted by Fırat AKTÜRK, defended on 17/01/2025 before the jury formed with the 13/01/2025 date and 2025/05 numbered decision of the GTU Graduate Administration Board, has been accepted as a MASTER of SCIENCE thesis in the Department of Civil Engineering, Earthquake and Structural Engineering Program .

### JURY

MEMBER

(THESIS ADVISOR) : Prof. Dr. Ferit ÇAKIR

MEMBER

: Asist. Prof. Ahu KÖMEÇ

MEMBER

: Asist. Prof. Ali YEŞİLYURT

### APPROVAL

Gebze Technical University Graduate Administration Board

...../...../..... date and ...../..... numbered decision.

SIGNATURE/SEAL



*To my Family*

## ABSTRACT

Structural Health Monitoring (SHM) is a comprehensive system supported by advanced technologies that aims to continuously assess the safety, durability, and performance of engineering structures. This system enables the early detection of potential damages by continuously monitoring the current state of structures, thereby facilitating maintenance and repair processes based on scientific data. Particularly in historical structures, the use of SHM systems has become an increasingly widespread approach both globally and in Türkiye, as it ensures precise and effective restoration processes. This study focuses on SHM activities carried out on the historically significant Oshki (Öşvank) Church, located in Uzundere District of Erzurum Province, and examines decision-making processes related to its restoration. Taking into account the current damaged condition of the church, measurements were conducted using various SHM devices, and the data obtained from these measurements were utilized to propose solutions for restoration efforts. Within the scope of SHM, sensors and monitoring equipment were employed to collect a wide range of data, including crack widths and propagation, humidity and temperature variations, as well as vibration analyses. These data facilitated the identification of the dynamic properties of the structure, such as natural frequencies, mode shapes, and damping ratios, thereby grounding restoration decisions on solid scientific foundations. In particular, crack measurements played a crucial role in understanding the stress distribution within the structure and the progression of damage. Continuous monitoring of humidity and temperature changes revealed the relationship between material degradation and environmental factors.

In conclusion, SHM systems contributed to the development of scientifically grounded restoration proposals by providing a detailed analysis of the current condition of the Oshki Church. This study highlights the critical role of SHM in preserving historical structures and exemplifies its contribution to restoration processes. SHM applications are emerging as essential tools for ensuring the safe transfer of historical structures to future generations, enabling more effective and accurate management of restoration processes.

**Keywords: Structural Health Monitoring, Decision-Making Mechanism, Restoration, Strengthening, Erzurum Oshki Church**

## ÖZET

Yapı Sağlığı İzleme (YSİ), mühendislik yapılarının güvenlik, dayanıklılık ve performansını sürekli olarak değerlendirmeyi amaçlayan, gelişmiş teknolojilerle desteklenen kapsamlı bir sistemdir. Bu sistem, yapıların mevcut durumunu sürekli izleyerek olası hasarları erken tespit etmeyi, bu sayede bakım ve onarım süreçlerinin bilimsel veriler ışığında planlanmasını mümkün kılmayı hedefler. Özellikle tarihi yapılarda, hassas ve etkili restorasyon süreçleri için YSİ sistemlerinin kullanımı, dünya genelinde olduğu gibi ülkemizde de giderek yaygınlaşan bir yaklaşım haline gelmiştir. Bu çalışmada, Erzurum İli Uzundere İlçesi'nde bulunan ve tarihi önemi haiz olan Oskhi (Öşvank) Kilisesi üzerinde gerçekleştirilen YSİ çalışmaları ele alınmış, bu kapsamda restorasyona yönelik karar verme süreçleri detaylı bir şekilde incelenmiştir. Oshki Kilisesi'nin mevcut hasarlı durumu göz önünde bulundurularak, farklı YSİ cihazlarıyla gerçekleştirilen ölçümler ve bu ölçümlerden elde edilen veriler, restorasyon çalışmalarına yönelik çözüm önerilerinin geliştirilmesine ışık tutmuştur. YSİ kapsamında kullanılan sensörler ve izleme ekipmanları, yapıdaki çatlakların genişliği ve gelişimi, nem ve sıcaklık değişimleri ile titreşim analizleri gibi çeşitli verilerin toplanmasını sağlamıştır. Bu veriler, yapının dinamik özelliklerini (örneğin doğal frekans, mod şekilleri ve sönüm oranı) belirlemeye yardımcı olmuş, böylece restorasyon kararlarının daha sağlam bilimsel temellere dayandırılmasını mümkün kılmıştır. Özellikle çatlak ölçümleri, yapı içindeki stres dağılımını ve hasarın ilerleyişini anlamak açısından kritik bir rol oynamıştır. Nem ve sıcaklık değişimlerinin sürekli izlenmesi ise malzeme bozulmasının çevresel faktörlerle olan ilişkisini ortaya koymuştur.

Sonuç olarak, YSİ sistemleri, Oshki Kilisesi'nin mevcut durumunu detaylı bir şekilde analiz ederek restorasyona yönelik bilimsel çözüm önerileri geliştirilmesine katkıda bulunmuştur. Bu çalışma, YSİ'nin tarihi yapıların korunması ve restorasyonu üzerindeki kritik rolünü somut bir örnek üzerinden göstermektedir. YSİ uygulamaları, tarihi yapıların geleceğe güvenle taşınmasında önemli bir araç olarak öne çıkmakta, restorasyon süreçlerinin daha etkin ve doğru bir şekilde yönetilmesine olanak tanımaktadır.

**Anahtar Kelimeler:** Yapı Sağlığı İzleme, Karar Verme Mekanizması, Restorasyon, Güçlendirme, Erzurum Oskhi Kilisesi

## ACKNOWLEDGEMENTS

I would like to express my sincere gratitude and appreciation to Prof. Dr. Ferit akır and Assoc. Prof. Abdullah Can Zülfikar for their invaluable guidance and assistance during the preparation of this thesis.

I would like to thanks to Prof. Dr. Bülent Akbař and Asst. Prof. Ahmet Anıl Dindar for their contributions in providing data and conducting fieldwork for the structural health monitoring studies.

I extend my gratitude and respect to the Ministry of Culture and Tourism for their support.

To my family, especially my brother Fuat Aktürk, a Ph.D. student at Gebze Technical University; my mother Gülten; and my sisters Ayper and Gülperi, who have given me boundless courage throughout my life, I offer my deepest thanks. My father Zarif, who is no longer with us but proudly supported my siblings and me in our education, will always remain in my memory.

Lastly, I am very thankful to my beloved wife, Selda, and my dear children, Elvin, Zarif Devran, and Asmin. This work would not have been possible without their support.

# TABLE OF CONTENTS

	<u>Page</u>
ABSTRACT	vi
ÖZET	vii
ACKNOWLEDGEMENTS	viii
TABLE OF CONTENTS	ix
LIST OF SYMBOLS AND ABBREVIATIONS	xi
LIST OF FIGURES	xii
LIST OF TABLES	xv
1. INTRODUCTION	1
1.1. Purpose of The Thesis	3
1.2 Scope and Content	3
2. LITERATURE REVIEW	5
3. STRUCTURAL HEALTH MONITORING (SHM)	18
3.1. Earthquake Regulations	20
3.1.1 Damage Detection	20
3.1.2 Instrumentation and Data Collection	22
3.1.3 Data Processing and Analysis	22
3.1.4 Decision-Making Mechanism	23
3.1.5 Restoration and Strengthening Works	23
3.1.6 Post-Intervention Monitoring and Follow-Up	24
3.2 Standards and Regulations for SHM	24
3.3 Threshold Levels for Decision-Making Mechanism	31
3.3.1 General Directorate of Foundations Guide of Turkey	31
3.3.2 FEMA 273, FEMA 356, ASCE 41 and Eurocode 8	36
4. SHM AT OSHKI CHURCH, ERZURUM	39
4.1. History of Erzurum Oshki Church	39
4.2 Plan and Architectural Features	44
4.3 Observed Damages in the Structure of Erzurum Oshki Church	47
4.4 Installation of SHM Devices	50
5. DECISION-MAKING FOR RESTORATION	56
5.1. Evaluation of Data Obtained from Crack Meters	57
5.2. Evaluation of Inclinator Data	69
5.3. Evaluation of Hygrometer Data	71
5.4. Evaluation of Thermometer Data	72
5.5. Evaluation of Accelerometer Data	72
6. RESTORATION AND STRENGTHENING RECOMMENDATIONS	77
6.1. Repair of Cracks in Structures	77
6.1.1. Cracks with a Width Less Than 1 mm	77
6.1.2. Cases Where Crack Width Ranges Between 1 mm and 5 mm	77
6.1.3. Cases Where Crack Width Ranges Between 5 mm and 50 mm	79
6.1.4. Cases Where Crack Width Ranges Between 50 mm and 150 mm	80
6.2. Repair of Section Losses	81
7. CONCLUSIONS	83

REFERENCES	85
BIOGRAPHY	88
PUBLICATIONS AND PRESENTATIONS FROM THE THESIS	89



## LIST OF SYMBOLS AND ABBREVIATIONS

<i>SHM</i>	: Structural Health Monitoring
<i>FEM</i>	: Finite Element Model
<i>IoT</i>	: Internet of Things
EdgeCVDMS	: Edge Computing Vision-based Displacement Measurement System
UUV	: Unnamed Underwater Vehicle
DOF	: Degrees of Freedom
CNT	: Carbon Nano Tube
<i>CFRP</i>	: Carbon Fiber-Reinforced Polymer
LRPCA	: Locally Robust Principal Component Analysis
GDD	: Gaussian Density Distance
PLS-SEM	: Partial Least Squares Structural Equation Modelling
CSB	: Clifton Suspension Bridge
TFT	: Temporal Fusion Transformer
ML	: Machine Learning
DT	: Digital Twin
BIM	: Building Information Modelling
CSS	: Capacitive Stress Sensor
FE	: Finite Element
NDT	: Non Destructive Test
RMS	: Root Mean Square
CNN	: Convolutional Neural Network
JDA	: Joint Distribution Adaptation
PRA	: Probabilistic Risk Assessment
FBG	: Fiber Bragg Grating
GPR	: Ground Penetrating Radar
ASCE	: American Society of Civil Engineer
UNESCO	: United Nations Education Society Culture Organization
NHL	: Natural Hydraulic Lime
FRP	: Fiber Reinforced Polymer
LVDT	: Linear Variable Differential Transformer
ISIS	: Intelligent Sensing for Innovative Structures
SAMCO	: Structural Assessment, Monitoring, and Control
ISO	: International Organization for Standardization
FHWA	: The Federal Highway Administration
ASTM	: American Society for Testing and Materials
ASCE	: American Society of Civil Engineers
AFAD	: Disaster and Emergency Management Authority
UTC	: Compatibility with Universal Time
LD	: Limited Damage
CD	: Controlled Damage
CP	: Collapse Prevention
I	: Building Importance Factor
Ra	: Unreduced Seismic Effects
FEMA	: Federal Emergency Management Agency

## LIST OF FIGURES

	<u>Page</u>
<b>Figure 3.1:</b> Flowchart for Restoration Decision-Making Using SHM Equipment.	21
<b>Figure 3.2:</b> Placement of Accelerometers.	30
<b>Figure 3.3:</b> Static Push Curve and Limit States.	33
<b>Figure 3.4:</b> Performance Levels in Relatively Ductile and Brittle Structures.	36
<b>Figure 4.1:</b> General View of Erzurum Oskhi Church.	40
<b>Figure 4.2:</b> External View of Erzurum Oskhi Church in Historical Photographs.	41
<b>Figure 4.3:</b> Internal View of Erzurum Oskhi Church in Historical Photographs.	43
<b>Figure 4.4:</b> Plan of Erzurum Oskhi Church.	45
<b>Figure 4.5:</b> South side view of Erzurum Oskhi Church.	45
<b>Figure 4.6:</b> West side view of Erzurum Oskhi Church.	46
<b>Figure 4.7:</b> Longitudinal Section of Erzurum Oskhi Church.	46
<b>Figure 4.8:</b> The Crack on the Western Facade of the Church and the Completely Collapsed Roof Section.	48
<b>Figure 4.9:</b> Damages Observed on the Main Dome and Eastern Facade of the Church.	48
<b>Figure 4.10:</b> Some Cracks Observed on the Exterior Facade of the Structure.	49
<b>Figure 4.11:</b> The Damaged Dome and Apse Section on the Interior Facade of the Structure.	49
<b>Figure 4.12:</b> Some Damages Observed on the Interior Facade of the Structure.	50
<b>Figure 4.13:</b> Some visuals of SHM Equipment.	51
<b>Figure 4.14:</b> Wall numbering study conducted within the scope of SHM work.	53
<b>Figure 4.15:</b> Placement detail of SHM equipment.	53
<b>Figure 5.16:</b> Crack 1 first & last data time : 2018_0709-11:20:00&2019_1011:00:00 First, last, ,max. ,min. : 0.0 , 0.044 , 0.578 , -0.119.	58
<b>Figure 5.17:</b> Crack 2 first & last data time : 2018_0709-11:20:00&2019_1011:00:00 First ,last ,max. , min. : 0.0 , -0.293 , 0.102 , -0.393.	58
<b>Figure 5.18:</b> Crack 3 first & last data time : 2018_0709 11:20:00&2019_1011:00:00 First ,last, max. ,min. : 0.0 , -0.02 , 0.196 , -0.141.	59
<b>Figure 5.19:</b> Crack 4 first &last data time : 2018_0709-11:20:00&2019_1011:00:00 First , last ,max. ,min. : 0.0 , -0.02 , 0.196 , -0.141.	59
<b>Figure 5.20:</b> Crack 5 first &last data time : 2018_0709-11:20:00&2019_1011:00:00 First , last ,max. ,min. : 0.0 , 0.356 , 1.605 , -0.145.	60
<b>Figure 5.21:</b> Crack 6 first &last data time : 2018_0709-11:20:00&2019_1011:00:00 First , last ,max. ,min. : 0.0 , 0.2 , 0.413 , -0.026.	60
<b>Figure 5.22:</b> Crack 7 first &last data time : 2018_0709-11:20:00&2019_101:	

11:00:00 First , last ,max. ,min. : 0.0 , -0.119 , 0.395 , -0.407.	61
<b>Figure 5.23:</b> Crack 8 first &last data time : 2018_0709-11:20:00&2019_101: 11:00:00 First , last ,max. ,min. : 0.0 , 0.105 , 0.293 , -0.186.	61
<b>Figure 5.24:</b> Crack 9 first &last data time : 2018_0709-11:20:00&2019_101: 11:00:00 First , last ,max. ,min. : 0.0 , 0.045 , 0.384 , -0.375.	62
<b>Figure 5.25:</b> Crack 10 first &last data time : 2018_0709-11:20:00&2019_10 11:00:00 First , last ,max. ,min. : 0.0 , 0.105 , 0.351 , -0.122.	62
<b>Figure 5.26:</b> Crack 11 first &last data time : 2018_0709-11:20:00&2019_10 11:00:00 First , last ,max. ,min. : 0.0 , 0.23 , 1.027 , -0.243.	63
<b>Figure 5.27:</b> Crack 12 first &last data time : 2018_0709-11:20:00&2019_10 11:00:00 First , last ,max. ,min. : 0.0 , 0.581 , 1.056 , -0.123.	63
<b>Figure 5.28:</b> Crack 13 first &last data time : 2018_0709-11:20:00&2019_10 11:00:00 First , last ,max. ,min. : 0.0 , 0.409 , 0.547 , -0.234.	64
<b>Figure 5.29:</b> Crack 14 first &last data time : 2018_0709-11:20:00&2019_10 11:00:00 First , last ,max. ,min. : 0.0 , -25.943 , 0.783 , -26.129.	64
<b>Figure 5.30:</b> Crack 15 first &last data time : 2018_0709-11:20:00&2019_10 11:00:00 First , last ,max. ,min. : 0.0 , 0.296 , 0.495 , -0.172.	65
<b>Figure 5.31:</b> Crack 16 first &last data time : 2018_0709-11:20:00&2019_10 11:00:00 First , last ,max. ,min. : 0.0 , 0.097 , 0.229 , -0.241.	65
<b>Figure 5.32:</b> Crack 17 first &last data time : 2018_0709-11:20:00&2019_10 11:00:00 First , last ,max. ,min. : 0.0 , 0.129 , 0.63 , -0.19.	66
<b>Figure 5.33:</b> Crack 18 first &last data time : 2018_0709-11:20:00&2019_10 11:00:00 First , last ,max. ,min. : 0.0 , 0.156 , 0.647 , -0.258.	66
<b>Figure 5.34:</b> Crack 19 first &last data time : 2018_0709-11:20:00&2019_10 11:00:00 First , last ,max. ,min. : 0.0 , -0.059 , 0.522 , -0.239.	67
<b>Figure 5.35:</b> Crack 20 first &last data time : 2018_0709-11:20:00&2019_10 11:00:00 First , last ,max. ,min. : 0.0 , 0.319 , 0.502 , -0.206.	67
<b>Figure 5.36:</b> Slope 1 XZ first &last data time : 2018_0709-11:20:00&2019_ 1015-11:00:00 First , last ,max. ,min. : 0.0 , 0.001 , 0.001 , -0.001	69
<b>Figure 5.37:</b> Slope 2 YZ first &last data time : 2018_0709-11:20:00&2019_ 1015-11:00:00 First , last ,max. ,min. : 0.0 , -0.0 , 0.001 , -0.001	69
<b>Figure 5.38:</b> Slope 3 XZ first &last data time : 2018_0709-11:20:00&2019_ 1015-11:00:00 First , last ,max. ,min. : 0.0 , 0.0 , 0.001 , -0.001.	70
<b>Figure 5.39:</b> Slope 4 YZ first &last data time : 2018_0709-11:20:00&2019_ 1015-11:00:00 First , last ,max. ,min. : 0.0 , -0.0 , 0.0 , -0.0.	70
<b>Figure 5.40:</b> Moisture first &last data time : 2018_0709-11:20:00&2019_10 11:00:00 First , last ,max. ,min. : 42.848 , 17.625 , 10.543 , 95.7	71
<b>Figure 5.41:</b> Moisture first &last data time : 2018_0709-11:20:00&2019_10 11:00:00 First , last ,max. ,min. : 42.848 , 17.625 , 10.543 , 95.7	72
<b>Figure 5.42:</b> Example of alarm set.	73
<b>Figure 5.43:</b> Acceleration Data Obtained in the X Direction.	74
<b>Figure 5.44:</b> Acceleration Data Obtained in the Y Direction.	74
<b>Figure 5.45:</b> Acceleration Data Obtained in the Z Direction.	75
<b>Figure 5.46:</b> Calculated frequency spectrum in X direction.	75

<b>Figure 5.47:</b> Calculated frequency spectrum in Y direction.	76
<b>Figure 5.48:</b> Calculated frequency spectrum in Z direction.	76
<b>Figure 6.1:</b> Injection Mortar Application Detail.	80
<b>Figure 6.2:</b> Reinforcement of Cracks Using Stitching Elements.	81



## LIST OF TABLES

	<b><u>Page</u></b>
<b>Table 3.1:</b> Worldwide SHM codes/standards.	25
<b>Table 3.2:</b> Minimum Number of Accelerometers.	29
<b>Table 3.3:</b> Accelerometer Specifications.	31
<b>Table 3.4:</b> Proposed Target Performance Levels.	34
<b>Table 3.5:</b> Performance levels of masonry structures according to ASCE 41.	37
<b>Table 3.6:</b> Performance levels of masonry structures according to FEMA 273 and FEMA 356.	38
<b>Table 3.7:</b> Performance levels of masonry structures according to Eurocode 8.	38
<b>Table 5.1:</b> Comparison of Data Obtained from Crack Gauges (mm).	68
<b>Table 5.2:</b> Comparison of data obtained from inclinometers (mm).	71
<b>Table 5.3:</b> Comparison of Data Obtained from Hygrometers (mm).	71
<b>Table 5.4:</b> Comparison of data obtained from thermometers (mm).	72
<b>Table 6.1:</b> Hydraulic Lime Binder Injection Grout (m <sup>3</sup> ).	78

# 1. INTRODUCTION

Historical structures are important elements that show the cultural history, processes and change of history of a society. These structures have been built by humans throughout history and used in various products. In the era of human history, different civilizations' own aesthetic understandings, construction techniques and structures of cultural characteristics emerge. The importance of historical structures and their multifaceted approach: cultural, educational, touristic and economic. They are considered as concrete examples of the cultural existence of a society. Each building or structure contains its own unique story and provides information about the social structure, beliefs, aesthetic understandings and lifestyle of the periods in which it was built. For example, while ancient temples reflect people's belief worlds, castles shed light on the military periods of different civilizations. In addition to aiding in the comprehensiveness of the past, structural structures offer cultural richness with distinctive architectural structures and details. Historical structures, while serving as invaluable testaments to the cultural, social, and architectural heritage of civilizations, face the inevitable effects of time, environmental factors, and human activity. Preserving these structures requires not only a deep understanding of their historical and cultural significance but also the application of modern technological solutions to ensure their longevity. This is where Structural Health Monitoring (SHM) plays a crucial role. By integrating advanced monitoring techniques with preservation efforts, SHM provides essential data to safeguard these treasures for future generations, bridging the gap between the historical past and the technological present. SHM covers processes performed to evaluate the safety, durability and performance of a structure. This process is used to monitor the current condition of the structure, detect possible damage, and anticipate problems that may occur over time. SHM typically includes the following components: Through sensors placed at various points of the structure, stresses, cracks, vibrations and deformations on the structure are constantly monitored. The exterior and interior conditions of the building are observed through regular visual inspections by expert teams. The collected data is analysed to evaluate the performance of the structure. These analyses help take the necessary precautions to ensure the safety of the structure. The results of the monitoring process are reported regularly and

presented to relevant stakeholders. Based on the monitoring results, the necessary maintenance and repair work for the structure is planned.

SHM is of great importance, especially in large construction projects, bridges, dams and historical structures. These applications play a critical role in both ensuring people's safety and minimizing economic losses. SHM is an important field in civil engineering and architecture, using a variety of strategies and technologies to ensure the longevity and safety of buildings and other structures. Further information can be summarized under the following headings. The purposes of SHM are providing safety of structures, maintenance and repairing, performance evaluation and long life by using monitoring methods of structural monitoring, crack monitoring, seismic monitoring, environmental monitoring. smart sensors, data collection systems, imaging technologies are used monitoring methods. SHM is used in building, bridges and roads, industrial facilities, historical structures.

SHM systems are used to evaluate the current condition of structures, their behaviour under dynamic loads, and changes before/after reinforcement. These systems allow restoration decisions to be based on scientific data, especially in historical and sensitive structures. SHM systems determine the dynamic properties of the structure and monitor changes in these properties over time. Detection of damage to the structure or re-evaluation of the structure after strengthening is done thanks to these systems. These data provide information about the stiffness and damage status of the structure. Data obtained from SHM systems helps make correct decisions about which areas need to be strengthened during restoration, which structural elements are more sensitive and how to intervene. Comparing the dynamic responses of the structure before and after strengthening reveals the effectiveness of the interventions. Restoration decisions are supported by experimental data and numerical modelling obtained with SHM. The dynamic properties of the structures are determined through experimental studies carried out before and after the reinforcement, and these data are verified with finite element models (FEM). Comparing both experimental and numerical analyses increases the accuracy and reliability of decisions made. SHM systems provide faster and more reliable results in restoration processes, providing advantages in terms of time and cost. In addition, these systems allow real-time monitoring of structures after restoration, allowing early intervention against any negativities that may occur in the future.

As a result, building health monitoring systems increase the accuracy of restoration decisions, ensuring that structures are long-lasting and safe. The use of SHM systems in restoration projects is of critical importance, especially for historical structures, because these systems accurately evaluate the current condition of the structures and detect possible future damage in advance.

## **1.1. Purpose of the Thesis**

The primary purpose of this thesis is to investigate the role of SHM in the preservation and restoration of historical structures, with a specific focus on the Oshki Church in Erzurum, Turkey. This study aims to analyse the structural condition of the Oshki Church using SHM techniques and provide data-driven recommendations for its restoration, protection, and strengthening.

The research seeks to demonstrate how SHM applications can identify existing damages, assess structural performance, and guide restoration decisions for historical monuments. By monitoring the church's dynamic behaviour, structural deformations, and material conditions, the study evaluates its current state and predicts potential vulnerabilities. Based on the data collected, tailored solutions are proposed to ensure the longevity and safety of the Oshki Church while preserving its historical and cultural significance.

Through this case study, the thesis aims to highlight the importance of integrating SHM technologies into the restoration processes of sensitive and historically significant structures. By doing so, it contributes to the broader understanding of how modern engineering practices can support the preservation of architectural heritage for future generations.

## **1.2. Scope and Content**

This thesis focuses on the application of SHM systems in the assessment and preservation of historical structures, with the Oshki Church in Erzurum serving as a case study. The scope of the research includes the evaluation of the structural integrity of the Oshki Church, the identification of damages and vulnerabilities, and the

development of restoration and strengthening recommendations based on the data obtained through SHM techniques.

The study begins with a review of the historical and architectural significance of the Oshki Church, providing context for its preservation. It then examines the theoretical foundations of SHM, detailing the methods and technologies used in structural monitoring, including sensor systems, data collection, and analysis techniques.

In the case of the Oshki Church, the thesis includes an in-depth analysis of the monitoring data, such as deformations, material degradation, and dynamic responses of the structure. The findings are used to propose targeted restoration and reinforcement strategies that align with the principles of historical preservation.

The content is organized as follows:

1. An introduction to the importance of SHM in historical preservation and an overview of the research objectives.
2. A detailed discussion of SHM methodologies and their application in civil engineering and restoration projects.
3. A historical and architectural analysis of the Oshki Church.
4. Data analysis and interpretation of the monitoring results obtained from the Oshki Church.
5. Recommendations for restoration and strengthening based on SHM findings.
6. Conclusions and implications of the research for future applications of SHM in historical preservation.

This thesis aims to provide a comprehensive understanding of how SHM can contribute to the effective and sustainable preservation of historical structures while ensuring their safety and resilience.

## 2. LITERATURE REVIEW

SHM plays a crucial role in providing real-time insights into the condition and performance of infrastructure, allowing for timely and cost-efficient maintenance, enhancing safety, and prolonging service life. Recently, computer vision-based non-contact sensors have gained attention as a viable alternative to traditional contact-based sensors for monitoring structural displacements in SHM applications. Most existing vision-based systems involve temporarily installing a camera at a distance from the structure, recording video data, and performing offline analysis to extract displacement information. However, this approach is often labour-intensive, inefficient, and more suitable for short-term monitoring. Advances in the Internet of Things (IoT) and edge computing have revolutionized this field, enabling real-time video analysis directly at the source. This eliminates the need for extensive data transmission, minimizes delays, and facilitates faster decision-making, surpassing the limitations of conventional offline processing methods. In this study, we propose a novel edge computing-based vision displacement measurement system (EdgeCVDMS). This system integrates video recording, real-time processing, and displacement tracking within an edge device, significantly reducing the amount of data sent to the cloud. The effectiveness of the EdgeCVDMS is validated through experimental testing on a laboratory-scale transmission tower model. The results demonstrate that the system is cost-efficient, easy to deploy, and holds significant potential for widespread use in monitoring aging civil infrastructure [1].

The structural integrity of underwater infrastructure, including bridges, dams, and pipelines, is continually compromised by factors such as aging, fatigue, unexpected loading conditions, and environmental degradation. Traditionally, inspections of these structures have relied on human divers; however, the growing demand for safer and more cost-efficient monitoring solutions has driven the development of unmanned underwater vehicles (UUVs) designed to perform subsea inspections. This paper offers a comprehensive and systematic review of the emerging technologies and methodologies associated with UUV deployment for infrastructure inspection. The existing literature is categorized into two primary areas: advancements in UUV design and operational capabilities, and innovations in instrumentation tailored for

underwater SHM. Following a thorough review, the paper identifies and discusses current challenges associated with UUV development and implementation. Finally, it presents recommendations for future research directions. By synthesizing recent advancements and highlighting gaps in the field, this study aims to provide researchers and industry professionals with a well-rounded perspective on the state of UUV-based inspection technologies and their potential evolution [2].

In vibration-based SHM, the early identification of sensor faults is critical to avoiding false alarms and incorrect assessments of the condition of monitored structures. Given that sensor networks often operate in harsh environments, they are susceptible to unexpected errors that can degrade the quality of the collected data. This paper introduces a novel approach for detecting and isolating faulty sensors using vibration response data. The method leverages an overdetermined system by establishing a relationship between the measured signals and the actual motion of the structure. It assumes that the monitored system exhibits rigid body motion, which can be described using a finite number of degrees of freedom (DOFs). This assumption allows for the formulation of an overdetermined relationship between sensor outputs and the system's DOFs. The methodology is further extended to systems not limited to rigid body motion by incorporating their vibration mode shapes into the analysis. The proposed approach's robustness is validated through experimental vibration data collected during a monitoring campaign, demonstrating its effectiveness in identifying and isolating sensor faults [3].

Sandwich composite structures are extensively utilized across various industrial sectors due to their exceptional bending strength, particularly in large-scale applications. Consequently, the need for SHM of sandwich structures to minimize maintenance costs over their service life has gained significant attention. This study focuses on the real-time monitoring of the structural health of sandwich composite structures featuring carbon nanotube (CNT)-dispersed cores and carbon fiber-reinforced polymers (CFRPs) using self-sensing data. Unlike previous self-sensing methods, which primarily detect damage and deformation within the elastic region, this work investigates multiple failure mechanisms in real time. A novel self-sensing health index system is proposed to evaluate damage severity in sandwich structures comprehensively. The self-sensing technique enables the detection and analysis of various damage types in both the skins and cores of sandwich structures. Additionally,

it facilitates the assessment of damage propagation, such as the length of core cracks, within the composite structure. The findings indicate that self-sensing SHM is an efficient and dependable approach for analysing sandwich structures, with significant potential applications in aircraft components, wind turbines, and personal aerial vehicles [4].

Freezing temperatures pose significant challenges to the long-term SHM of civil structures, particularly bridges. One critical issue is the abrupt and sharp increase in structural modal frequencies caused by freezing, which can lead to false alarms and errors in detecting structural changes. This study introduces a novel unsupervised approach for normalization method to address the adverse effects of freezing temperatures. The proposed approach, termed GDD-LRPCA, utilizes locally robust principal component analysis (LRPCA) in conjunction with Gaussian density distance (GDD) clustering to identify the optimal cluster number without manual input. Initially, the original modal frequency data are partitioned into clusters using the GDD clustering technique. Each cluster is then modelled with an independent LRPCA framework to extract normalized modal frequencies that are insensitive to freezing effects. The innovative aspect of this research lies in developing an integrated unsupervised normalization framework by utilizing advanced machine learning concepts, including local learning, robust learning, and hybrid unsupervised learning. A key advantage of the proposed method is its non-parametric design, which eliminates the need for additional hyperparameter optimization techniques. The validity and performance of the GDD-LRPCA method are evaluated using real-world bridge data, accompanied by comparative analyses against other methods. Results confirm that the proposed method effectively mitigates the impact of freezing temperatures on modal frequencies and surpasses existing techniques in unsupervised data normalization for SHM applications [5].

Civil engineering infrastructures are increasingly vulnerable to seismic loads, necessitating innovative methods to enhance structural resilience. This study explores the IoT technologies to strengthen resilience in seismically active regions. Through a comprehensive review of the literature, key aspects of seismic resilience were identified, including adaptive structural control, data acquisition and transmission, early warning systems, compliance with building standards and codes, and real-time monitoring and analytics. To investigate the practical applications of IoT in seismic

regions, a survey was conducted among 239 participants, achieving a robust response rate of 58.99%, underscoring substantial interest in the study. Using Partial Least Squares Structural Equation Modelling (PLS-SEM), the researchers developed and validated a measurement model to assess the reliability and validity of IoT-related constructs. Additionally, bootstrap resampling techniques were employed to rigorously test five hypotheses. The findings demonstrate strong associations between adaptive structural control, data acquisition, early warning systems, integration with building codes, real-time analytics, and IoT, collectively contributing to enhanced seismic resilience. These results offer valuable management insights for infrastructure developers and provide a validated framework for researchers to guide future empirical investigations into IoT-based seismic resilience strategies [6].

Automated damage detection forms a critical component of SHM systems. Typically, sensor measurements are processed to extract damage-sensitive features, which are then evaluated statistically to generate diagnostic values. However, not all data variations are attributable to damage; confounding factors, such as environmental and operational conditions, can also influence the measurements. Therefore, it is essential to identify and mitigate the effects of these factors to ensure accurate damage detection. Existing methods for correcting confounding effects often rely on mean regression techniques, that overlook variations in the higher-order statistical moments. Notably, output covariances play a vital role in generating robust diagnostics. This study introduces a novel approach to explicitly quantify covariance changes using conditional covariance matrices derived from a non-parametric, kernel-based estimator. The proposed method is validated using data from the Munich Test Bridge and the KW51 Railway Bridge in Leuven, incorporating both raw sensor measurements (acceleration, strain, inclination) and extracted damage-sensitive features (e.g., natural frequencies). Results reveal that covariances between sensors, such as vibration or inclination sensors, and natural frequencies are significantly affected by temperature variations. The study further demonstrates how conditional covariances can be integrated with standard damage detection methods, including the Mahala Nobis distance and principal component analysis, to enhance diagnostic reliability. By leveraging this approach, more accurate diagnostic values can be achieved with reduced false alarm rates, advancing the effectiveness of SHM systems [7].

Non-destructive testing (NDT) using acoustic waves has emerged as a promising technology for enhancing the safety of elastic structures while minimizing life-cycle costs. Despite significant advancements in this field, normal operational conditions, such as applied stresses, can compromise the reliability of defect detection. To address this, the nonlinear interactions between mechanical stress and acoustic wave propagation, known as acoustoelasticity, have been extensively studied. Acoustoelastic effects are intricately linked to acoustic wave modes, propagation directions, and material nonlinearity. Understanding these phenomena is critical to fully leveraging the potential of acoustic-based NDT. For instance, as applied stress and structural damage both affect wave phase velocity, it is essential to differentiate between stress-induced and damage-induced changes. Furthermore, a comprehensive understanding of stress-induced changes opens avenues for stress measurement in structural materials. To the best of the authors' knowledge, no comprehensive review has been published on acoustoelastic effects. This paper aims to fill that gap by systematically reviewing studies on the topic over the past 23 years, with a particular focus on applications in NDT and SHM. The review consolidates current knowledge, highlights areas of debate and ambiguity, and examines the relationship between initial stress and material symmetry. Through a comprehensive examination of the state of the art, this study endeavours to further the understanding and utilization of acoustoelastic effects in engineering applications [8].

This article presents a comprehensive review of the application of wavelet transform techniques in the analysis of durability and SHM of automotive components. Over the past three decades, research in automotive engineering has increasingly transitioned from traditional laboratory-based experiments to signal processing and simulation-based methodologies. This paradigm shift has driven researchers to investigate the utility of wavelet transforms as a powerful tool for signal processing in structural integrity analysis. The study is organized into five sections. The first section introduces the concept of durability analysis in automotive applications, providing an overview of evolving research trends in the field. The second section explores traditional signal processing approaches in the time and frequency domains, highlighting their limitations. The third section offers a detailed theoretical background on wavelet transform, covering both continuous and discrete wavelet transforms. The fourth section focuses on the practical applications of wavelet transform as a signal

processing technique for analysing durability and SHM in automotive components. Finally, the summary underscores the significance of wavelet transform in advancing automotive engineering by offering a robust approach to signal processing for structural analysis and monitoring [9].

SHM plays a vital role in maintaining the safety and durability of the engineering infrastructure integral to our daily lives. Traditional SHM techniques, while effective, often involve high costs and require specialized instruments and expertise. Advancements in computational capabilities and the declining costs of components have positioned photogrammetry, a method for deriving quantitative data from images, as a cost-efficient option for SHM applications. By investigating the use of proven photogrammetric methods in this emerging area, this study introduces a new technique called Mean Intensity Mapping (MIM). Both methods were subjected to experimental testing and benchmarked against conventional, high-cost techniques like laser vibrometers and accelerometers to assess their accuracy, usability, and implementation simplicity. Initial analyses focused on factors such as mass, structural damage, and frame complexity, with findings further validated through field testing on the Clifton Suspension Bridge (CSB). The experiments were designed to assess a low-cost method of obtaining modal data from video recordings, with applications in SHM. Using an entry-level Panasonic camcorder (£200) with high optical zoom, modal frequencies were detected remotely under favourable conditions. The proposed method employed brightness-based virtual sensors alongside conventional tracking algorithms. The measured frequencies were cross-verified with models and prior studies on the CSB, demonstrating a remarkable level of accuracy (approximately 0.5% error). This underscores the viability of photogrammetric methods as a low-cost alternative to conventional techniques, enabling non-contact, remote observations and detections within minutes. While photogrammetry shows great promise, several challenges remain, including visibility issues due to weather conditions, refractive index variations caused by wind and temperature, difficulties in low-light or nighttime data collection, longer processing times, and instability in mounting equipment such as tripods. Nonetheless, with the ongoing reduction in optical equipment costs and advancements in computational capabilities, photogrammetric methods are poised to become a crucial tool in the future of SHM [10].

Detecting anomalies in the vibrational characteristics of historical buildings is a critical component of SHM. SHM techniques utilize data from onsite measurements and environmental factors to determine dynamic properties, such as natural frequencies, and identify deviations or unusual behaviour over time. This study explores the application of the Temporal Fusion Transformer (TFT), a deep learning algorithm initially developed for multi-horizon time series forecasting in domains such as electricity, traffic, retail, and volatility, to SHM. Specifically, the TFT framework is employed to analyse the long-term dynamic behaviour of the Guinigi Tower in Lucca, Italy, which has been subjected to an extensive monitoring campaign. The TFT model is trained on experimental frequency data from the tower, supplemented by environmental parameters. Once trained, the network predicts vibrational features such as natural frequencies and root mean square (RMS) values of the velocity time series. Anomalies or unexpected events are identified by analysing deviations between the predicted and actual frequencies. This methodology is applied to assess the impact of the Viareggio earthquake on 6 February 2022, as well as structural damage induced under three simulated damage scenarios. The results demonstrate the potential of the TFT approach in accurately predicting vibrational features and detecting anomalies, offering a robust tool for the SHM of historic and age-old structures [11] .

SHM systems are increasingly being deployed on bridges worldwide, delivering critical data for assessing structural conditions and planning maintenance. Machine Learning (ML), with its efficiency in tasks such as classification and regression, has gained prominence due to its capacity to improve accuracy through data-driven learning without explicit programming instructions. In recent years, ML-based approaches have become increasingly prominent in bridge SHM, driven by their ability to detect material degradation in concrete and steel and to deliver comprehensive assessments of structural conditions. Although ML applications in SHM have been covered in various review articles, most of these reviews present overarching discussions applicable to diverse civil engineering structures. This article centers on the use of ML techniques specifically within the context of bridge SHM, offering a detailed summary and discussion of various methodologies. A critical evaluation of different ML approaches is presented, highlighting their strengths and limitations. Furthermore, the paper identifies existing research gaps and provides recommendations for future studies to advance the integration of ML techniques in

bridge SHM, promoting enhanced accuracy and reliability in damage detection and condition assessment [12].

SHM has become an essential component of civil engineering for enhancing the operational performance and longevity of aging infrastructure. Recent advancements in Industry 4.0 technologies—such as the IoT, Big Data analytics, cloud computing, and cybersecurity—have been leveraged to automate SHM processes. Despite these advancements, significant challenges remain in seamlessly integrating these technologies and establishing a fully autonomous digital framework for SHM applications. One major challenge lies in the real-time visualization of processed SHM data through digital interfaces, which is hindered by issues such as delays in data transfer and reliance on offline tools for manual data processing. Addressing these challenges, this paper investigates the integration of Building Information Modelling (BIM) and IoT using an Arduino microcontroller for tracking and visualizing time- and frequency-domain data. The proposed methodology develops strategies for continuous data acquisition, monitoring, and processing, enabling real-time structural response analysis. A web-based database is employed to query and store data, eliminating the need for offline resources that require manual intervention. The approach is validated through two experimental case studies: (1) a dynamically moving vehicle over a simply supported bridge prototype and (2) a randomly excited three-story structure. Both experiments demonstrate real-time visualization of time- and frequency-domain information under undamaged and damaged conditions. This research establishes an early-phase Digital Twin (DT), integrating static and real-time dynamic data into a BIM-rich database, thus advancing the development of comprehensive, automated SHM frameworks for civil infrastructure [13].

SHM of existing masonry structures poses significant challenges and has been a subject of extensive research within the scientific community. This study investigates the application of low-cost Capacitive Stress Sensors (CSSs) as an effective tool for detecting the compression state within mortar joints of masonry constructions. The research employs Finite Element (FE) simulations to replicate the mechanical response of an innovative CSS prototype, recently patented, under compression forces representative of typical serviceability conditions in masonry structures. To validate the sensor's constitutive behaviour, a pilot laboratory experiment was conducted on a cylindrical mortar specimen equipped with CSSs and Linear Variable Differential

Transformers (LVDTs). The specimen was subjected to cyclic uniaxial compression, and the results were compared against the numerical predictions. The FE model is designed to simulate the capacitive sensor embedded within the mortar material, enabling a correlation analysis between the numerical stress-strain outputs of the sensor and the experimental data. The validation process demonstrates strong agreement between the FE results and the experimental measurements obtained through the LVDTs. Additionally, the FE model is utilized to perform a parametric analysis to evaluate the influence of mortar stiffness and strength on the effectiveness of SHM using CSSs. Based on this analysis, optimal serviceability configurations are identified, providing insights into the practical application of CSS technology in masonry structure monitoring [14].

While structures are typically inspected during manufacturing using Non-Destructive Testing (NDT) methods, there is a growing emphasis on monitoring their integrity throughout their entire life cycle through SHM strategies. This approach is particularly critical for aircraft structures, which are subjected to high strains and extreme atmospheric conditions. Although a substantial body of literature exists on SHM in aviation, comprehensive methodologies are rarely addressed. This paper presents a novel methodology, an electronic SHM device, and the validation tests performed on it. The proposed SHM prototype employs ultrasonic techniques utilizing piezoelectric transducers. Designed with a lightweight architecture, the device features USB 2.0 connectivity and integrated data pre-processing algorithms to enhance its performance. It supports both pitch-catch and pulse-echo operational modes, enabling the application of both passive and active SHM techniques. Passive techniques are employed to detect sudden events, such as impacts or fiber breakage in composite materials, while active techniques are used to identify a range of damage types. These include abrupt damage as well as progressive issues caused by factors like corrosion, delamination, or fatigue. The comprehensive design and functionality of the device provide a robust framework for the SHM of aircraft structures, addressing the need for continuous and reliable monitoring throughout their service life [15].

This research presents a cutting-edge SHM approach based on a non-destructive self-sensing technique designed for large-scale carbon fiber-reinforced polymers (CFRPs). Three types of CFRPs underwent cyclic point bending tests to analyse damage severity and localization, classified via four separate convolutional neural network (CNN)

architectures. Electrical resistance images were used as input data to train each CNN architecture for conducting damage analysis. An improved CNN model for analysing CFRP damage was designed using electrical resistance data, and its performance was assessed in comparison to standard CNN-based methods. The proposed SHM approach was evaluated by examining previously undetected damage in CFRPs, showcasing its effectiveness. This study improves upon previous self-sensing approaches by decreasing the electrode count, which reduces data complexity and enlarges the effective sensing area of CFRPs. The methodology achieved high accuracy, exceeding 90%, in identifying both damage severity and localization, irrespective of the carbon fiber variety or the stacking arrangement of the composite structures. These findings highlight the significant potential of this SHM methodology for efficient and reliable damage analysis in CFRPs [16].

Recent occurrences of vortex-induced vibrations in several prominent engineering structures in China have highlighted the need for effective monitoring and evaluation methods. These events involved large mono-frequency periodic vibrations, prompting further investigation. This study analyses data recorded from the SHM system of a suspension bridge, aiming to develop indicators for identifying abnormal vibrations and potential changes in structural health conditions. The analysis involves plotting the power spectrum of measured acceleration responses in a three-dimensional space of time, frequency, and power. Data from 16 acceleration sensors installed on the bridge deck were collected over 233 days, providing a comprehensive dataset for evaluating dynamic behaviours. The study examines the evolution of dynamic parameters during periods of significant vortex-induced vibrations, revealing their strong correlation with temporary installations on the bridge deck and measures taken to suppress vibrations. Changes in vibration power at various natural frequencies of the structure illustrate the progression of these unexpected events. The observed trends and abrupt shifts in natural frequencies and modal components indicate energy flow between different vibration modes. To enhance detection capabilities, two state vectors are derived from the power spectrum, enabling automatic identification of abnormal vibrations and structural states using a novelty detection method with predefined thresholds. The study demonstrates the effectiveness of the proposed methodology through the analysis of SHM acceleration data from the bridge deck. The results validate the implementation process and highlight the potential of this approach for As

damage tolerance design principles gain prominence, health monitoring systems have become essential for the effective operation and maintenance of engineering structures. A critical component of these systems is the damage indicator, a metric that quantifies the structural integrity level and requires continuous monitoring. Damage indicators are typically derived from structural response data, with various quantities such as natural mode shape, strain energy, frequency, curvature, and statistical measures like z-, t-, and F-statistics being commonly proposed. This paper introduces a novel damage indicator derived from Euler-Bernoulli beam theory, applicable in both the time and frequency domains. The proposed approach was tested through numerical simulations of a cracked beam, where the nonlinear deformation emerges from vibrational contact interactions of the crack faces. The damage indicator is estimated across multiple observation points on the beam, providing a comprehensive assessment of structural integrity. In addition, the proposed method is compared to traditional damage detection techniques based on changes in natural frequency and mode shape. The results demonstrate that the proposed damage indicator exhibits higher sensitivity in detecting cracks than conventional methods. These findings underscore the potential of the proposed approach as a robust tool for identifying damage and enhancing the reliability of health monitoring systems in engineering structures [17].

Structural repairs inherently alter the physical properties of a structure, resulting in changes to its responses under both normal and damaged conditions. These alterations create a shift between pre- and post-repair data distributions, posing challenges for conventional data-driven SHM methods. Such methods typically assume that the data distribution remains consistent between training and testing phases. When this assumption is violated, as in the case of structural repairs, algorithms often fail to generalize effectively because pre-repair labels become inapplicable to post-repair data. Transfer learning, particularly in the form of domain adaptation, offers a promising solution to this challenge. Domain adaptation seeks to map the pre- and post-repair data distributions onto a shared latent space where their distributions are aligned. This mapping enables the use of pre-repair label knowledge to classify post-repair data accurately. This paper demonstrates the feasibility of domain adaptation in addressing the challenges posed by structural repairs using a dataset from a Gnat trainer aircraft. Furthermore, the study introduces a novel modification to an existing

domain adaptation technique, joint distribution adaptation (JDA). The proposed metric-informed joint distribution adaptation method enhances the semi-supervised learning phase of the algorithm by incorporating a metric-informed approach. Benchmarking results show that the proposed metric-informed JDA algorithm outperforms both traditional data-based methods and other domain adaptation techniques. This advancement highlights the potential of domain adaptation as a robust framework for addressing the complexities introduced by structural repairs in SHM applications [18].

The implementation of SHM systems is largely motivated by the need for informed and efficient decisions in managing structural operations and maintenance. Probabilistic Risk Assessment (PRA) is a widely recognized approach that supports engineers in making risk-informed decisions for designing and operating safety-critical and high-value assets, with applications in industries like nuclear and aerospace. This study introduces a risk-based decision-making framework for SHM, combining principles of PRA with the current SHM paradigm. The framework utilizes probabilistic graphical models, ideal for reasoning and making decisions in the presence of uncertainty. Structural failure modes are modelled using Bayesian networks derived from fault trees, which are further enhanced by incorporating costs or utilities linked to failure events. The fault trees enable the flow of information from probabilistic classifiers to influence diagrams representing decision-making processes. The graphical models include nodes that can be queried to derive marginal probability distributions for localized damage states in a structure. Optimal maintenance or operational strategies for structures are determined by identifying actions that maximize expected utility within the framework. The proposed risk-based framework is validated through its application to a realistic truss-like structure, with support from experimental data. The results illustrate how the integration of PRA with SHM facilitates informed decision-making processes. The paper concludes with a discussion on the broader implications of adopting a risk-based approach and identifies challenges that need to be addressed for effective decision-making within the SHM context [19].

The integration of machine learning into SHM has demonstrated considerable success across various applications. However, most machine learning techniques rely on the assumption that training and test data originate from the same underlying distribution. Consequently, when test data are collected from systems operating under different

conditions or from different structures, the predictions made by models trained on the original data are often inaccurate. This limitation poses a significant challenge for SHM, where recollecting new training data and labels for every new structure is both costly and impractical. Transfer learning, specifically in the form of domain adaptation, offers an innovative solution to this problem. Domain adaptation techniques enable the mapping of feature and label distributions from different structures—referred to as the labelled source and unlabelled target domains—into a shared latent space. This approach allows classifiers trained on labelled data from a source structure to generalize effectively to unlabelled target structures. The paper provides an extensive analysis of domain adaptation's applicability, highlighting its role in population-based SHM. Additionally, three domain adaptation methods are showcased through four distinct case studies, presenting novel frameworks for addressing challenges in SHM. These findings highlight the potential of domain adaptation to significantly reduce the need for structure-specific data collection while maintaining robust predictive performance in diverse SHM scenarios [20] .

### **3. STRUCTURAL HEALTH MONITORING (SHM)**

SHM is a system used to monitor the safety and performance of buildings, bridges, dams, tunnels and similar engineering structures. In this process, factors such as damage, deformation, vibration, stress and temperature that may occur in the structure are measured and analysed continuously or at regular intervals through sensors and other monitoring devices placed on the structure. The aim is to evaluate the performance of the structure over time, detect damage early, and plan maintenance and repair works to extend the life of the structure. SHM is important to ensure the safety of critical structures, especially those facing earthquakes, overloads, material fatigue and other environmental impacts. While the system offers long-term monitoring for large structures, it minimizes the need for intervention by working integrated with damage detection systems. Sensor technology (accelerometers, strain gauges, fiber optic sensors, etc.), data analysis systems and software are the basic components of SHM.

The history of the SHM concept dates back to the mid-20th century, driven by the need to continuously monitor the safety and performance of engineering structures (Abdo, 2014). This process evolved in parallel with technological advancements and developments in engineering disciplines. The idea of SHM emerged primarily from the necessity to ensure the safety of large engineering projects. After World War II (From 1940), the safety of large structures such as bridges, dams, and other major infrastructures became a critical concern. During this period, monitoring was generally conducted through visual inspections, manual measurements, and basic tests to analyse the responses of structures. These methods were mostly reactive and relied on simple techniques for assessing the condition of the structures. From the 1960s onwards, the field of SHM became more sophisticated as technology advanced. Accelerometers, strain gauges, and simple electronic monitoring devices were integrated into engineering projects. These tools were particularly used in large bridge and dam projects to continuously monitor the dynamic responses of the structures and detect potential structural issues at an early stage. In the 1980s, advancements in microelectronics and computer technologies allowed SHM systems to become more complex. During this period, real-time data collection and analysis capabilities

improved, and sensor networks were installed on large structures. These networks enabled the continuous monitoring of stress, deformation, and vibrations at different points within a structure. With the growing computational power of computers, this data was analysed more comprehensively, allowing for more accurate predictions about the structures' performance and lifespan. Additionally, SHM systems played a crucial role in earthquake engineering, helping assess the safety of buildings and structures after major seismic events. Since the 2000s, SHM has undergone a significant evolution due to rapid developments in sensor technology and wireless communication. Fiber optic sensors, piezoelectric sensors, and wireless sensor networks have provided more precise and reliable measurements. During this time, advanced analytical methods such as artificial intelligence and machine learning were applied to large datasets to predict the performance of structures and improve damage detection accuracy. Advanced data processing systems and algorithms also enhanced the capability to perform real-time dynamic analysis of structures. SHM systems have become widespread, particularly in critical infrastructure (e.g., bridges, dams, tall buildings, tunnels) and historic structures. The development of SHM has been shaped by technological progress aimed at ensuring the safety and sustainability of engineering structures. It has become especially critical in regions prone to seismic activity, where SHM helps assess structural safety after major events, and continues to evolve with the advancement of monitoring and analytical technologies.

In SHM systems, the condition of structures is constantly monitored using various sensors and devices. The main tools used in SHM are Accelerometers, Strain Gauges, Fiber Optic Sensors, Laser Displacement Sensors, Piezometric Sensors, Tiltmeters, Displacement Sensors, Inclinator, Fiber Bragg Gratings – FBG, Thermal Cameras, Ultrasonic Testing Equipment, Wireless Sensor Networks, Ground Penetrating Radar – GPR, Acoustic Emission Sensors.

SHM has become an increasingly important issue in regulations and standards. The application of SHM systems has been made mandatory in some regulations in order to monitor the safety of structures, especially in earthquake zones and critical infrastructures. Regulations in this area may vary from country to country and depending on the size of engineering projects [21].

## 3.1. Structural Health Monitoring Processes

SHM is a technology used to evaluate, ensure, and sustainably manage the performance, safety, and integrity of structures. SHM systems consist of sensors, data collection devices, and analytical methods that continuously or periodically monitor the condition of structures and assess potential risks or damage. These systems are commonly applied to large-scale structures such as bridges, dams, tall buildings, and historical structures, as well as those located in earthquake-prone regions. The SHM process is structured into six main stages, each critical to ensuring the safe and efficient functionality of a structure. The flowchart for SHM processing is shown in **Figure 3.1**.

### 3.1.1. Damage Detection

- **Anomaly Detection:** At this initial stage, the current condition of the structure is compared with a predefined reference or "healthy" state. Data collected from sensors is analysed to identify unexpected deviations or anomalies. For example, sudden changes in vibration frequencies of a bridge could indicate potential issues. This step is vital for the early detection of damage.
- **Damage Localization and Severity Assessment:** Once anomalies are identified, the precise location and severity of the damage are determined. Detailed sensor data analysis pinpoints the affected sections of the structure. This evaluation also helps ascertain whether the damage is superficial or deep, and whether immediate intervention is required. For instance, the location and extent of cracks in a building column can provide crucial insights into the overall stability of the structure.

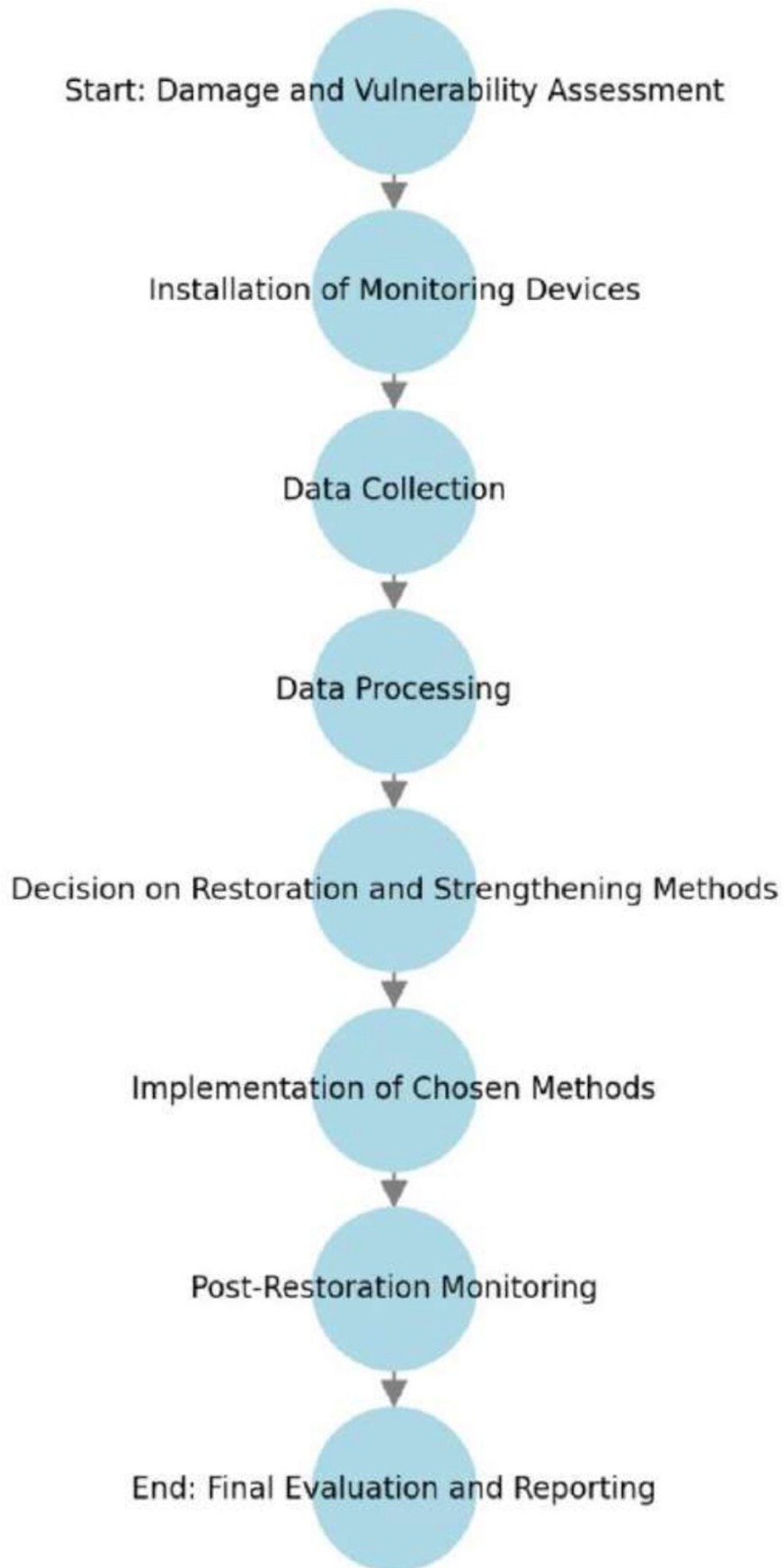


**Figure 3.1:** Flowchart for Restoration Decision-Making Using SHM Equipment.

### 3.1.2. Instrumentation and Data Collection

- **Sensors:** A variety of sensors measure different physical parameters of the structure. Accelerometers monitor vibrations, strain gauges measure stresses on materials, fiber-optic sensors provide high-precision temperature and strain readings, and Linear Variable Differential Transformers (LVDTs) are used for displacement and deformation measurements. These sensors are strategically installed at critical points to create a comprehensive and reliable dataset.
- **Data Recorders:** Sensor data is transferred to high-capacity and reliable data recording devices, ensuring accurate and uninterrupted data collection. Time-stamped recordings allow for tracking changes over time.
- **Remote Monitoring:** Cloud-based systems enable real-time monitoring and analysis of the collected data. Engineers and decision-makers can remotely track the structure's condition, such as monitoring water pressure sensors in a dam to identify potential risks.

### 3.1.3. Data Processing and Analysis

- **Preprocessing:** Raw data is cleaned to remove noise and filtered to prevent environmental factors from compromising data quality. Consistency and reliability are verified through validation processes, identifying and correcting issues such as sensor failures or communication interruptions.
- **Modelling and Simulation:** Structural behaviour is modelled using numerical analysis techniques like the Finite Element Method (FEM). Digital twin models replicate the real structure virtually, allowing simulations of various scenarios to predict the effects of loads or potential damages.
- **Feature Extraction:** Processed data is used to derive dynamic and static characteristics of the structure, such as natural frequencies, mode shapes, and damping ratios. These parameters reflect the structure's current state and performance, enabling the identification of changes and potential damage over time.

### 3.1.4. Decision-Making Mechanism

The decision-making phase is critical, as it consolidates all data and analysis results to make important determinations about the structure's safety and usage. Risk assessments are conducted, and restrictions or shutdowns may be imposed if necessary. Key considerations in this phase include:

- **Risk Assessment:**
  - **Natural Hazards:** Analysing the effects of earthquakes, wind loads, floods, and temperature changes on the structure.
  - **Human-Induced Hazards:** Evaluating damages caused by overloading, vibrations, explosions, or accidents.
  - **Time-Dependent Hazards:** Assessing material degradation, corrosion, or crack propagation over time.
- **Defining Critical Thresholds:**
  - **Dynamic Behaviour Parameters:** Changes in natural frequency, damping ratio, and mode shapes help detect stiffness loss or damage localization.
  - **Load and Stress Limits:** Exceeding design load capacities or stress thresholds indicates a breach in safety.
- Simulating responses to potential future hazards such as earthquakes or environmental stressors.

### 3.1.5. Restoration and Strengthening Works

Based on the decisions made, restoration and strengthening works are planned and executed to address identified damages and weaknesses. Examples include:

- **Material Replacement:** Replacing damaged or deteriorated materials with new ones.
- **Structural Reinforcements:** Adding steel or carbon fiber reinforcements to improve the structure's strength.
- **Repair Works:** Filling cracks, removing corrosion, or other measures to extend the structure's lifespan.

### 3.1.6. Post-Intervention Monitoring and Follow-Up

After restoration and strengthening works, SHM systems continue to monitor the structure to assess the effectiveness of interventions and track its future performance. Continuous monitoring ensures:

- **Intervention Effectiveness:** Evaluating how well the repairs and reinforcements have improved the structure's behaviour.
- **Early Warning Systems:** Detecting potential new damages early.
- **Maintenance Planning:** Proactively scheduling future maintenance and repairs based on real-time data.

This six-step process highlights the comprehensive and systematic nature of SHM, emphasizing its growing importance in ensuring the safe and sustainable service of structures. Advances in sensor technology and data analysis methods are continually enhancing the effectiveness and reliability of SHM applications.

## 3.2. Standards and Regulations for SHM

Structural Health Monitoring (SHM) systems play a crucial role in ensuring the safety, reliability, and longevity of structures. To standardize the design, implementation, and assessment of SHM systems, various international and national standards and regulations have been established. These standards serve as guidelines for engineers, researchers, and practitioners in the field. Below are the key standards and regulatory frameworks relevant to SHM.

SHM practices vary across countries due to differences in seismicity, infrastructure, and technological advancements. National standards and regulations play a crucial role in defining the methodologies, design requirements, and performance evaluation criteria for SHM systems. These standards ensure uniformity, reliability, and safety in monitoring critical structures. **Table 3.1** provides a summary of standards and regulations related to SHM from various countries.

**Table 3.1:** Worldwide SHM codes/standards [22].

<b>Country /Region</b>	<b>Standard Code and Name</b>	<b>Responsible Organization</b>	<b>Year</b>
Australia	AS 5100: Bridge Design	Standards Australia	2017
China	Structural health monitoring system technical specification for bridges in Tianjin	Tianjin Municipal Government	2011
	GB 50982: Technical code for monitoring of building and bridge structures	Ministry of Housing and Urban-Rural Development of PRC; General Administration of Quality Supervision, Inspection and Quarantine of the People's Republic of China.	2014
	Design standard for structural health monitoring systems	China association for engineering construction standardization	2012
	Technical code for construction process analysing and monitoring of building engineering	Ministry of housing and urban-rural development of China	2013
	Technical code for monitoring of building and bridge structures	Ministry of housing and urban-rural development of China	2014
Canada	Guidelines for structural health monitoring	Intelligent Sensing for Innovative Structures (ISIS)	2001

Table 3.1:Continued			
	Reinforcing concrete structures with fiber-reinforced polymers (FRPs)	Intelligent Sensing for Innovative Structures (ISIS)	2007
European Union	Strategic research agenda	Structural Assessment, Monitoring, and Control (SAMCO)	2006
	SAMCO monitoring glossary	Structural Assessment, Monitoring, and Control (SAMCO)	2006
	Ambient vibration monitoring	Structural Assessment, Monitoring, and Control (SAMCO)	2006
	Case studies	Structural Assessment, Monitoring, and Control (SAMCO)	2006
	Guidelines for structural control	Structural Assessment, Monitoring, and Control (SAMCO)	2006
	SAMCO history and events	Structural Assessment, Monitoring, and Control (SAMCO)	2006
	Guideline for the assessment of existing structures	Structural Assessment, Monitoring, and Control (SAMCO)	2006

Table 3.1 : Continued			
	Guideline for structural health monitoring	Structural Assessment, Monitoring, and Control (SAMCO)	2006
	Report on bridge management	Structural Assessment, Monitoring, and Control (SAMCO)	2006
	EN 1998: Eurocode 8: Design of structures for earthquake resistance	European Committee For Standardization	2004
UK	CIRIA C788: Structural Health Monitoring for civil engineering	The Construction Industry Research and Information Association (CIRIA)	2020
India	IS 1893: Criteria For Earthquake Resistant Design of Structures	Bureau Of Indian Standards Manak Bhavan, New Delhi	2002
International	ISO 13374: Condition monitoring and diagnostics of machines — Data processing, communication and presentation	International Organization for Standardization (ISO)	2003
	ISO 2394: General principles on reliability for structures	International Organization for Standardization (ISO)	2015

Table 3.1: Continued			
	ISO 13822: Bases for design of structures — Assessment of existing structures	International Organization for Standardization (ISO)	2010
Japan	Building Standard Law of Japan	Building Guidance Division, Housing Bureau, Ministry of Land, Infrastructure and Transport	2000
Switzerland	Fundamentals of the conservation of structures	Swiss society of engineers and architects	2011
United States	Development of a model health monitoring guide for major bridges	The Federal Highway Administration (FHWA)	2003
	Long-term bridge performance (LTBP) Program Protocols	The Federal Highway Administration (FHWA)	2016
	ASTM E2983: Standard Guide for Application of Acoustic Emission for Structural Health Monitoring	American Society for Testing and Materials (ASTM)	2019
	ASCE 41: Seismic Evaluation and Retrofit of Existing Buildings.	American Society of Civil Engineers (ASCE)	2023

The Structural Health Monitoring System Implementation Directive was submitted by the Disaster and Emergency Management Authority (AFAD) to the Ministry of Interior's Directorate General of Strategy Development on January 10, 2020, under directive number 76388967-15.20.1-111. In this directive the accelerometers used in SHM systems will be synchronized with at least 24-bit resolution and connected to a

GPS-timestamped digital recording system. The system will continuously record vibration data and transfer it in real time to designated centers via the internet, modem, satellite, or similar channels. It will also include batteries or necessary equipment to operate for at least one week in the event of power or communication failures and will have the capability to store data internally. Additionally, accelerometers, data acquisition devices, and other system components will be safeguarded against fire and impact, with necessary precautions taken.

To ensure synchronized operation, the accelerometers to be installed on a building as part of the SHM system will be connected to the same central recording system via cables. The cables used to connect the accelerometers and data acquisition devices will be resistant to fire and impacts. Where wireless or fiber-optic cables are used, precautions will be taken to prevent interruptions and ensure system security, particularly at cable connection points, which will be installed to minimize potential external damage. The system will use a precise time synchronization method such as GPS to ensure compatibility with universal time (UTC). If needed, an NTP server can also be employed for this purpose. The signal cables of the sensors will be installed within protective channels and positioned in a way that ensures their safety under adverse conditions. The data acquisition devices will have both continuous recording and trigger mode capabilities. In trigger mode, the triggering level can be set at a minimum of 0.005 g (5 gal) acceleration. When the trigger level is exceeded, recording will begin, and data will continue to be recorded for 30 seconds before and 600 seconds after the event. In cases of earthquakes or other emergencies, the system will allow AFAD or the authorized owner to remotely control the equipment and transfer the recorded data to the designated central station via secure communication channels. The minimum number of accelerometers to be used is provided in **Table 3.2**.

**Table 3.2:** Minimum Number of Accelerometers.

<b>Building Height Above Ground Level (m)</b>	<b>Minimum Number of Channels</b>
105–155	16
156–205	24
>205	32

The placement of accelerometers in the building should follow the specified locations and numbers as illustrated in **Figure 3.2**. Depending on the building's characteristics and if deemed necessary by AFAD, the number of accelerometers may be increased. On the top floor, sensors should be positioned to measure maximum displacements, with at least two sensors aligned in orthogonal directions and placed at a distance from each other. On the ground floor, at least two sensors should be placed orthogonally to each other. In the basement, four sensors should be installed in two orthogonal directions to measure the rotational movement of the rigid base. Additionally, for evaluating torsional movements, sensors should be placed in parallel and orthogonal directions at the specified locations. At least two orthogonal sensors should also be placed at defined floor levels, including those outside the base level. On the basement floor, additional sensors should be positioned to measure the rigid body rotation of the base.

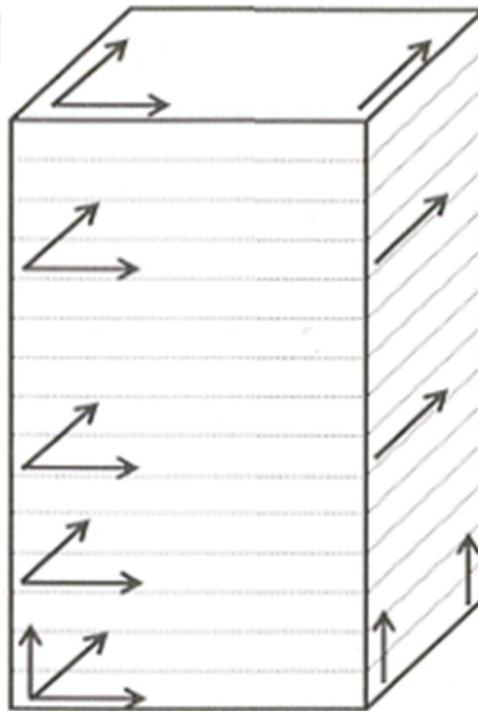


**Figure 3.2:** Placement of Accelerometers (The number of accelerometers varies depending on the floor level).

Accelerometers to be installed in the building must meet at least the minimum specifications outlined in **Table 3.3**.

**Table 3.3:** Accelerometer Specifications.

Specification	Value
Dynamic Range	>144 dB+
Frequency Range	0.01 – 200 Hz
Noise Level	<1 $\mu$ g RMS
Measurement Range	$\pm 2$ g

### 3.3. Threshold Levels for Decision-Making Mechanism

Threshold levels play a critical role in the assessment and management of structural health, particularly for masonry structures, which are highly susceptible to damage due to their material composition and construction techniques. Various national and international codes and standards provide specific threshold values for evaluating the vulnerability and damage levels of such structures. These thresholds are essential for establishing decision-making mechanisms that guide interventions, including maintenance, strengthening, or restoration efforts. In this section, the focus will be on reviewing the threshold levels outlined in prominent regulatory frameworks, such as the General Directorate of Foundations Guide of Turkey, Eurocode 8, FEMA 273, FEMA 356 and ASCE 41. By comparing these standards, the study aims to identify critical parameters, such as allowable deformations, stress limits, and crack widths, which serve as benchmarks for determining the safety and performance levels of masonry structures. This analysis provides a foundation for developing scientifically grounded and contextually relevant strategies for preserving historical masonry buildings, including the Oshki Church.

#### 3.3.1. General Directorate of Foundations Guide of Turkey

The Acceptable Damage Level for a historical structure can be defined based on its significance, function, and the number of users and visitors. For structures of global

importance that attract large numbers of visitors, the target level of damage tolerability remains minimal. However, for a historical structure of local significance that is primarily visited externally without entry, relatively higher levels of damage may be considered acceptable. The concept of performance has been developed to assess the seismic safety of existing structures, and its definition is influenced by two key factors. The first factor involves realistically considering both the capacity of the structural system and the demands imposed by the earthquake on the structural system during elastic and inelastic behaviour under seismic effects. The second factor involves using advanced knowledge of structural behaviour and detailed computational techniques provided by modern software to numerically define the accepted level of damage in the structure (controlled inelastic deformations) in greater detail and reflect this in seismic safety assessments. When conducting detailed mathematical analyses, it is crucial not to overlook that all obtained results depend on the assumptions made in defining the structural behaviour and seismic effects. It must be remembered that, due to uncertainties in a historical structure, the material properties and structural parameters used in the analysis can only be determined with limited accuracy. For this reason, it is evident that the assumptions and mathematical methods used in the evaluation of a historical structure should be kept as simple as possible.

The following Structural Performance Levels can be defined for historical structures subjected to a specific earthquake effect:

**b.1. Limited Damage (LD) Performance Level:** This level corresponds to a state where the structural elements of the building sustain limited damage, with minimal non-linear behaviour.

**b.2. Controlled Damage (CD) Performance Level:** This level corresponds to a state where the structural elements of the building sustain damage that is largely repairable and remains under controlled conditions.

**b.3. Collapse Prevention (CP) Performance Level:** This level corresponds to a state where the structural elements of the building sustain severe and extensive damage, nearing partial or total collapse, but collapse is successfully prevented (**Figure 3.3**).

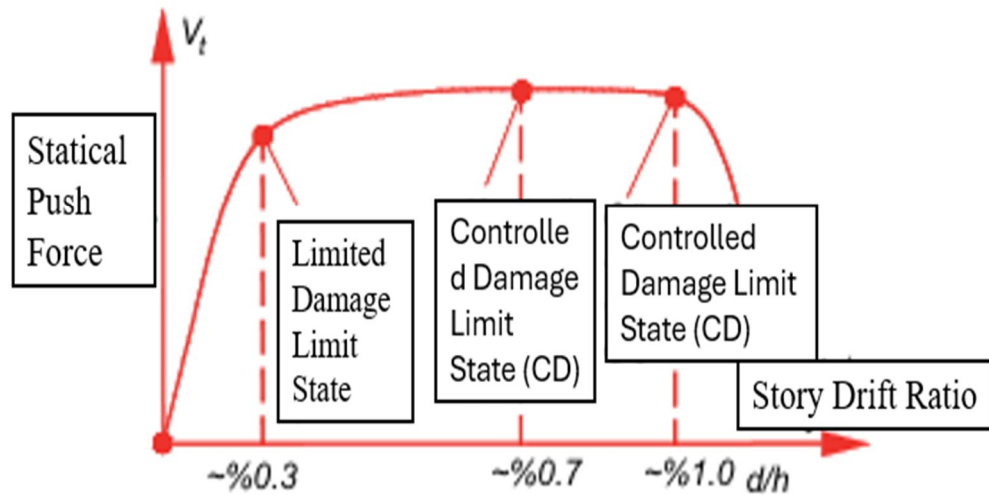


**Figure 3.3:** Limit States for Masonry Structures.

In the evaluation of structural system safety, either Strength-Based Assessment or Deformation-Based Assessment is commonly applied. The Earthquake Code stipulates the following design principles for earthquake-resistant buildings:

- Structural and non-structural elements should experience no damage during low-intensity earthquakes.
- Damage to structural and non-structural elements during moderate-intensity earthquakes should remain limited and repairable.
- During severe earthquakes, permanent structural damage should be restricted to ensure controlled damage is maintained.

The design provisions outlined in the Earthquake Code can be categorized into three main sections as follows:

**Design Earthquake and Building Importance Factor (I = 1):**

The code defines the design earthquake for buildings with a Building Importance Factor of  $I = 1$  as an event with a 10% probability of exceedance in 50 years for the relevant region. Using the specified rules, the loads acting on the structural system under seismic effects are calculated considering the increase in system capacity due to inelastic behaviour and the reduction in earthquake demand. The design ensures that

reduced seismic loads and related vertical loads are adequately accounted for in cross-sectional effects.

**Limiting Damage to Non-Structural Elements:**

The code requires that damage to non-structural elements under frequent earthquakes be limited. This can be interpreted as either restricting second-order effects or minimizing damage to non-structural system elements within buildings.

**Preventing Total Structural Collapse:**

The code accounts for the possibility of less frequent but more severe earthquake effects and ensures that the structural system does not reach total collapse under such scenarios. As explained in the following sections, strength-based assessment is appropriate when the damage (inelastic deformations) in the structure is minor. However, when the damage is substantial but remains controlled and does not lead to collapse, deformation-based assessment is preferred. Nevertheless, it is possible to extend the application range of strength-based assessment by using an appropriate seismic load reduction factor. Similarly, deformation-based design can be applied in such damage scenarios by defining appropriate limit values (**Table 3.4**).

**Table 3.4: Proposed Target Performance Levels.**

Performance Levels That Can be Selected According to the Importance of Historical Structures	Nationally Significant Historical Structure Group I	Globally Significant Historical Structure	
		DD-3 (50%/50, 72 years) Limited Damage Level (LD)	DD-2 (50%/10, 475 years) Limited Damage Level (LD)
Locally Significant Historical Structure Group II	DD-3 (50%/50, 72 years) Controlled Damage Level (CD)	DD-2 (50%/10, 475 years) Controlled Damage Level (CD)	DD-1 (50%/2, 2475 years) Controlled Damage Level (CD)
	DD-3 (50%/50, 72 years) Limited Damage Level (LD)	DD-2 (50%/10, 475 years) Collapse Prevention Level (CP)	DD-1 (50%/2, 2475 years) Collapse Prevention Level (CP)

In strength-based assessment, the stresses in structural elements are calculated under vertical loads combined with seismic effects reduced by the accepted seismic load reduction factor ( $R_a \leq 3$ ). These stresses are then compared to the allowable stress limits for the relevant material. If the structure is expected to experience minimal damage under the anticipated seismic effects, meaning it remains within the Limited Damage (LD) region, it is required that the stresses under the unreduced seismic effects ( $R_a = 1$ ) do not exceed the allowable limits. If the goal is to prevent total collapse of the structure, the stresses caused by vertical loads and reduced seismic effects may be permitted to exceed the allowable limits by a certain margin (e.g., 50%). In cases of controlled damage, which fall between these two damage states, it is expected that the stresses under reduced seismic effects do not exceed the allowable limits. The seismic load reduction factor is determined based on the ductility of the structural system. For historical structures, particularly masonry ones, where ductility is limited,  $R_a \leq 3$  is typically adopted.

It is important to ensure two conditions are met in this type of assessment. First, for the comparison to be valid, the structure must have sufficient post-elastic deformation and displacement capacity necessary for the behaviour. In structures that are entirely brittle or lack adequate ductility, the use of such seismic load reduction factors is not appropriate. For example, applying a high seismic load reduction factor to a masonry structure with low ductility renders the assessment meaningless. Second, the post-elastic deformations or displacements (controlled damage) anticipated in the structural system must be acceptable. For instance, controlled damage (post-elastic deformation or displacement) that might be acceptable for a locally significant historical structure under a specific earthquake may not be acceptable for a nationally significant historical structure. In all damage scenarios, the global behavior of the structural system under unreduced seismic effects must be controlled by limiting the drift ratio. For historical structures, the drift ratio is calculated as the difference in horizontal displacements at different levels divided by the height difference (**Figure 3.4**).

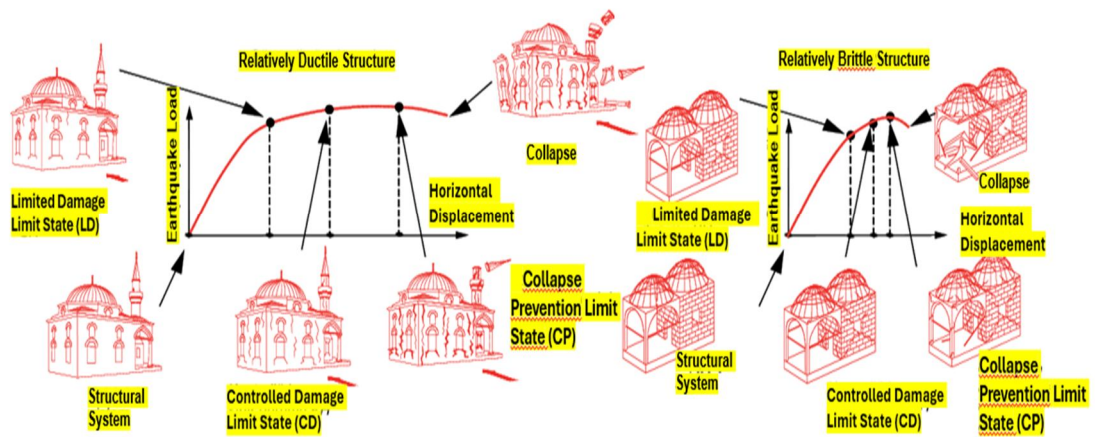


**Figure 3.4:** Performance Levels in Relatively Ductile And Brittle Structural Systems [23] .

### 3.3.2. FEMA 273, FEMA 356, ASCE 41 and Eurocode 8

FEMA 273 (1997) and FEMA 356 (2000) are guidelines developed by the Federal Emergency Management Agency in the United States to assess and improve the seismic performance of existing buildings. These documents provide comprehensive methodologies for evaluating structural and non-structural components of buildings, including masonry structures, under seismic loads. FEMA 273 introduces performance-based seismic evaluation, categorizing structural performance levels into "Operational," "Immediate Occupancy," "Life Safety," and "Collapse Prevention." FEMA 356 builds on these concepts, offering detailed procedures for nonlinear static (pushover) analysis and damage assessment, as well as repair and strengthening strategies tailored to various structural systems.

ASCE 41, the "Seismic Evaluation and Retrofit of Existing Buildings" standard published by the American Society of Civil Engineers, evolves from FEMA 356 and offers more refined and updated guidance. It introduces detailed performance objectives, including both structural and non-structural components, and provides threshold values for damage levels specific to material types, including masonry. ASCE 41 emphasizes nonlinear dynamic analysis for more accurate assessments and ensures compliance with modern engineering practices.

Eurocode 8, a European standard for the design of structures for earthquake resistance, provides comprehensive guidelines for new buildings as well as recommendations for assessing and retrofitting existing structures. It includes provisions specific to masonry buildings, focusing on material properties, allowable stresses, and deformation limits. Eurocode 8 categorizes damage levels into "No Damage," "Slight Damage," "Moderate Damage," and "Severe Damage," linking them to quantifiable parameters such as inter-story drift ratios, stress distributions, and crack widths. It also emphasizes the use of performance-based design and analysis to ensure that buildings meet specific safety and functionality requirements under seismic conditions.

Together, these guidelines and standards provide critical threshold levels and decision-making frameworks for assessing the vulnerability of masonry structures. They serve as essential references for engineers and researchers in developing restoration and strengthening strategies that comply with international best practices while addressing the specific challenges of seismic risk and material deterioration in historical buildings. The evaluation of performance levels for masonry structures according to different codes is summarized in **Table 3.5** to **Table 3.7**.

**Table 3.5:** Performance levels of masonry structures according to FEMA 273 and FEMA 356 [24].

Regulation	Structural Behaviour	Primary Elements: Immediate Occupancy (IO) (%)	Primary Elements: Life Safety (LS) (%)	Primary Elements: Collapse Prevention (CP) (%)	Secondary Elements: Life Safety (LS) (%)	Secondary Elements: Collapse Prevention (CP) (%)
FEMA 273	Shear	0.1	0.3	0.4	0.6	0.8
FEMA 273	Overturning	0.1	$0.3heff/L$	$0.4heff/L$	$0.6heff/L$	$0.8heff/L$
FEMA 356	Shear	0.1	0.3	0.4	0.6	0.8
FEMA 356	Overturning	0.1	$0.3heff/L$	$0.4heff/L$	$0.6heff/L$	$0.8heff/L$
heff = Height of the Lateral Force Application						
L = Height of the Column or Wall						

**Table 3.6:** Performance levels of masonry structures according to ASCE 41 [24].

		Performans Levels		
Regulations	Structural Behaviour	Immediate Occupancy (IO) (%)	Life Safety (LS) (%)	Collapse Prevention (CP) (%)
ASCE 41	Shear	0.1	0.75	1
ASCE 41	Overturning	0.1	0 / heff and <2.25%	100 $\Delta_{tc,r}$ /heff and <2.25%
heff = Height of the Lateral Force Application				
$\Delta_{tc,r}$ = Lateral Displacement Associated with the Onset of Cracking at the Base				

**Table 3.7:** Performance levels of masonry structures according to Eurocode 8 [24].

Regulation	Structural Behaviour	Primary Elements: Damage Limitation (DL) (%)	Primary Elements: Significant Damage (SD) (%)	Primary Elements: Collapse Prevention (CP) (%)	Secondary Elements: Significant Damage (SD) (%)	Secondary Elements: Collapse Prevention (CP) (%)
Eurocode 8	In-Plane (Shear Controlled)	-	0.40H <sub>o</sub> /D	0.53H <sub>o</sub> /D	0.60H <sub>o</sub> /D	0.80H <sub>o</sub> /D
Eurocode 8	Out-of-Plane (Flexure Controlled)	-	0.80H <sub>o</sub> /D	1.06H <sub>o</sub> /D	1.20H <sub>o</sub> /D	1.60H <sub>o</sub> /D
H <sub>o</sub> = Distance Between the Section Where Flexural Capacity is Achieved and the Point of Reverse Curvature						
D = Planar Horizontal Dimension (Depth) of the Wall						

## **4. SHM AT OSHKI CHURCH, ERZURUM**

### **4.1. History of Erzurum Oshki Church**

Erzurum, a historic crossroads of cultures and civilizations, has long served as a social, cultural, and strategic centre. Over the centuries, it has preserved cultural traces left by each civilization that inhabited it. Due to its geographical location and geopolitical importance, Erzurum fell under the influence of several prominent empires, including the Assyrians, Sasanians, Persians, Arabs, Romans, and Byzantines, and has remained one of the most significant cities in the region throughout history.

In 979, as a reward for the support provided to the Byzantine Empire, the plains of Erzurum and the region of Pasinler were granted to the Kingdom of Bagratids, which already controlled the areas of İspir and Oltu. After the death of King David of the Bagratids, the territories under Bagratid rule were incorporated into the Byzantine Empire. Following the Battle of Manzikert, the Saltukids—who established the first Turkish state in Eastern Anatolia—took control of the Erzurum and Kars regions.

During the Mongol invasions in Anatolia, Erzurum briefly came under the rule of the Ilkhanids and later the Eretnids. After the collapse of the Ilkhanate in 1336, Erzurum experienced nearly 200 years of conflict and devastation until it was conquered by the Ottoman Empire in 1514. The Ottomans ruled Erzurum and its surroundings until the establishment of the Republic of Turkey in 1923.

Erzurum, covering an area of 25,066 square kilometres, ranks as Turkey's fourth-largest province and the largest in the Eastern Anatolia Region. Geographically, about 30% of Erzurum lies in the Eastern Black Sea Region, while the remaining 70% is within Eastern Anatolia. The province is bordered by Rize to the north, Ağrı to the east, Erzincan to the west, Artvin, Ardahan, and Kars to the northeast, Bayburt to the northwest, Muş to the south, and Bingöl to the southwest. Erzurum consists of a total of 20 districts, 3 of which are central districts.

Erzurum's city center sits at an elevation of 1,852 meters above sea level. The southern part of Erzurum features rugged terrain due to the Karasu-Aras Mountains. In this

region, the Palandöken, Şahvelet, and the northern half of the Bingöl Mountains are prominent. To the north of Erzurum lie the secondary mountain ranges of the Northern Anatolian Mountains, with notable peaks including the Mescid Mountains between İspir and Erzurum, the Kargapazarı Mountains to the east, and the Allahu Ekber Mountains, partially extending to the Kars border.

Between these northern and southern mountain ranges are expansive plains, namely the Erzurum and Pasinler plains. The lowest point of the Erzurum Plain is 1,850 meters, while that of the Pasinler Plain is 1,650 meters.

Erzurum holds a strategically significant position in terms of commerce, military, and economy, making it a site where people have settled and left numerous artifacts since the earliest historical periods. Among these invaluable structures is the Oshki Church in Erzurum (**Figure 4.1**). Located in the village of Camliyamac in the Uzundere district of Erzurum, the church is situated 50 km north of Erzurum's Tortum district and 13 km off the Erzurum-Artvin highway. The church, along with the accompanying library and refectory, constitutes the Oshki Monastery complex. The renowned Georgian historian and archaeologist Ekvtime Takaishvili states that the monastery was initially built as a monastic community comprising a library and refectory. However, these structures are currently in a fragile state, barely standing.



**Figure 4.1:** General View of Erzurum Oshki Church [25].

The construction date of the Erzurum Oshki Church is indicated by two important Georgian inscriptions. The first is situated on the pediment of the door on the southern cross arm, while the second is positioned beneath the 'Presentation of the Temple' depiction on the same arm. According to these inscriptions, the church was commissioned by the sons of King Adarnase III (d. 961), Bagrat (d. 966), and David the Great Kuropalat (d. 1001). Takaishvili, analysing the inscription over the southern entrance, suggests that the church was built between 958 and 966 by an architect named "Grigor of Oshki"; he further interprets that the construction was initiated by King Adarnase III, but, following the king's death in 961, was completed during the reign of his son, King Magistros Bagrat (961-966) (Özkan, 2010). The renowned Georgian historian Wachtang Djobadze, on the other hand, asserts that construction began on March 25, 963, and, based on the inscription near the angel figure on the eastern pediment indicating a ten-year construction period, claims that the church was completed in 973 [25] (Figures 4.2-4.3).

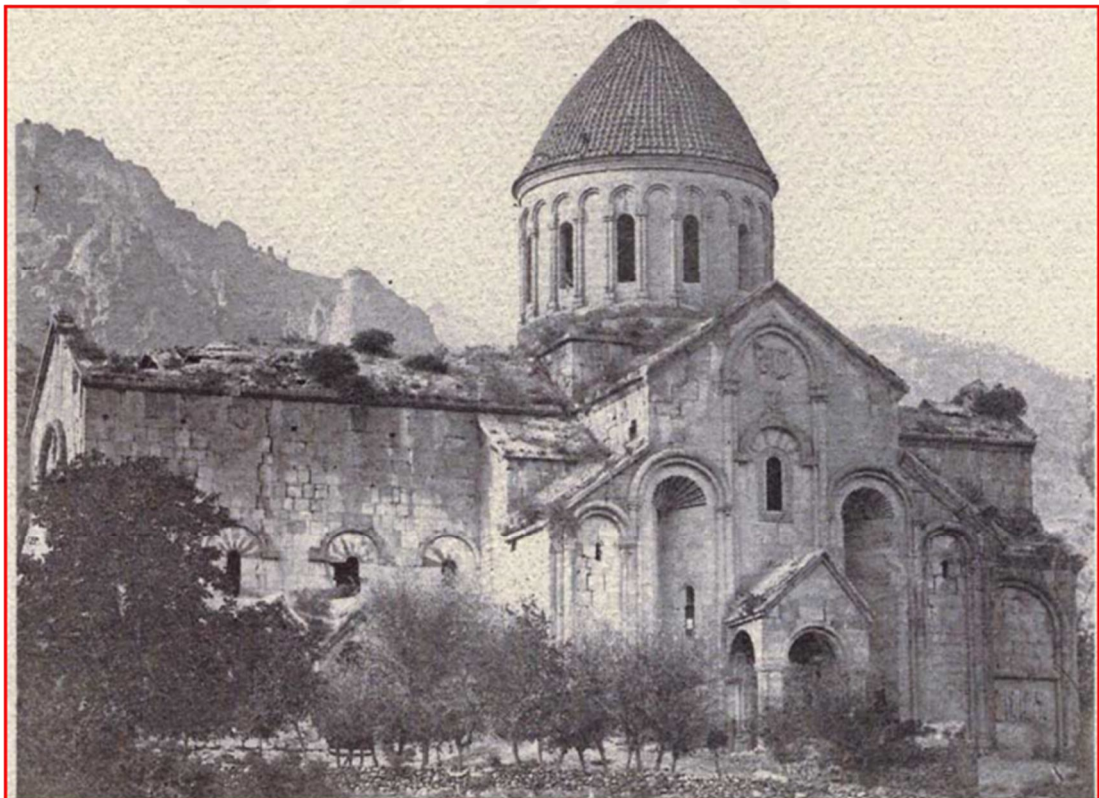


**Figure 4.2:** External View of Erzurum Oshki Church In Historical Photographs [25].

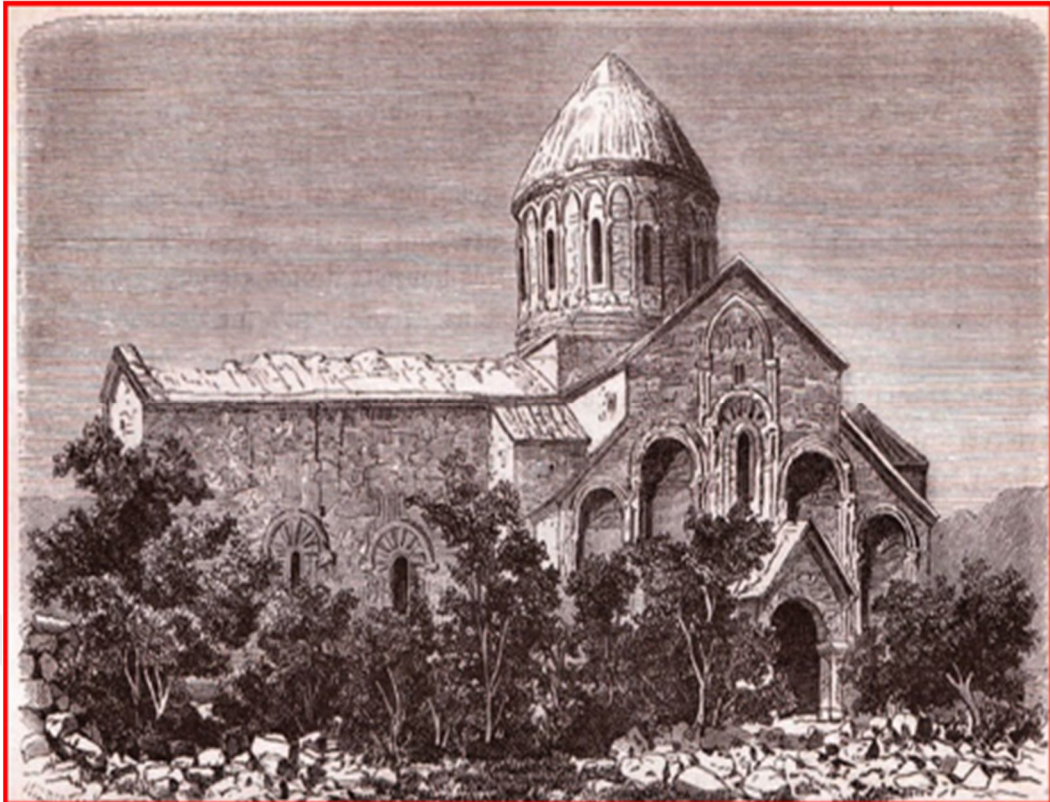


**Figure 4.2 Continued:** External View of Erzurum Oshki Church In Historical Photographs” [25].



**Figure 4.3:** Internal View of Erzurum Oshki Church In Historical Photographs [25].

## 4.2. Plan and Architectural Features

The Oshki Church has external dimensions of 29.70 x 43.80 meters and is designed in a cruciform shape. The square central area is covered with a conical dome supported by four main structural columns, each approximately two meters in diameter. This square-centered space is expanded by the arms of the cross extending in four directions. In the eastern arm of the cross lies a semicircular apsis. The naos, which forms the main worship area of the church, and the arms of the cross are arranged as a single-story structure. The Oshki Church features a hybrid plan that combines triconch and basilica layouts, with the naos section designed in the form of a closed Greek cross. By extending the three arms (except for the western arm) with semicircular domes, a triconch layout is achieved. The western arm, with its rectangular extension, exhibits basilical characteristics. The spaces adjacent to the apsis, known as pastophorion cells, along with the areas on either side of the northern and southern exedras, and the section located north of the western cross arm, are arranged as two-story structures. An architectural order is displayed on the facades, with similar features repeated with slight variations, except for the western facade. These facades are enlivened with five large pilasters resembling columns, arranged in arches. The central arch is higher than the others, giving the facade a tiered appearance that gradually decreases in height from the center outward.

The naos section, forming the primary worship area of the church, and the arms of the cross are arranged as a single-story structure. Conversely, the pastophorion cells near the apsis, the areas flanking the northern and southern exedras, and the section situated north of the western arm of the cross are constructed with two stories. An architectural order featuring similar characteristics, with minor variations, is displayed on all facades except the western one. These facades are enlivened by five arches formed by large moldings resembling pilasters. The central arch is set higher than the others, giving the facade a tiered appearance that gradually decreases in height toward the sides (**Figures 4.4-4.7**).



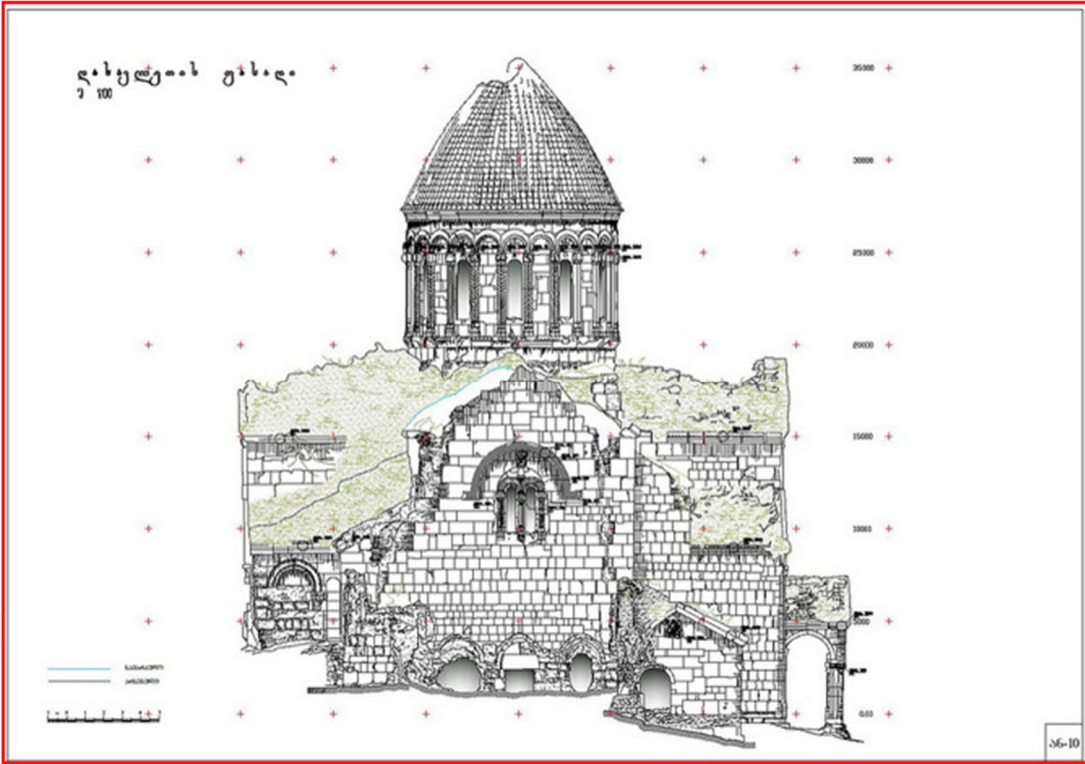


Figure 4.6: West side view of Erzurum Oshki Church [25].

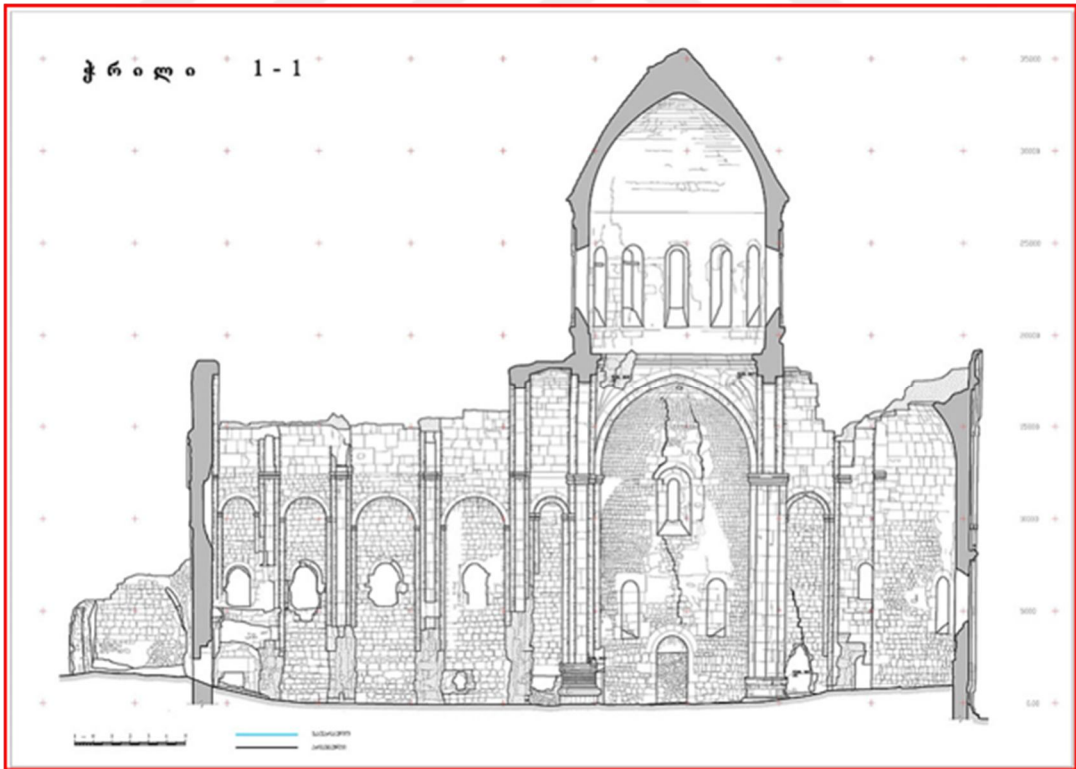


Figure 4.7: Longitudinal Section of Erzurum Oshki Church [25].

### **4.3. Observed Damages in the Structure of Erzurum Oshki Church**

In determining the seismic behaviour of historical structures, it is essential first to identify the characteristics of the structural system. Additionally, it is necessary to investigate structural issues, construction details, and any previous damage, repairs, or reinforcements. As a result, this part of the study concentrates on identifying structural problems observed on-site in the historic Oshki Church and researching its construction features.

Due to environmental conditions, neglect, and abandonment, a variety of damages can be observed in the structure. The roof on the western facade has completely collapsed, leaving the structure exposed and unprotected. Cracks of varying sizes have developed in different areas, particularly on the upper sections of the walls and around the main dome. Notably, a significant crack runs along the height of the wall where the western and southern facades meet, especially on the western side. In its current state, this crack, resulting from the substantial separation between the western and southern walls, poses the greatest structural threat. The crack runs vertically from the top of the wall to its foundation. On-site data indicate that the crack width spans from 2 cm to 30 cm, implying a structural detachment between the southern and western walls. Similar damage was observed in the southern section, resembling the issues found in the northern section. It was noted that certain vault sections, particularly those on the southern facade, which aid in load transfer, have collapsed, leading to issues in load transmission to the foundation.

In the interior, particularly in the lower sections, material losses and collapses near the entrance areas are noticeable. Joint gaps resulting from environmental factors are also evident. These gaps, which have spread throughout the structure over time, have caused parts of the church to separate, with the materials composing the structure showing localized deterioration. Additionally, joint gaps and material losses have allowed rain and snow to penetrate the structure, resulting in decay of the original stones and the growth of vegetation on the stone surfaces. Some of the damages observed in various parts of the structure are illustrated in **Figures 4.8-4.12**.



**Figure 4.8:** The Crack on the Western Facade of the Church and the Completely Collapsed Roof Section.



**Figure 4.9:** Damages Observed on the Main Dome and Eastern Facade of the Church.



**Figure 4.10:** Some Cracks Observed on the Exterior Facade of the Structure.



**Figure 4.11:** The Damaged Dome and Apse Section on the Interior Facade of the Structure.



**Figure 4.12:** Some Damages Observed on the Interior Facade of the Structure.

#### **4.4. Installation of SHM Devices**

SHM is a comprehensive system that has recently gained widespread use globally in the fields of civil and earthquake engineering. Through advanced technological devices and sensors, SHM allows for the real-time monitoring of structures. In other words, SHM can be defined as a method of continuously or periodically monitoring a structure based on specific indicators, analysing crucial structural parameters (both static and dynamic) obtained from this monitoring. The first SHM systems were developed and put into use at the beginning of the 20th century. With advancements in communication and information technology, health monitoring systems have made significant progress, and the advent of digital, portable monitoring devices has led to the widespread adoption of SHM.

The Erzurum Oshki Church has been scheduled for examination as part of a restoration project conducted by the Ministry of Culture and Tourism, General Directorate of Cultural Heritage and Museums, and Erzurum Directorate of Surveying and Monuments, with the aim of preserving its structural integrity and historical value. To support this examination, a 12-month monitoring study has been proposed to understand the dynamic characteristics of the structure at the start of the restoration

and to assess the progression of observed damages. To observe the current state of damage in the church's load-bearing system, crack gauges, two biaxial inclinometers, a thermometer for indoor temperature monitoring, a hygrometer for humidity measurement, and a triaxial accelerometer to monitor dynamic effects have been installed (**Figure 4.13**). The crack gauges were positioned inside the church to track the progression of cracks at various levels. The inclinometers and accelerometer were installed on the upper sections of the church walls, while the temperature sensor was placed in the pastophorion room.



**Figure 4.13:** Some visuals of SHM Equipment .



**Figure 4.13 Continued:** Some visuals of SHM Equipment”.

As a result of the inspection studies conducted in the church, SHM equipment was placed in locations where the maximum amount of data could be obtained. During the placement of the instruments, the church walls were numbered (**Figure 4.14**). After the instruments were installed, each was assigned a number, and their interactions were monitored through an online platform. The detailed placement of the SHM instruments on the church is shown in **Figure 4.15**.

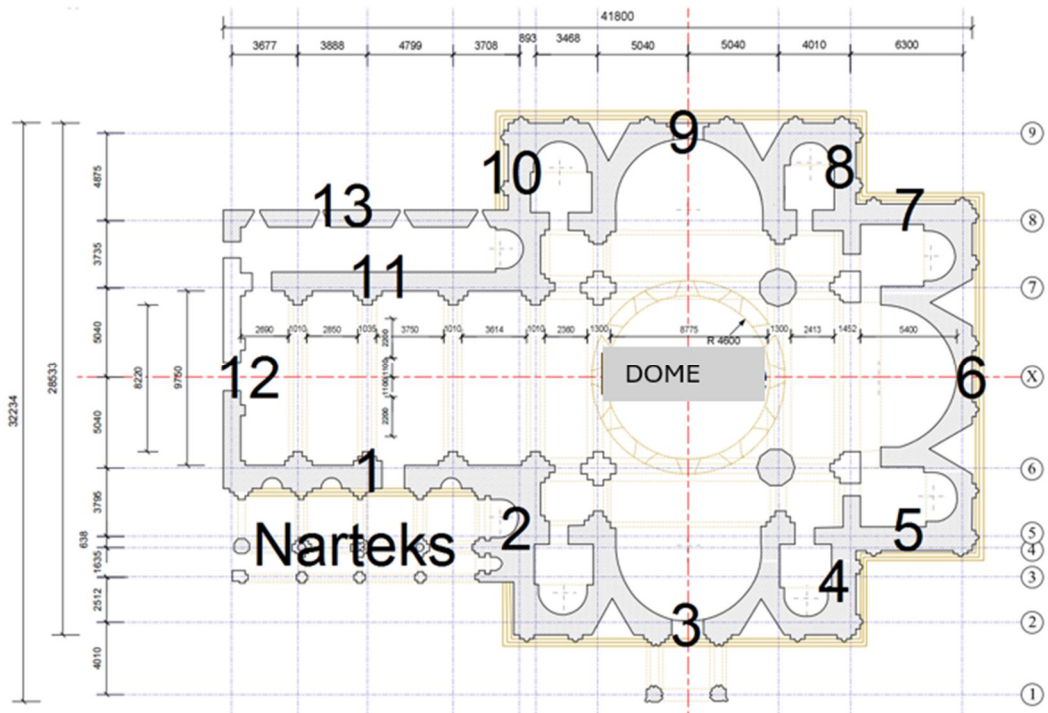


**Figure 4.14:** Wall numbering study conducted within the scope of SHM work

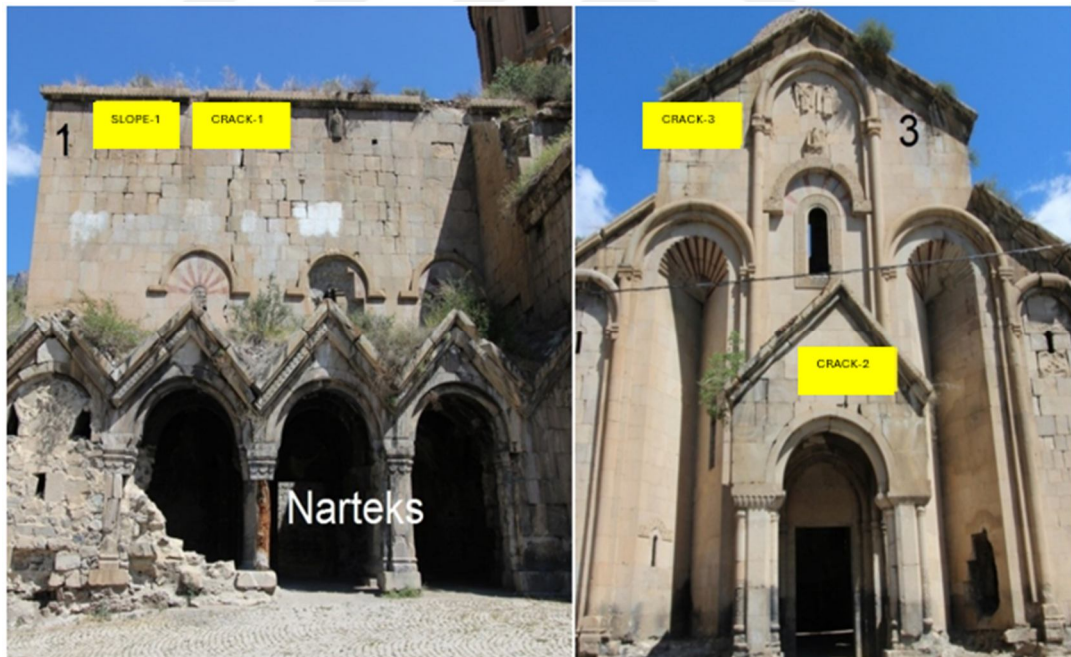


**Figure 4.15:** Placement detail of SHM equipment

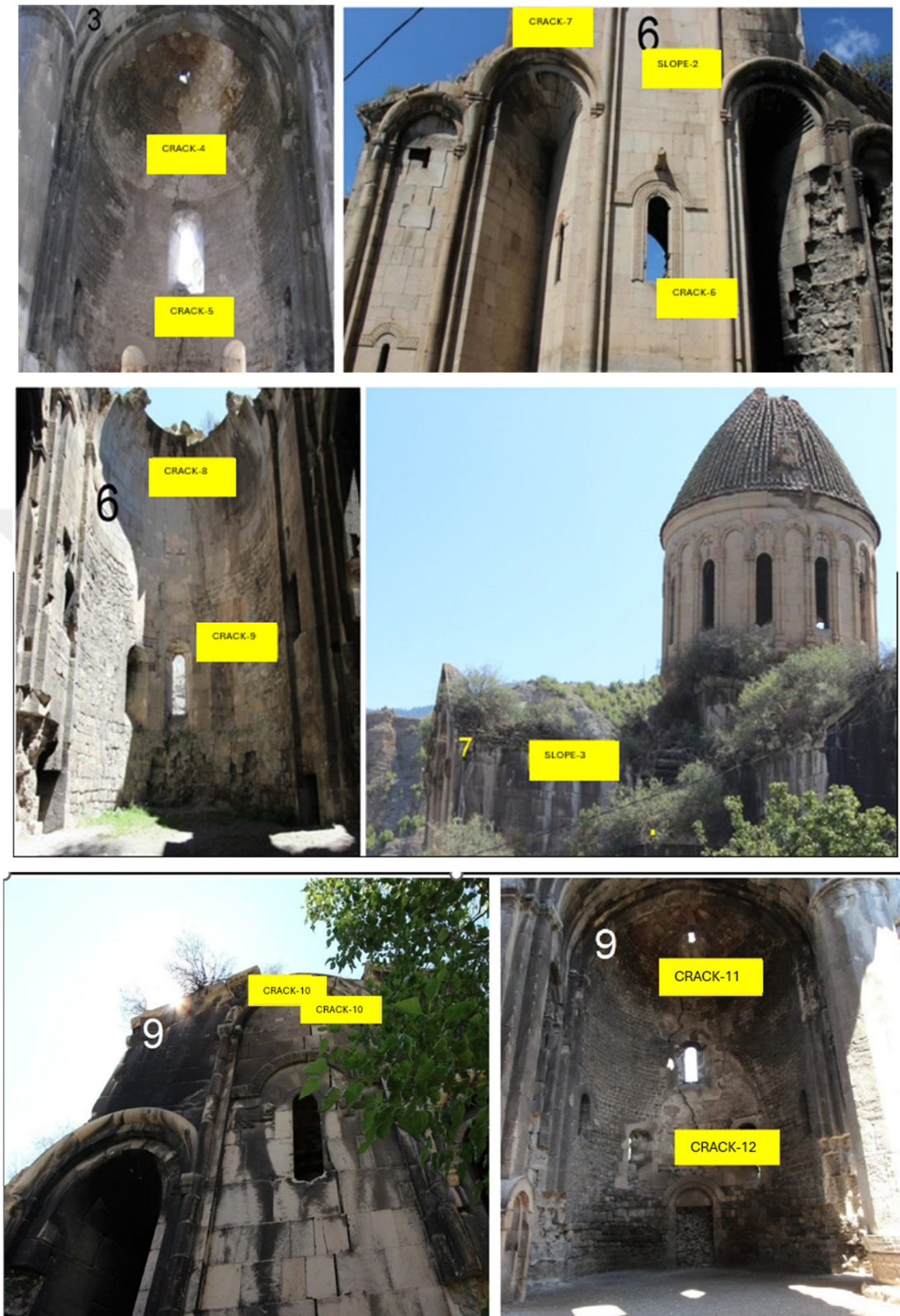


**Figure 4.15 Continued:** Placement detail of SHM equipment.

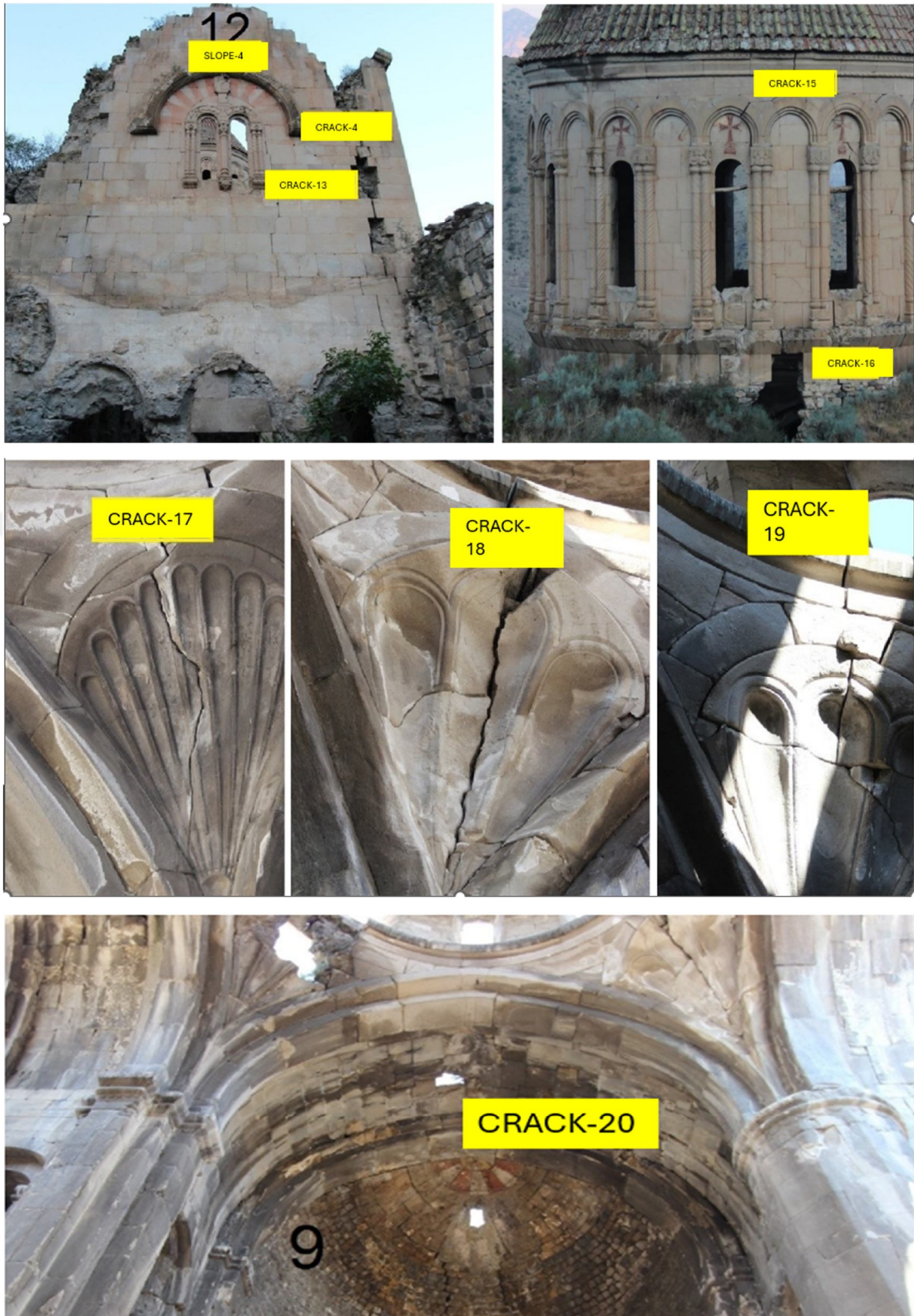


**Figure 4.15 Continued:** Placement detail of SHM equipment

## 5. DECISION-MAKING FOR RESTORATION

The process of decision-making for restoration is crucial in ensuring that structural interventions are both effective and sensitive to the historical and cultural significance of the church. In the case of the Oshki Church, detailed SHM was conducted to assess the current condition, identify existing damage, and evaluate its overall structural performance. Based on the data collected from sensors and visual inspections, several critical decisions were made regarding restoration and strengthening measures.

The monitoring results highlighted key areas of concern, such as material degradation, deformation, and localized structural weaknesses, which required immediate attention. For example, certain sections of the masonry exhibited signs of cracking and displacement due to historical seismic events and environmental factors. The SHM data revealed that these damages were within tolerable limits according to international guidelines, but they were close to exceeding the thresholds for safety and longevity.

Following the analysis of these findings, the decision-making process for restoration involved a combination of preservation techniques and structural reinforcement. Key decisions included:

1. **Strengthening of Load-Bearing Capacity of the Walls:** Based on the data showing significant deformations in the load-bearing walls, it was decided that these areas should be reinforced with hydraulic lime based injection mortar to enhance their seismic resilience while maintaining the aesthetic integrity of the church.
2. **Crack Repair and Stabilization:** The presence of cracks in certain masonry sections was addressed through targeted stabilization techniques, including the use of injection grouting and localized repointing of mortar joints. This intervention was aimed at halting further deterioration and preventing the spread of damage.
3. **Completion of Incomplete Sections and Ensuring Structural Integrity:** One of the key recommendations was to complete incomplete sections of the building, particularly where portions of the masonry had been damaged or

removed over time. These sections were restored to ensure continuity and structural integrity. By reinforcing these areas, the overall structural cohesion of the building was achieved, reducing vulnerabilities and enhancing its overall resilience.

4. **Monitoring System Upgrade:** Given the importance of continuous data collection, a decision was made to upgrade the SHM system to include more advanced sensors capable of monitoring real-time conditions and providing early warning signs of potential future damage.
5. **Preservation of Historical Features:** While structural interventions were necessary, special care was taken to ensure that any modifications or additions did not compromise the church's historical and architectural features. All restoration work was carried out in compliance with preservation standards and in consultation with heritage experts to maintain the church's cultural significance.

These decisions were made based on a comprehensive analysis of the monitoring data, ensuring that the restoration efforts would not only restore the structural integrity of the Oskhi Church but also preserve its historical value for future generations. The combination of advanced SHM techniques and careful decision-making highlights the importance of data-driven restoration strategies in maintaining the safety, sustainability, and cultural heritage of historical structures.

## **5.1. Evaluation of Data Obtained from Crack Meters**

To monitor the widening of 20 cracks identified on the church walls, a displacement gauge was placed perpendicular to each crack. By measuring the displacement changes between the fixed points on either side of the cracks, the movement characteristics of these cracks over the monitoring period will be determined. The time series, where the first recorded data is taken as the reference, are presented in **Figure 4.16-4.35**.

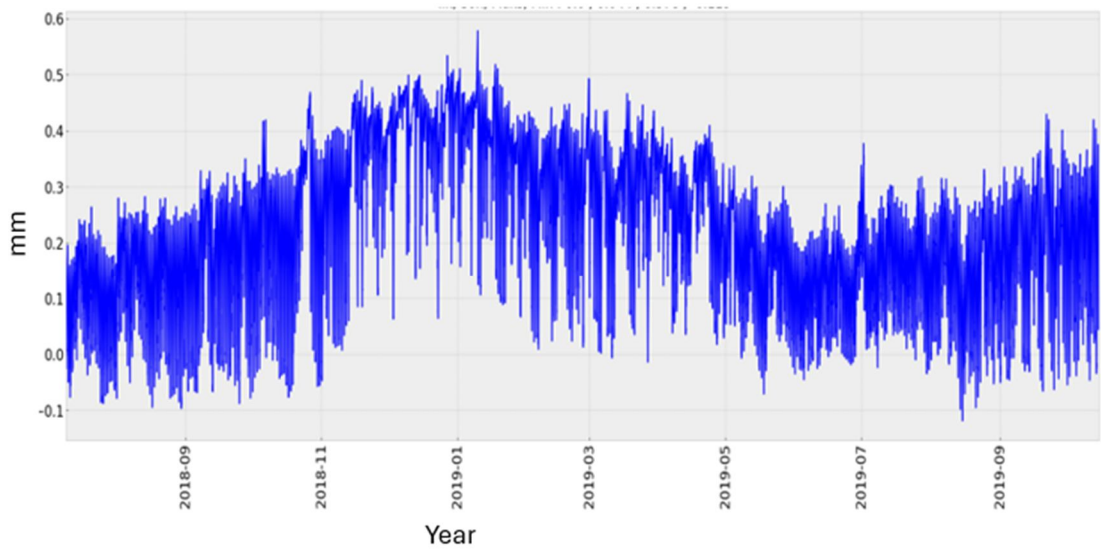


**Figure 5.16:** Crack 1 first & last data time : 2018\_0709-11:20:00&2019\_1015-11:00:00 First ,last ,max. ,min.: 0.0 , 0.044 , 0.578 , -0.119

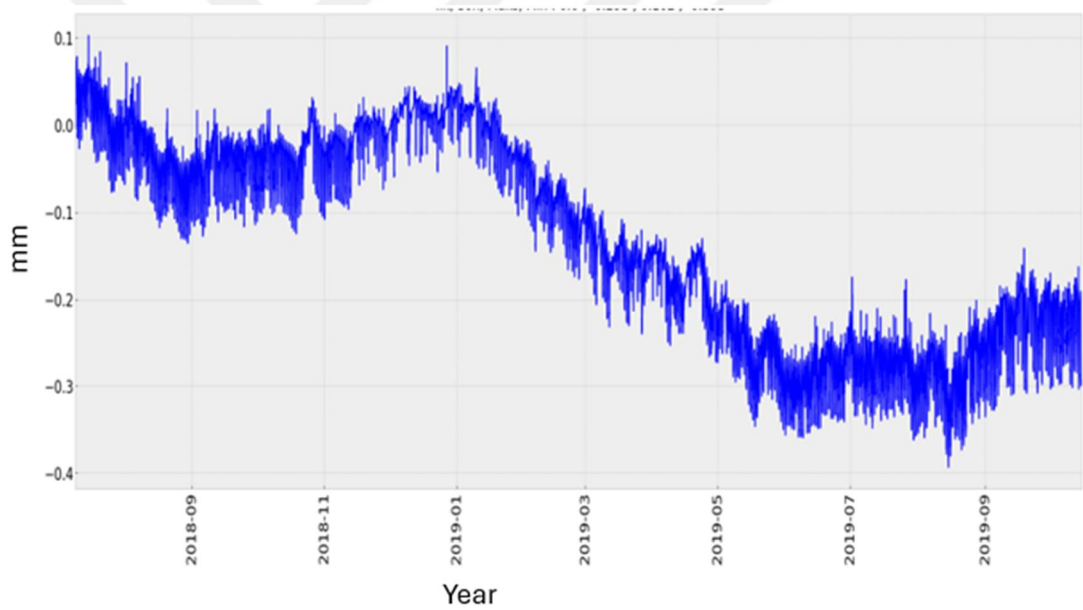


**Figure 5.17:** Crack 2 first & last data time : 2018\_0709-11:20:00&2019\_1015-11:00:00 First ,last ,max. , min. : 0.0 , -0.293 , 0.102 , -0.393

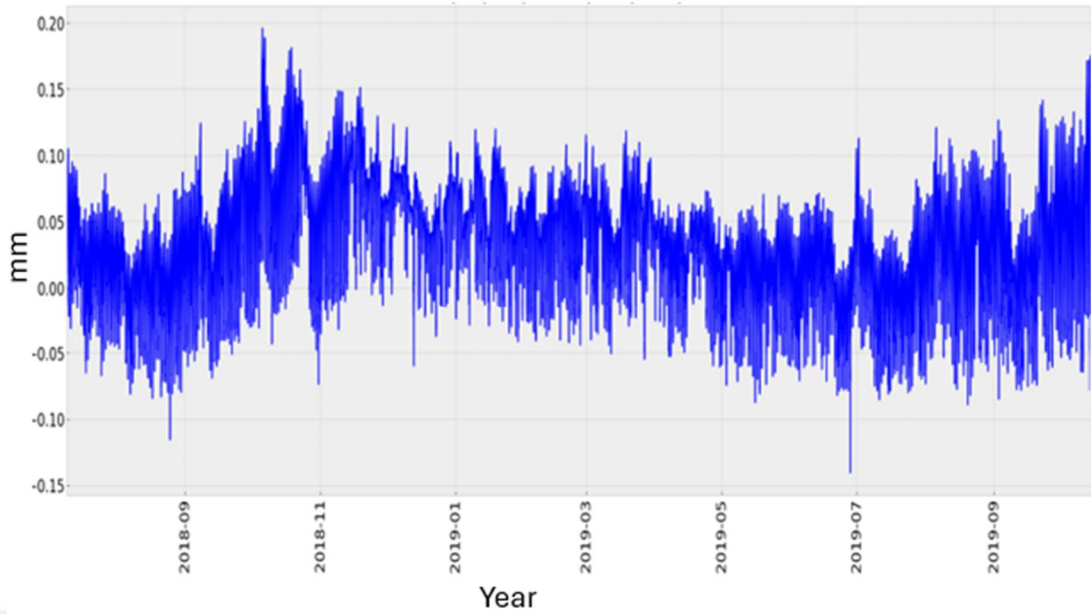


**Figure 5.18:** Crack 3 first & last data time : 2018\_0709-11:20:00&2019\_1015-11:00:00 First ,last, max. ,min. : 0.0 , -0.02 , 0.196 , -0.141

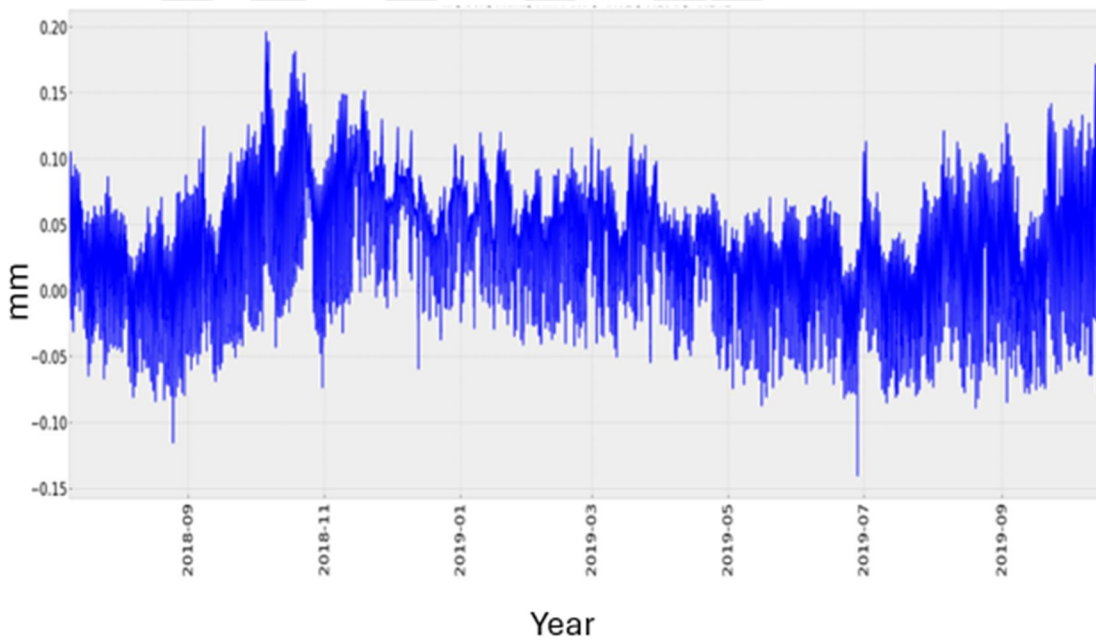


**Figure 5.19:** Crack 4 first & last data time : 2018\_0709-11:20:00&2019\_1015-11:00:00 First , last ,max. ,min. : 0.0 , -0.02 , 0.196 , -0.141

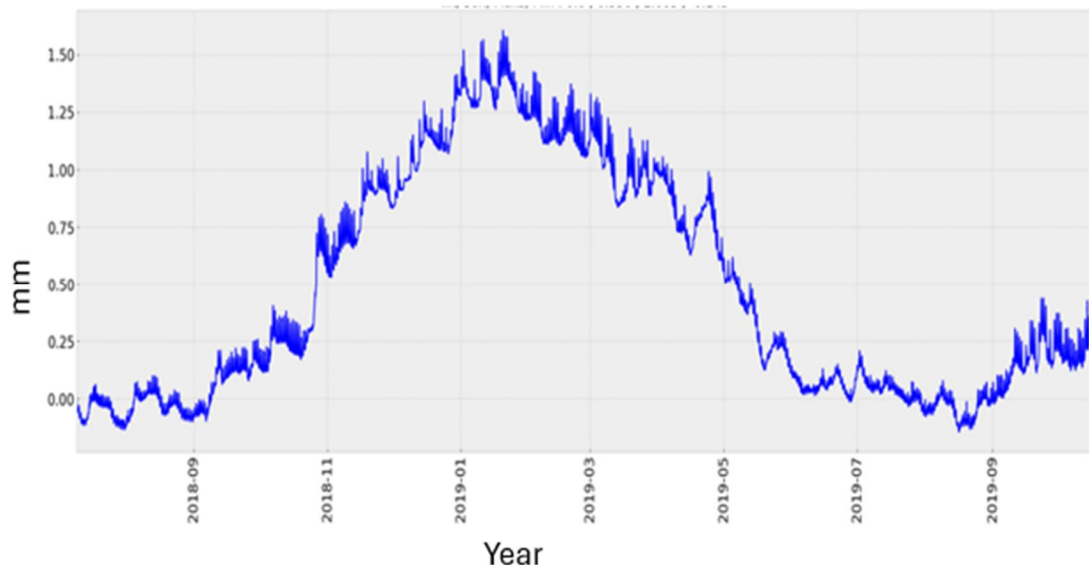


**Figure 5.20:** Crack 5 first &last data time : 2018\_0709-11:20:00&2019\_1015-11:00:00 First , last ,max. ,min. : 0.0 , 0.356 , 1.605 , -0.145

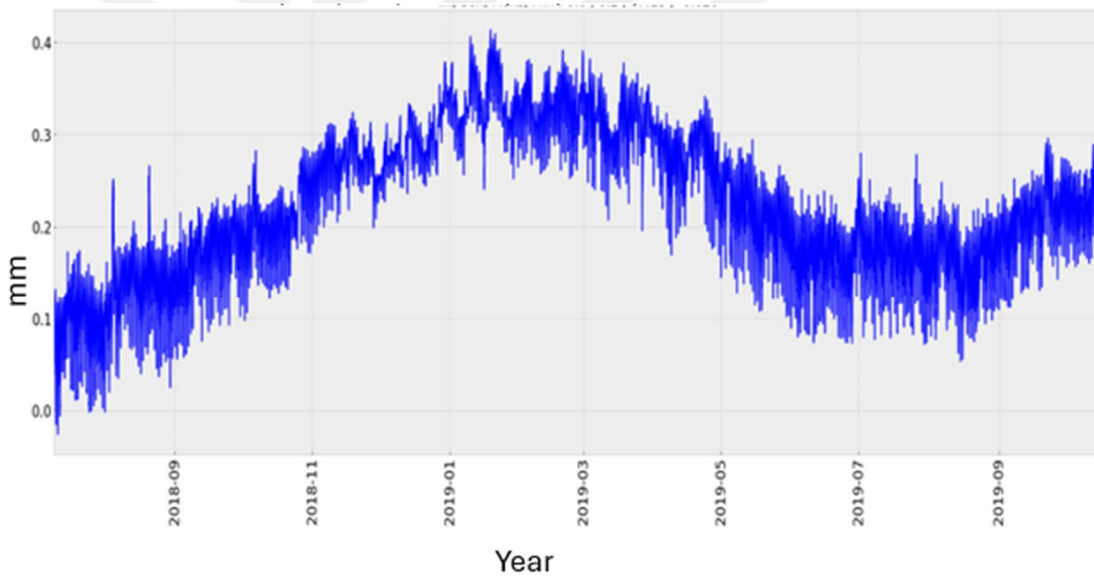


**Figure 5.21:** Crack 6 first &last data time : 2018\_0709-11:20:00&2019\_1015-11:00:00 First , last ,max. ,min. : 0.0 , 0.2 , 0.413 , -0.026

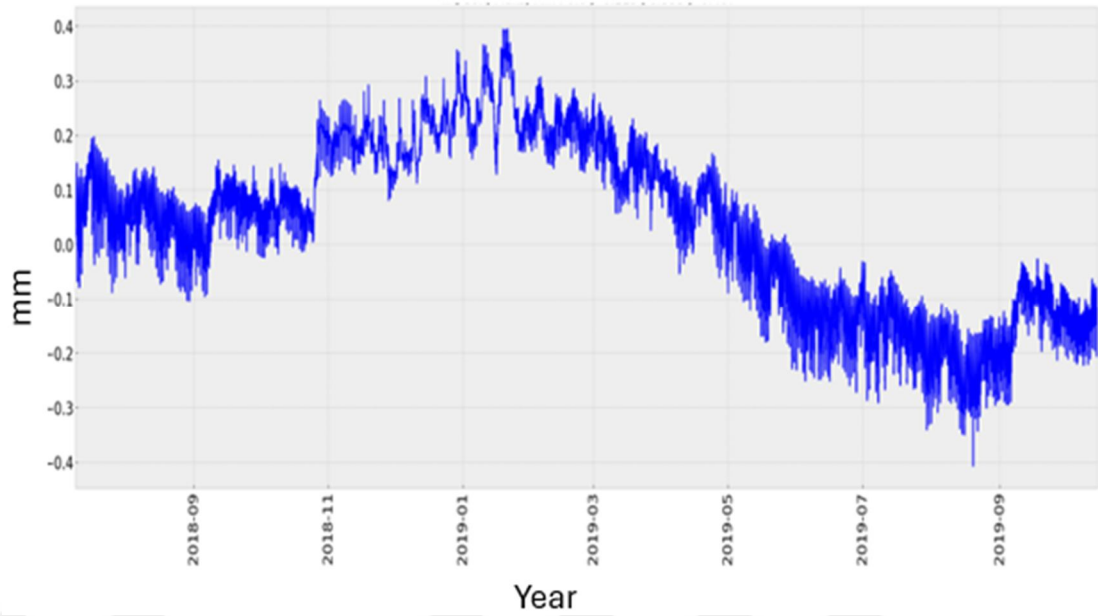


**Figure 5.22:** Crack 7 first &last data time : 2018\_0709-11:20:00&2019\_1015-11:00:00 First , last ,max. ,min. : 0.0 , -0.119 , 0.395 , -0.407

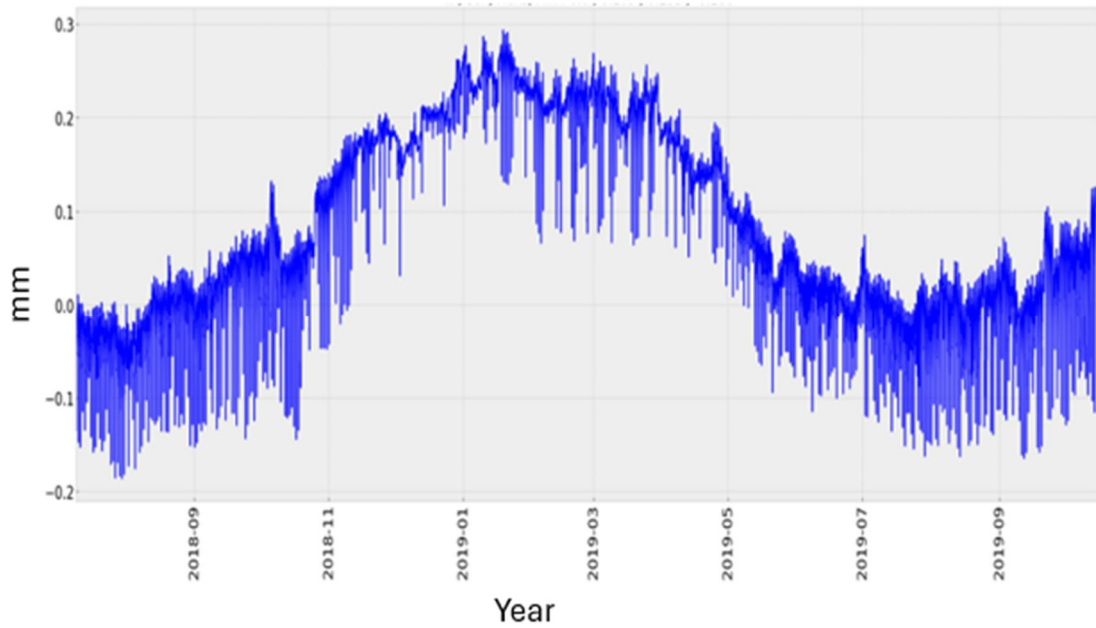


**Figure 5.23:** Crack 8 first &last data time : 2018\_0709-11:20:00&2019\_1015-11:00:00 First , last ,max. ,min. : 0.0 , 0.105 , 0.293 , -0.186

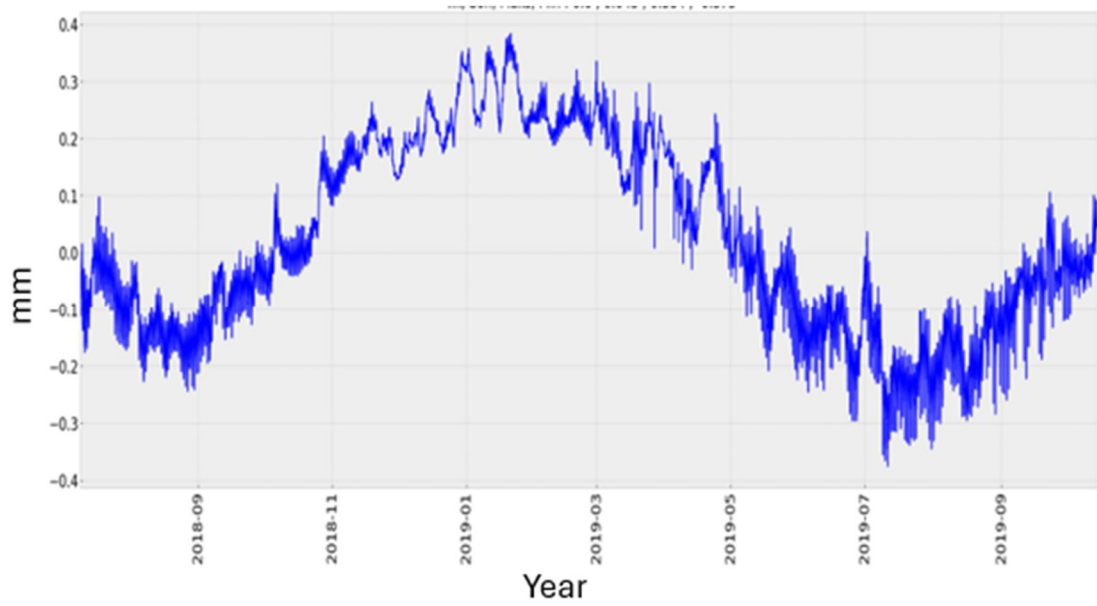


**Figure 5.24:** Crack 9 first &last data time : 2018\_0709-11:20:00&2019\_1015-11:00:00 First , last ,max. ,min. : 0.0 , 0.045 , 0.384 , -0.375

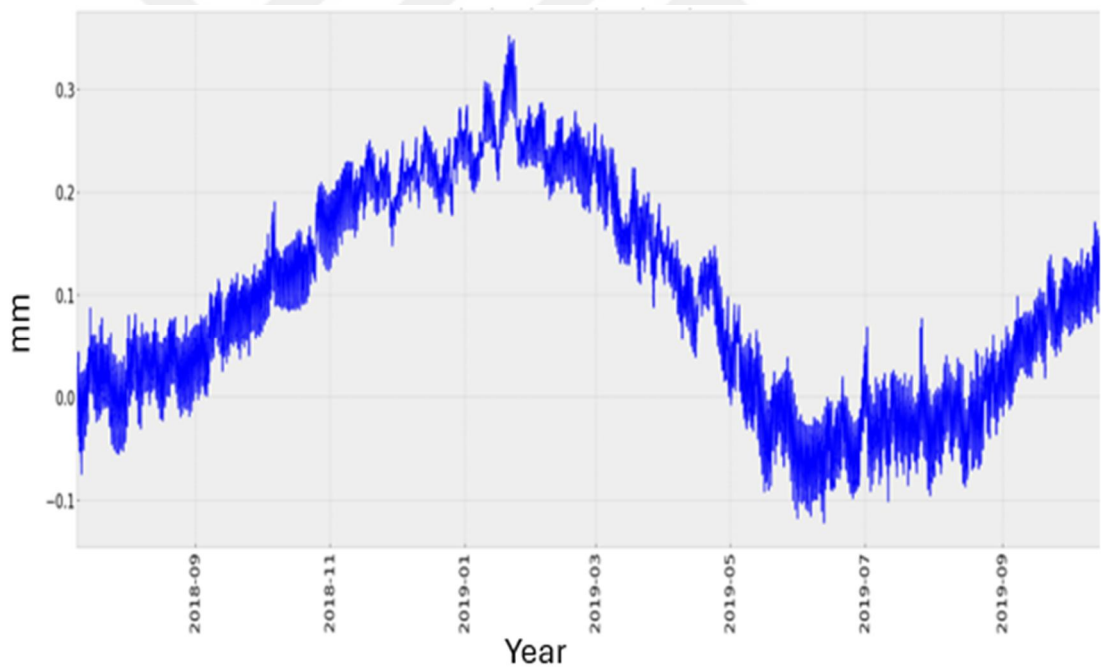


**Figure 5.25:** Crack 10 first &last data time : 2018\_0709-11:20:00&2019\_1015-11:00:00 First , last ,max. ,min. : 0.0 , 0.105 , 0.351 , -0.122

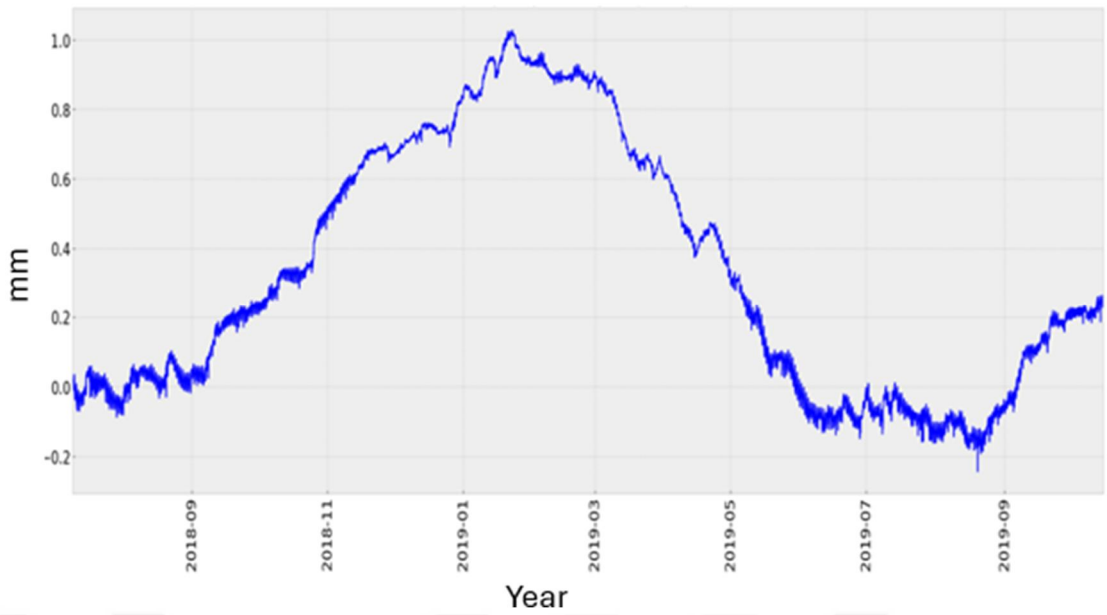


**Figure 5.26:** Crack 11 first &last data time : 2018\_0709-11:20:00&2019\_1015-11:00:00 First , last ,max. ,min. : 0.0 , 0.23 , 1.027 , -0.243

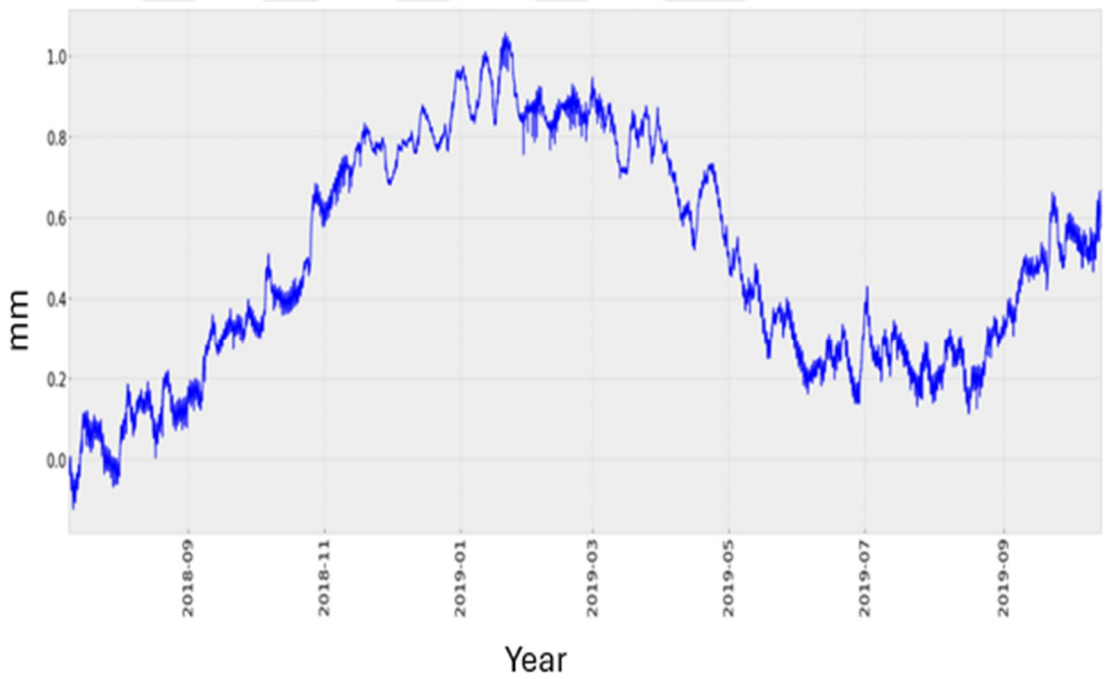


**Figure 5.27:** Crack 12 first &last data time : 2018\_0709-11:20:00&2019\_1015-11:00:00 First , last ,max. ,min. : 0.0 , 0.581 , 1.056 , -0.123

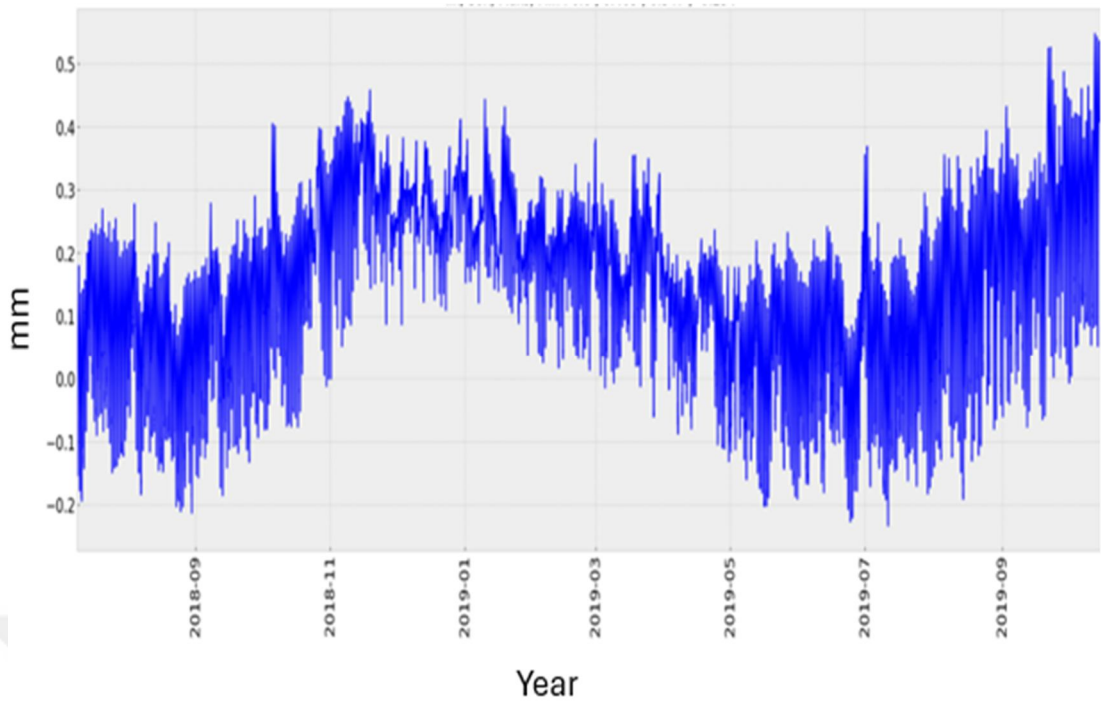


**Figure 5.28:** Crack 13 first &last data time : 2018\_0709-11:20:00&2019\_1015-11:00:00 First , last ,max. ,min. : 0.0 , 0.409 , 0.547 , -0.234

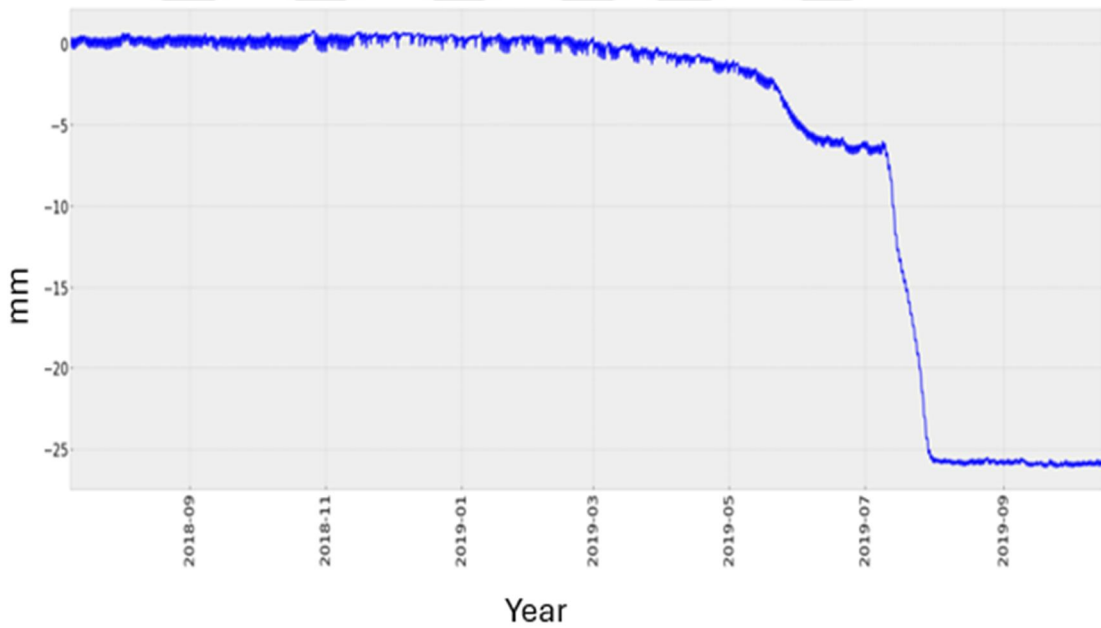


**Figure 5.29:** Crack 14 first &last data time : 2018\_0709-11:20:00&2019\_1015-11:00:00 First , last ,max. ,min. : 0.0 , -25.943 , 0.783 , -26.129

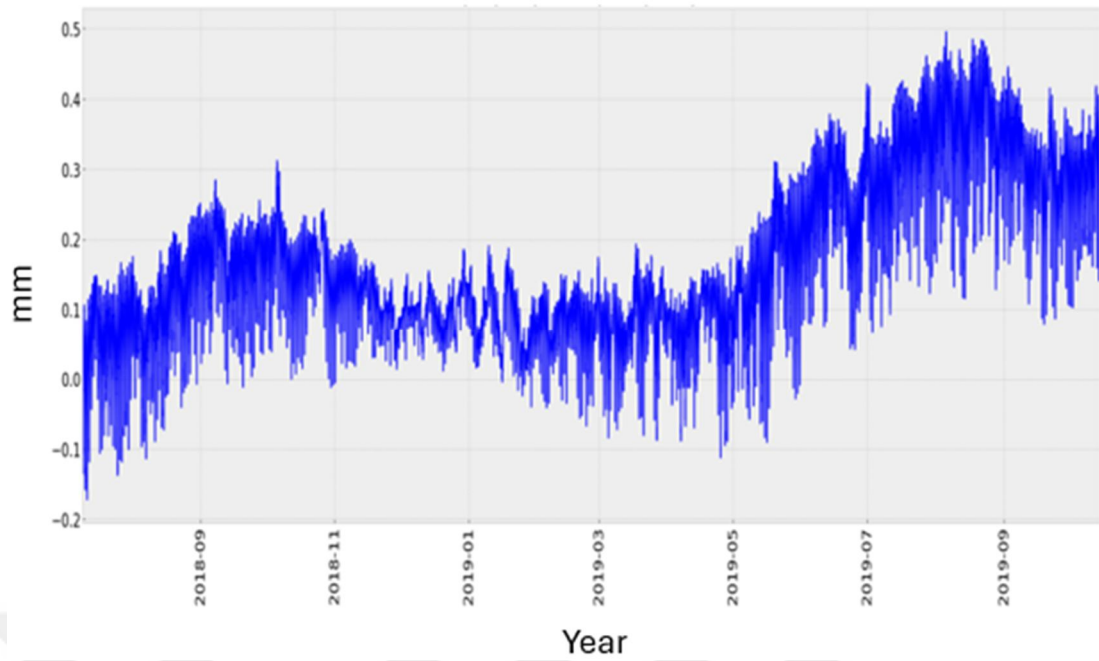


**Figure 5.30:** Crack 15 first &last data time : 2018\_0709-11:20:00&2019\_1015-11:00:00 First , last ,max. ,min. : 0.0 , 0.296 , 0.495 , -0.172

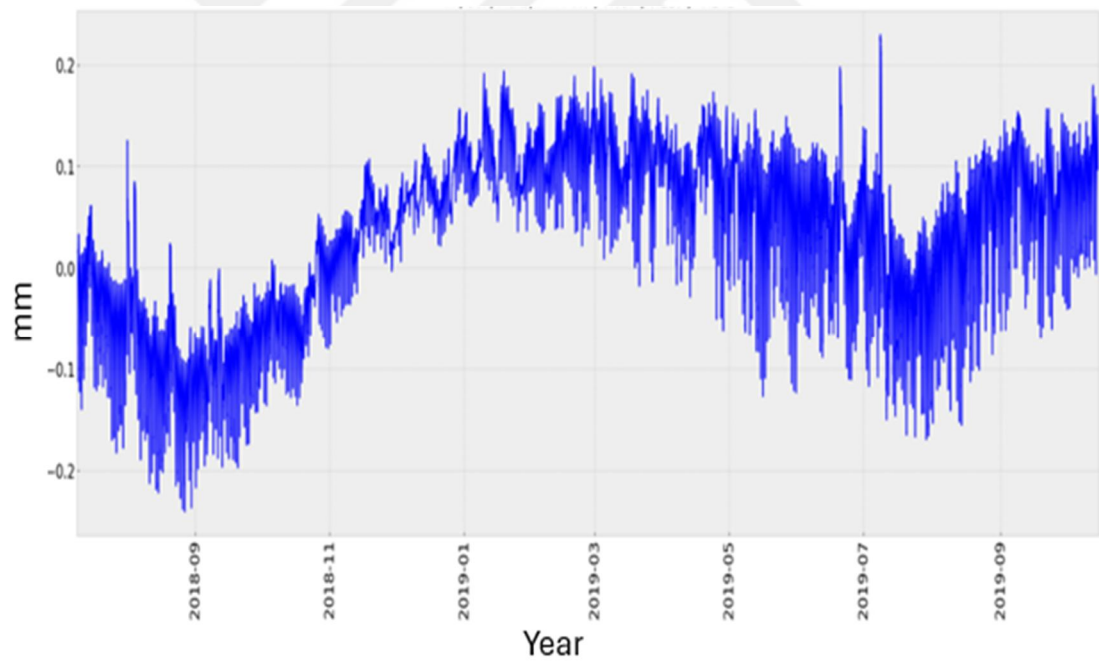


**Figure 5.31:** Crack 16 first &last data time : 2018\_0709-11:20:00&2019\_1015-11:00:00 First , last ,max. ,min. : 0.0 , 0.097 , 0.229 , -0.241

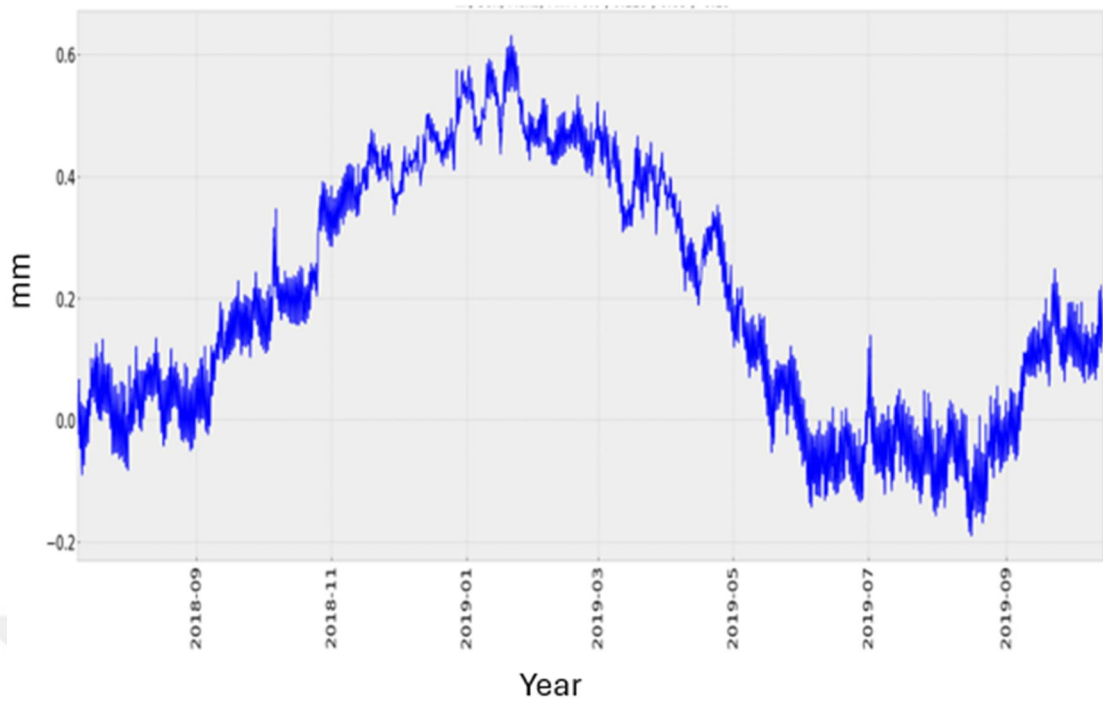


**Figure 5.32:** Crack 17 first &last data time : 2018\_0709-11:20:00&2019\_1015-11:00:00 First , last ,max. ,min. : 0.0 , 0.129 , 0.63 , -0.19

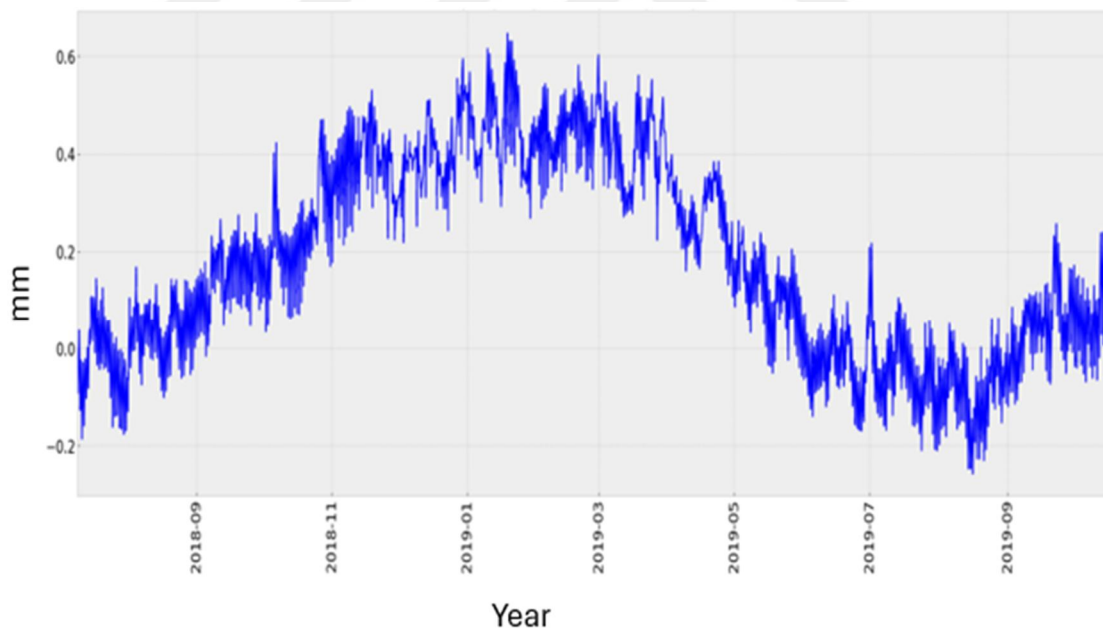


**Figure 5.33:** Crack 18 first &last data time : 2018\_0709-11:20:00&2019\_1015-11:00:00 First , last ,max. ,min. : 0.0 , 0.156 , 0.647 , -0.258

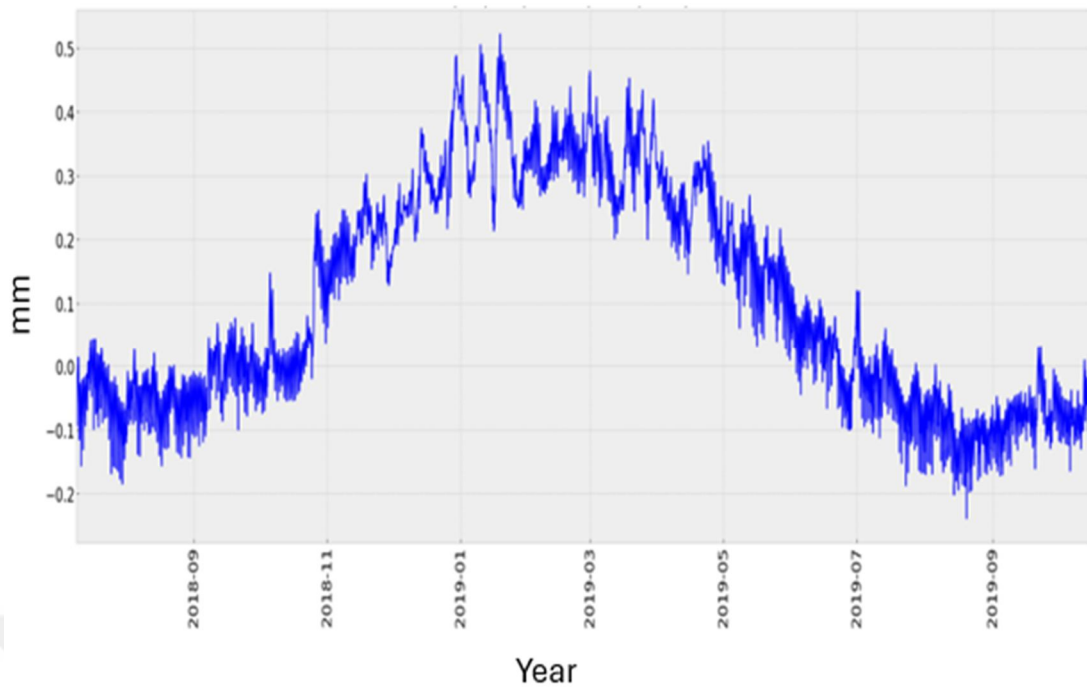


**Figure 5.34:** Crack 19 first &last data time : 2018\_0709-11:20:00&2019\_1015-11:00:00 First , last ,max. ,min. : 0.0 , -0.059 , 0.522 , -0.239

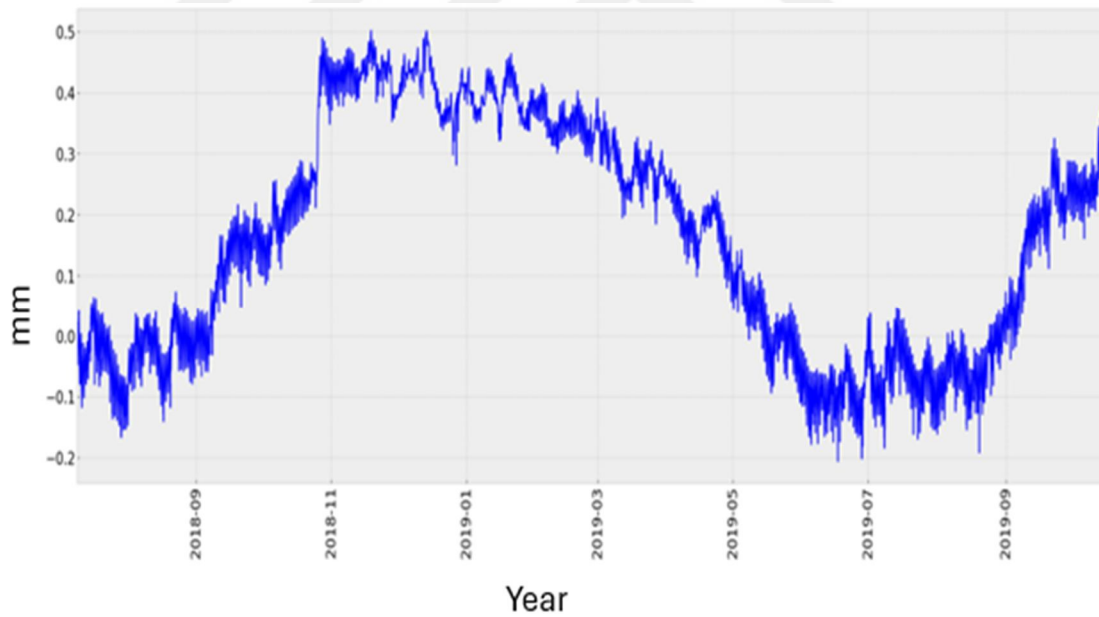


**Figure 5.35:** Crack 20 first &last data time : 2018\_0709-11:20:00&2019\_1015-11:00:00 First , last ,max. ,min. : 0.0 , 0.319 , 0.502 , -0.206

To facilitate the evaluation of time series, the latest observed values, as well as the maximum and minimum values, are presented in **Table 5.1**.

**Table 5.1:** Comparison of Data Obtained from Crack Gauges (mm).

<b>Crack Meter</b>	<b>Last Value</b>	<b>Maximum</b>	<b>Minimum</b>	<b>Margin</b>
1	0.044	0.578	-0.119	0.697
2	-0.293	0.102	-0.393	0.496
3	-0.02	0.196	-0.141	0.336
4	0.092	0.523	-0.104	0.626
5	0.356	1.605	-0.145	1.749
6	0.200	0.413	-0.026	0.439
7	-0.119	0.395	-0.407	0.802
8	0.105	0.293	-0.186	0.480
9	0.045	0.384	-0.375	0.759
10	0.105	0.351	-0.122	0.474
11	0.230	1.027	-0.243	1.270
12	0.581	1.056	-0.123	1.179
13	0.409	0.547	-0.234	0.781
14	-25.943	0.783	-26.129	26.912
15	0.296	0.495	-0.172	0.667
16	0.097	0.229	-0.241	0.470
17	0.129	0.630	-0.190	0.820
18	0.156	0.647	-0.258	0.904
19	-0.059	0.522	-0.239	0.761
20	0.319	0.502	-0.206	0.708

As observed, the largest change in crack gauge readings occurred at crack number 14. This crack gauge, located on the associated wall, showed an opening of 2.7 cm from the start of the monitoring period.

## 5.2. Evaluation of Inclinometer Data

A biaxial inclinometer was used to determine the tilting of the church walls within two perpendicular planes. The data obtained from the inclinometer is shown in **Figure 5.36-5.39**.

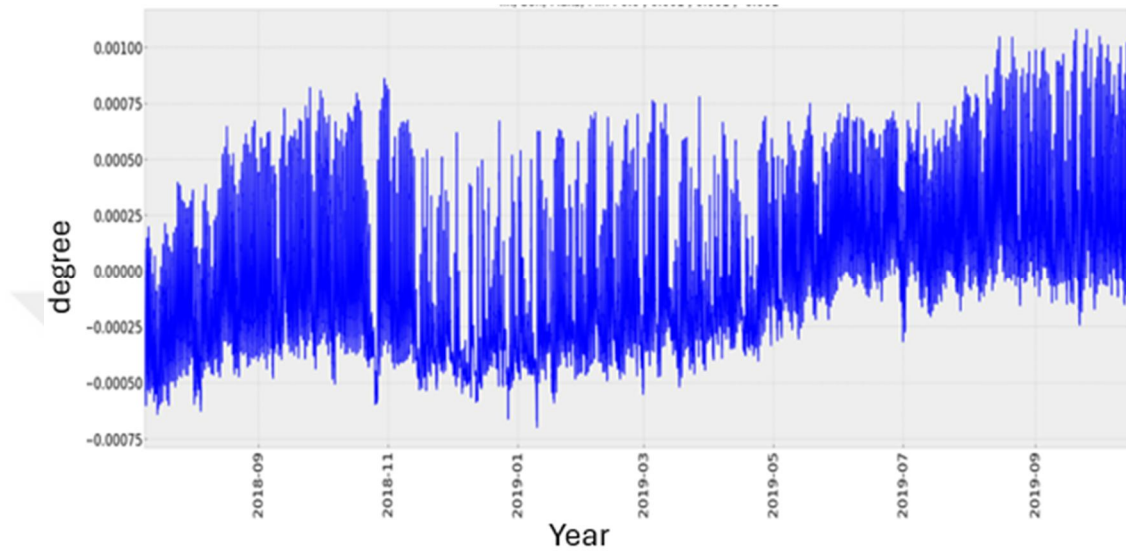


**Figure 5.36:** Slope 1 XZ first &last data time : 2018\_0709-11:20:00&2019\_1015-11:00:00 First , last ,max. ,min. : 0.0 , 0.001 , 0.001 , -0.001

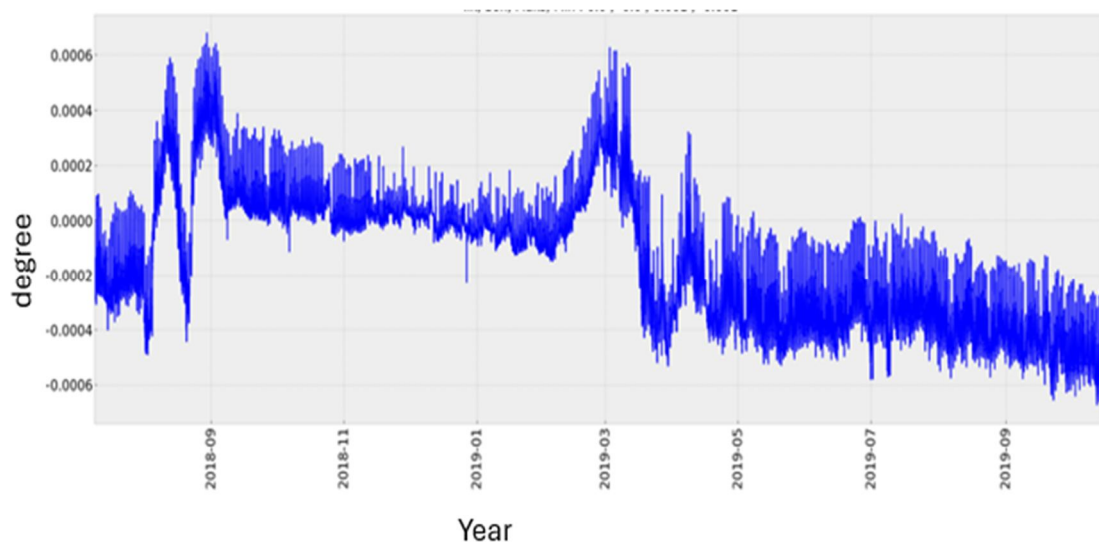


**Figure 5.37:** Slope 2 YZ first &last data time : 2018\_0709-11:20:00&2019\_1015-11:00:00 First , last ,max. ,min. : 0.0 , -0.0 , 0.001 , -0.001

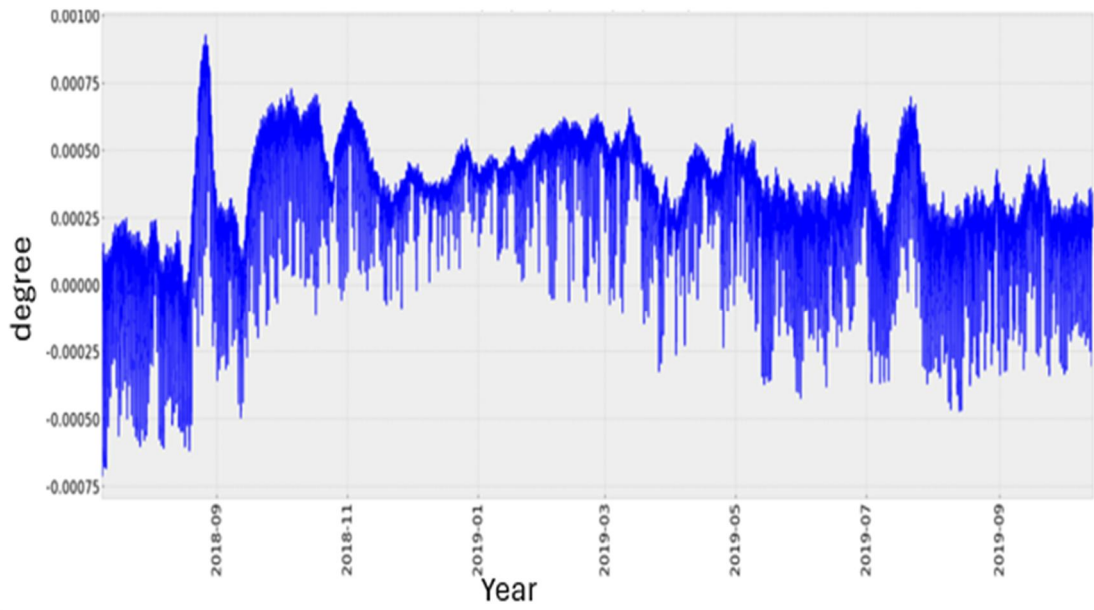


**Figure 5.38:** Slope 3 XZ first &last data time : 2018\_0709-11:20:00&2019\_1015-11:00:00 First , last ,max. ,min. : 0.0 , 0.0 , 0.001 , -0.001

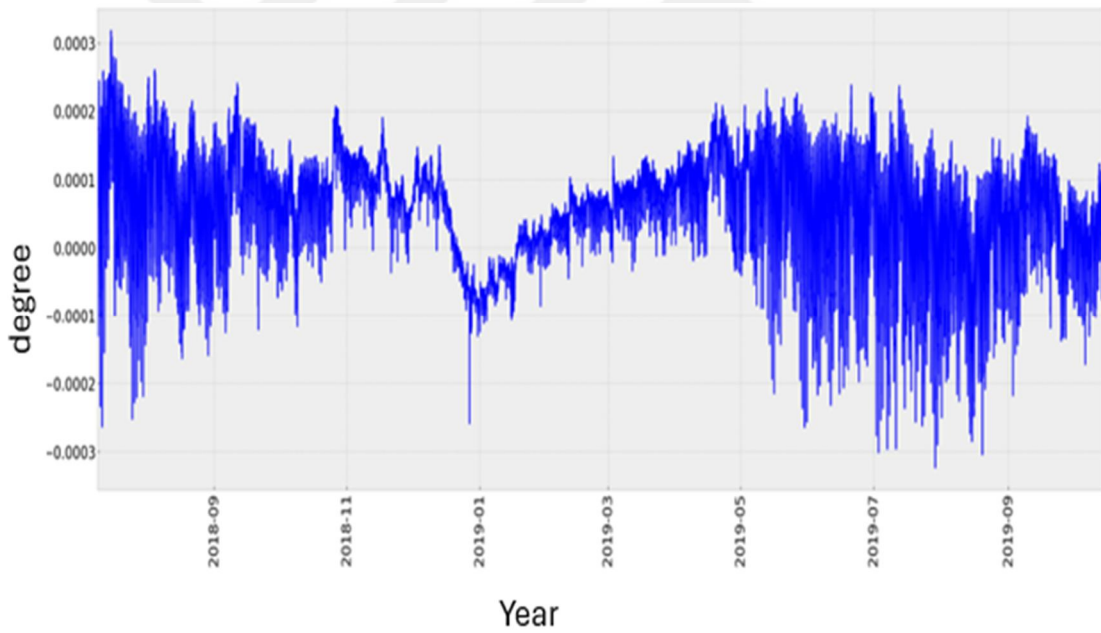


**Figure 5.39:** Slope 4 YZ first &last data time : 2018\_0709-11:20:00&2019\_1015-11:00:00 First , last ,max. ,min. : 0.0 , -0.0 , 0.0 , -0.0

To facilitate the evaluation of time series, the latest observed values, along with the maximum and minimum values, are presented in **Table 5.2**.

**Table 5.2:** Comparison of data obtained from inclinometers (mm).

Inclinometer	Last Value	Maximum	Minimum	Margin
Slope 1 XZ	0.00085	0.00108	-0.0007	0.00178
Slope 2 YZ	-0.00039	0.00068	-0.00067	0.00135
Slope 3 XZ	-0.00002	0.00032	-0.00032	0.00064
Slope 4 YZ	0.00024	0.00093	-0.00071	0.00164

### 5.3. Evaluation of Hygrometer Data

The time series of humidity values inside the church is presented in **Figure 4.42**. To facilitate the evaluation of the time series, the latest observed, maximum, and minimum values are displayed in Table 5.3.

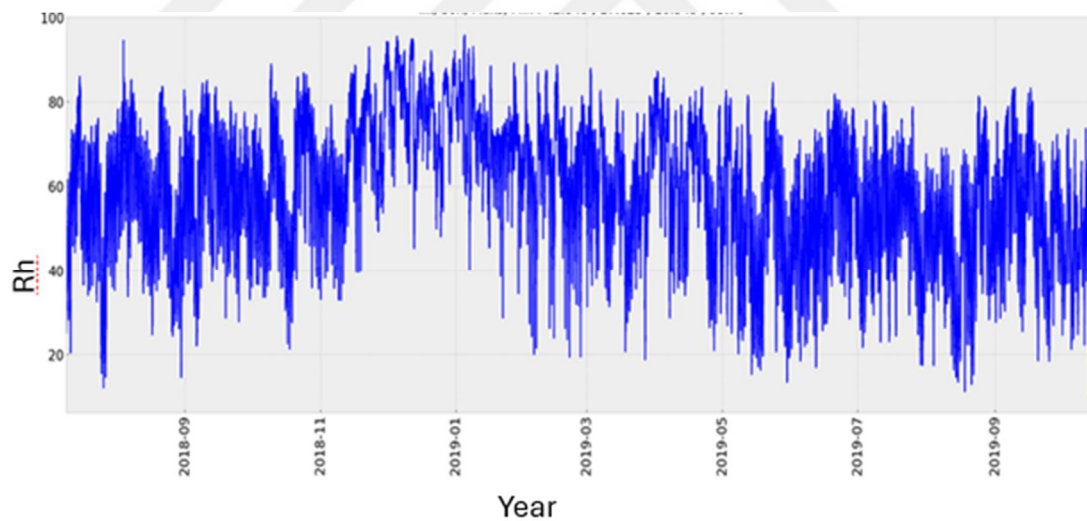


**Figure 5.40:** Moisture first &last data time : 2018\_0709-11:20:00&2019\_1015-11:00:00 First , last ,max. ,min. : 42.848 , 17.625 , 10.543 , 95.76

**Table 5.3:** Comparison of Data Obtained from Hygrometers (mm).

Hygrometer	First Value	Last Value	Maximum	Minimum	Margin
1	42.848	17.625	95.76	10.543	85.22

## 5.4. Evaluation of Thermometer Data

The time series for temperature values inside the church is presented in **Figure 5.41**. To facilitate the evaluation of the time series, the latest observed values, along with the maximum and minimum values, are shown in **Table 5.4**.

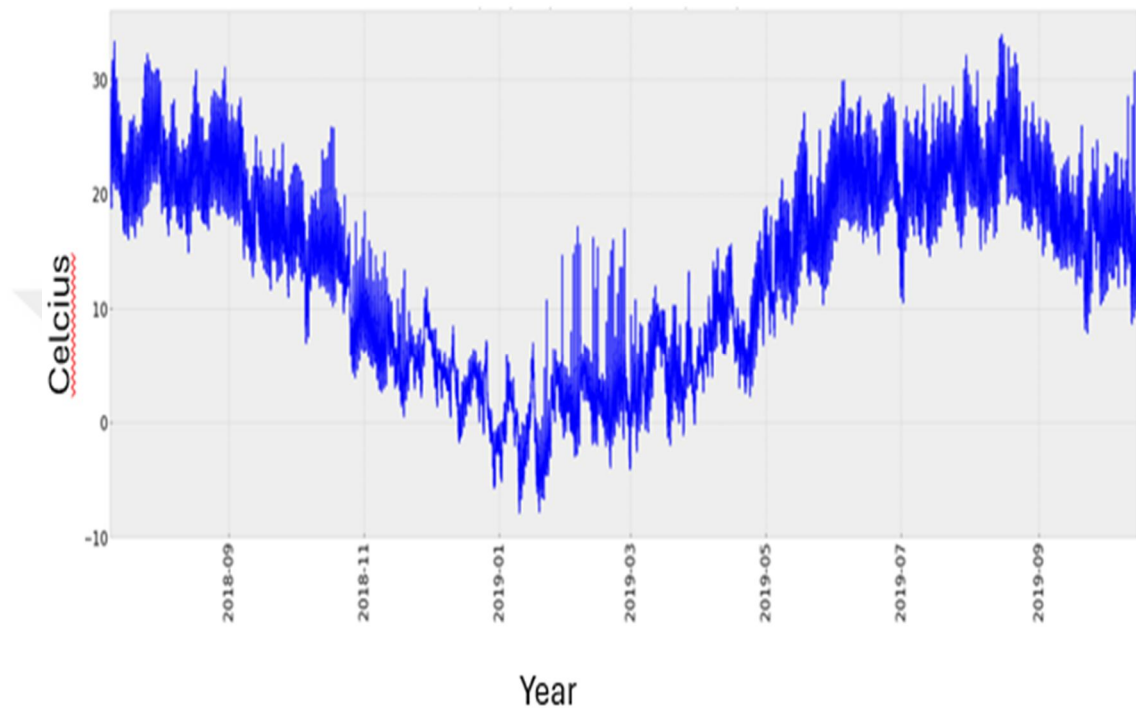


**Figure 5.41:** Moisture first &last data time : 2018\_0709-11:20:00&2019\_1015-11:00:00 First , last ,max. ,min. : 42.848 , 17.625 , 10.543 , 95.76

**Table 5.4:** Comparison of data obtained from thermometers (mm).

Temperature	First Value	Last Value	Maximum	Minimum	Margin
Inside	26.29	18.086	33.306	-7.894	41.2

## 5.5. Evaluation of Accelerometer Data

A triaxial accelerometer on the structure collects data at a 100Hz sampling rate. The collected data is stored on a computer on-site. Each day, one-hour segments covering 08:00 and 20:00 are used for free vibration analysis. Additionally, due to an on-site setup, an alarm condition is triggered if the accelerometer data exceeds a threshold of 0.05g. In such cases, a data package with a 200Hz sampling rate is created for a

duration of 2.5 minutes. During the fourth semi-annual reporting period, a total of 80 alarm files were generated. Upon review, it was found that these alarms were not due to strong ground motion but rather due to a systematic issue (**Figure 5.42**). All reviewed alarm files indicated that the data was generated due to fluctuations caused by electrical issues.

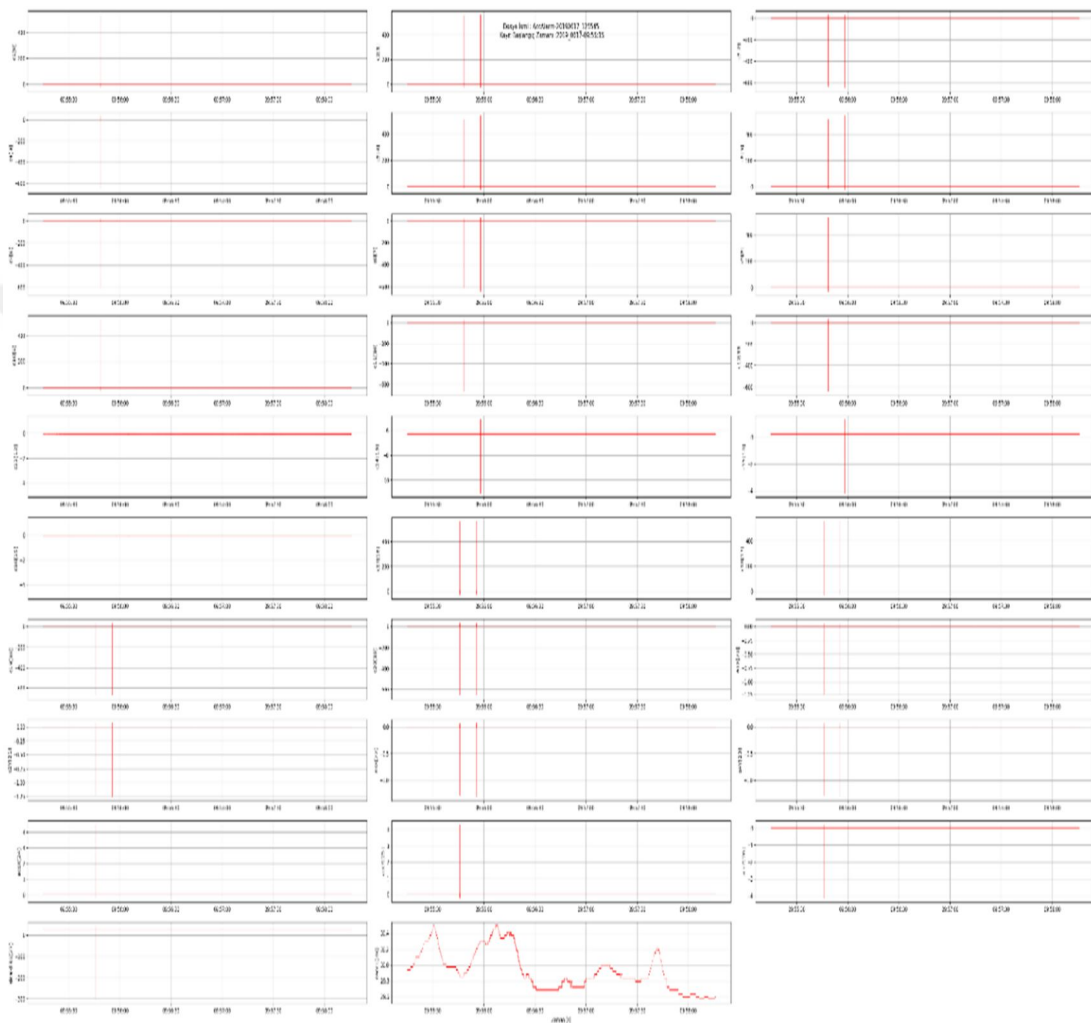


**Figure 5.42:** Example of alarm set

Additionally, recordings under environmental conditions, excluding alarm situations, were examined for the structural element where the accelerometer is placed. Although the file duration is 1 hour, a 200-second segment was analysed (**Figure 5.43-5.45**).

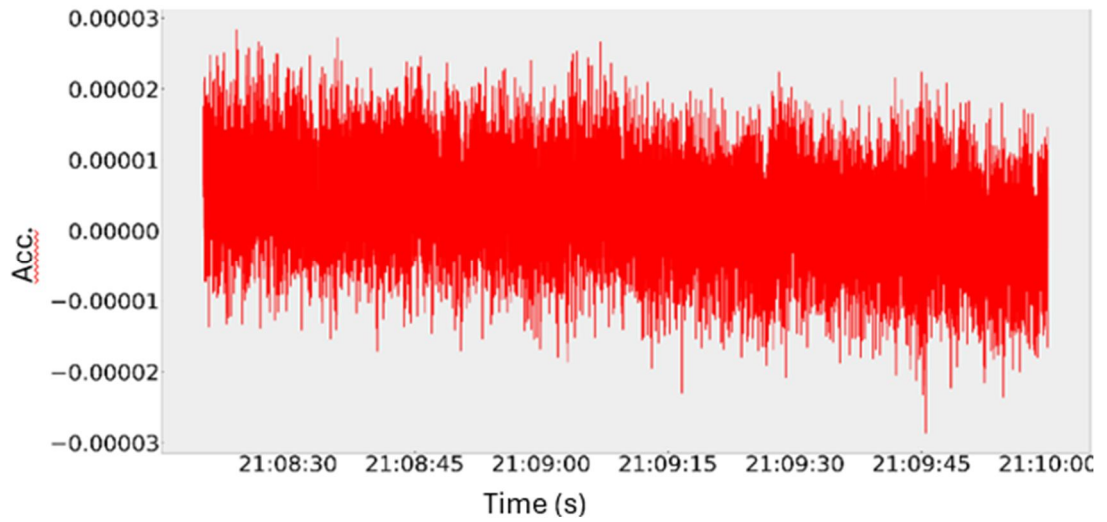


**Figure 5.43:** Acceleration Data Obtained in the X Direction

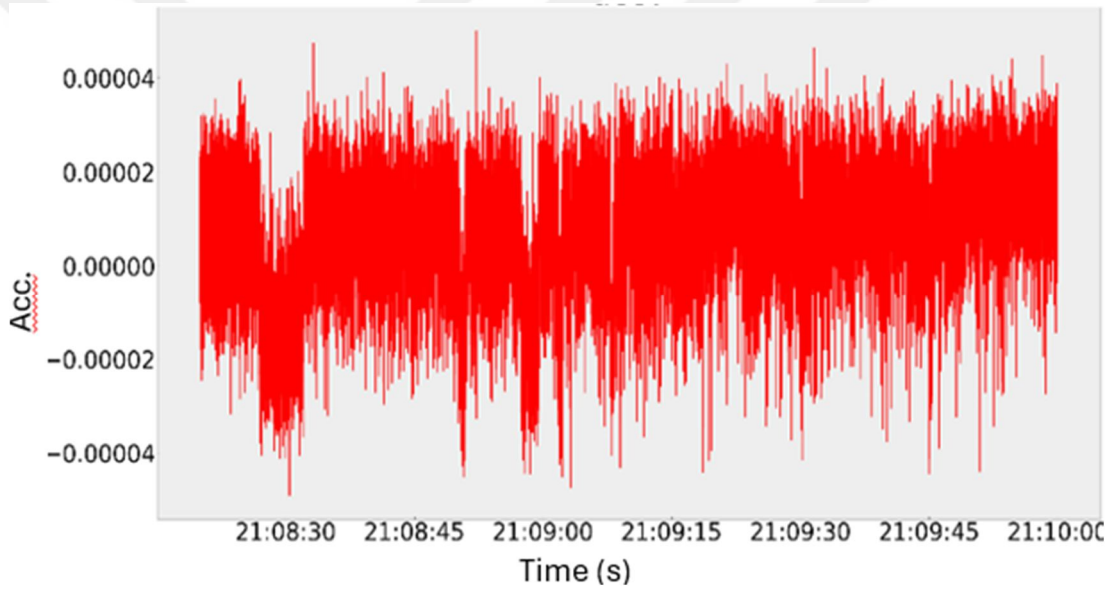


**Figure 5.44:** Acceleration Data Obtained in the Y Direction

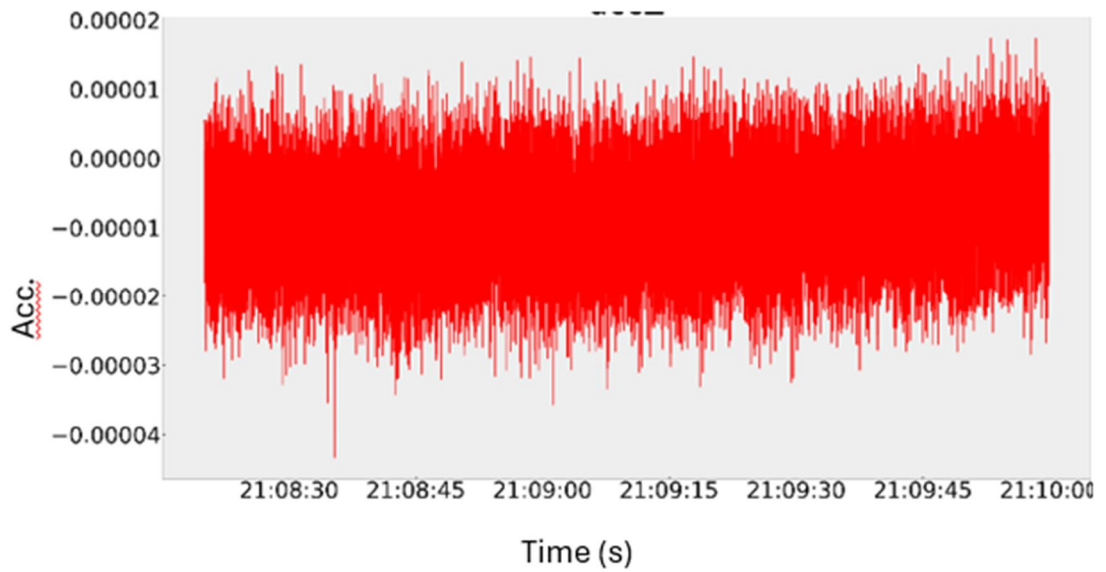


**Figure 5.45:** Acceleration Data Obtained in the Z Direction

After filtering the recorded vibration acceleration data with a 4th-order Butterworth filter in the range of 0.05 to 20Hz, frequency domain analysis was performed. This diagnostic process identified dominant frequencies in the vibration directions, resulting in values of 0.28Hz, 0.1Hz, and 0.15Hz for the X, Y, and Z planes, respectively (**Figure 5.46-5.48**).

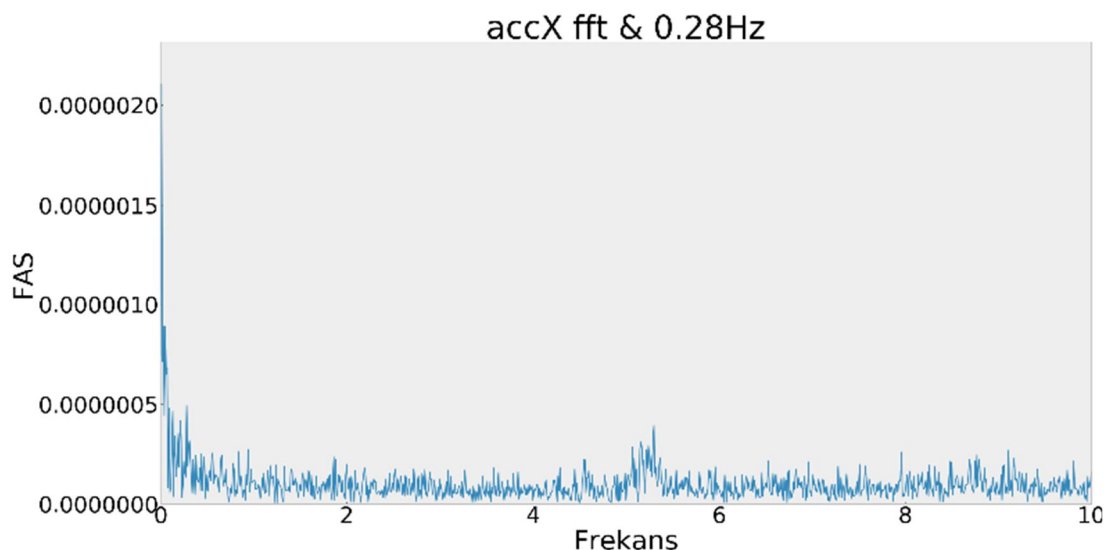


**Figure 5.46:** Calculated frequency spectrum in X direction

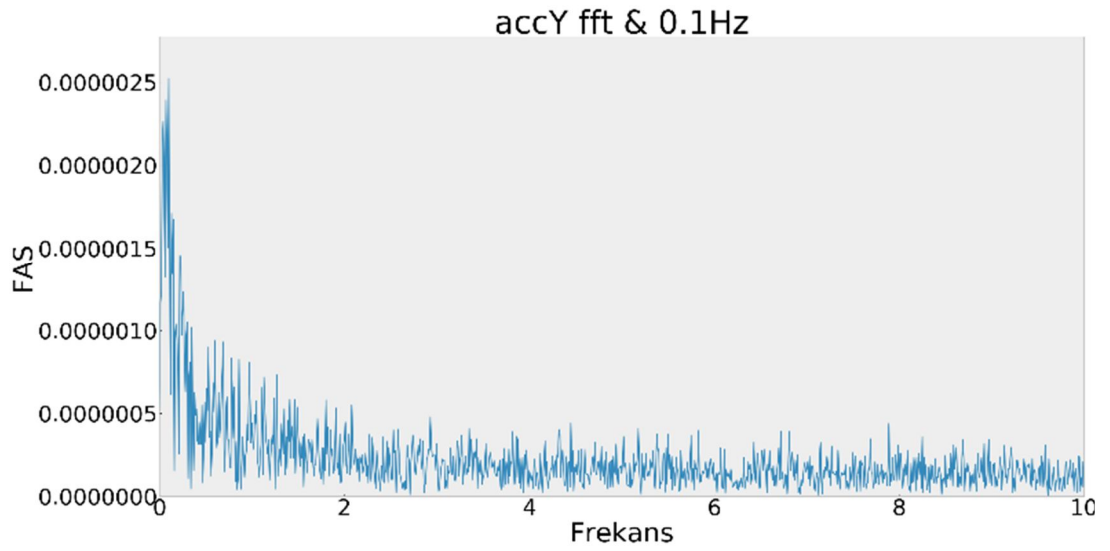


**Figure 5.47:** Calculated frequency spectrum in Y direction

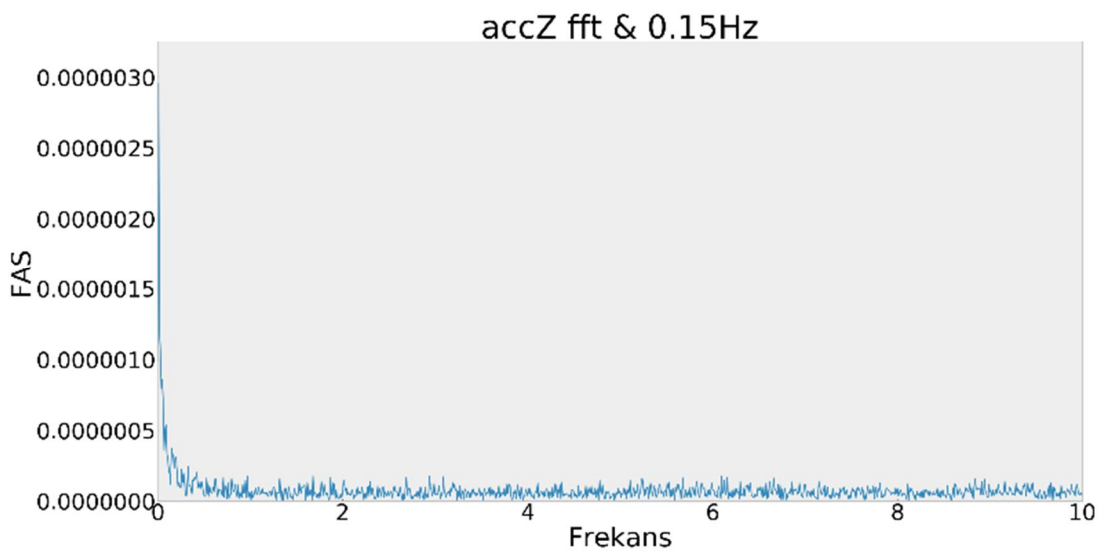


**Figure 5.48:** Calculated frequency spectrum in Z direction

## **6. RESTORATION AND STRENGTHENING RECOMMENDATIONS**

Based on the comprehensive analysis of the Structural Health Monitoring (SHM) data and the condition assessment of the Oskhi Church, several restoration and strengthening recommendations were formulated to ensure the long-term preservation and structural stability of the building. These recommendations aim to address the current vulnerabilities while preserving the historical integrity and cultural significance of the church.

### **6.1. Repair of Cracks in Structures**

Masonry structures are traditional constructions created by assembling natural materials like stone or brick, which are weak against tensile stresses. During the repair of cracks, all plaster and cement-based joints on the crack surfaces must be cleaned, and all cracks should be clearly exposed. The application surface should be cleaned of dust, oil, and construction debris using water, and any damaged or loose parts should be removed from the surface. If there is water leakage on the surface, it should be drained or sealed using an appropriate plug. Detailed measurements and documentation should be carried out on all opened and cleaned cracks to record their width, depth, and current condition. Once the documentation is complete, the cracks should be categorized based on their width and depth, and specific repair methods should be applied for each category.

#### **6.1.1. Cracks with a Width Less Than 1 mm**

If structural cracks are capillary, they should be repaired using a hydraulic lime-based plaster without cement, with a flexural strength greater than 2 MPa and a compressive strength greater than 5 MPa.

#### **6.1.2. Cases Where Crack Width Ranges Between 1 mm and 5 mm**

Depending on the width, depth, and environmental conditions of the crack, holes should be drilled at appropriate intervals (30–50 cm) on both sides of the crack plane

in a staggered pattern. These holes must penetrate through the crack plane and extend to the other side, forming an angle of approximately 45 degrees with the crack plane. The drilled holes should be cleaned using compressed air to remove dust and loose particles, and plastic tubes should be inserted, secured, and fixed tightly in place.

After placing all the tubes, the areas around the tubes and the surface of the crack should be plastered using a natural hydraulic lime-based plaster. This plaster should include natural silica aggregates and inorganic fibers, and should not contain cement. This ensures the crack is sealed to prevent leakage. Depending on the ambient and weather conditions, injection should commence at least 24 hours later using a suitable injection pump and the injection mortar recommended in **Table 6.1**.

The injection materials used in the application are expected to meet the following criteria:

- **High fluidity** without bleeding (measured using a Marsh cone).
- **Low hydration heat** and limited water-soluble salts (Normal 13-83).
- **Resistance to sulfates.**
- **High vapor permeability** (UNI EN 1015/19).
- **Mechanical properties** in accordance with EN 998/2.
- **Strong adhesion to steel or FRP rods.**

**Table 6.1:** Hydraulic Lime Binder Injection Grout (m<sup>3</sup>).

Compliant with TS EN 459-1 and TS EN 459-2, using NHL 3.5 grade natural hydraulic lime	Ton	0,335
Brick dust or roof tile dust	Ton	0,472
Natural stone dust	Ton	0,50
Water	m <sup>3</sup>	0,52
Adherence and Water Impermeability Additive	Kg	10,40

### 6.1.3. Cases Where Crack Width Ranges Between 5 mm and 50 mm

Based on the crack width, depth, and environmental conditions, pneumatic tubes should be installed in the cracks at appropriate intervals (75–100 cm). Loose particles inside the cracks must be removed using compressed air. After all the tubes are placed, the areas around the tubes and the crack surface should be sealed with a natural hydraulic lime-based plaster, commonly used for coating historical masonry structures. This plaster should include natural silica aggregates and inorganic fibers and must not contain cement to ensure watertightness. Depending on ambient and weather conditions, injection should begin at least 24 hours later using an appropriate injection pump and a mortar containing pozzolanic lime and micronized carbonates, specifically designed for the structural repair of masonry components (**Figure 6.1**). For hydraulic lime-based injections to fill cracks and/or voids in the prepared surfaces, the following steps should be followed. The injection points on the stones of the wall, arch, vault, or column must first be determined. These points should align with the surface joints, and holes with a diameter of up to Ø25 mm and a depth of at least half the wall thickness should be drilled with a drill. Before the application, the areas to be injected should be dampened with water. If there is plaster on the surface, any damaged areas must be fully removed, and the damage must be cleaned in detail. The application surface should be cleaned of dust, oil, and construction debris, and any damaged and loose parts should be removed from the surface. If there is water leakage, it must be drained or appropriately redirected. To ensure tightness in the tubes and allow all the injection material to enter the wall, the areas around the injection tubes should be sealed with NHL 3.5 class hydraulic lime mortar (Specification no: V.0104E). After drilling the holes, a ventilated compressor should be used to thoroughly clean dust and loose particles from inside and around the holes. The injection holes should be placed at intervals of 30–50 cm, aligned with the most suitable joint spacing, and arranged approximately in the shape of an equilateral triangle. Injection tubes should fit tightly into the cleaned holes. After completing all these steps, the tubes should adhere completely to the surface, and the process should be left to settle for 24 hours to prepare for injection. The prepared injection mortar should be applied using an injection machine. During the application, a pressure of no more than 2 bar should be used, and the injection should start from the lowest tube, continuing until the injection material overflows from another tube. Before proceeding to a new tube, the end of the injected

tube must be sealed. After completing the injection process on all tubes on the surface, the material must be left to cure for the duration required to achieve its strength. Once the injection has set, the ends of the remaining tubes on the surface should be cut. For every 50 m<sup>2</sup>, and at least three locations in total, the wall's strength should be checked before and after injection using non-destructive testing methods. The injection materials used in the application must meet the following criteria: exhibit very high fluidity without bleeding (Marsh cone), have low hydration heat, limit water-soluble salts (Normal 13-83), resist sulfates, provide high vapor permeability (UNI EN 1015/19), comply with mechanical properties outlined in EN 998/2, and exhibit strong adhesion to steel or FRP rods.

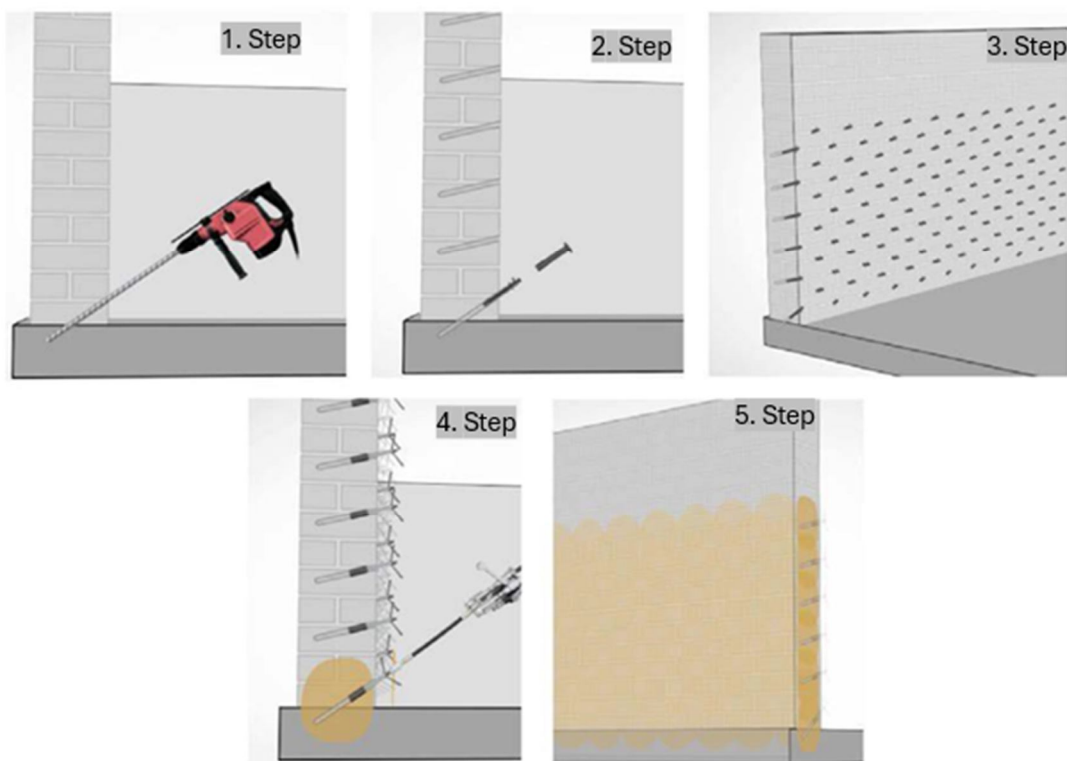


**Figure 6.1:** Injection Mortar Application Detail [26].

#### **6.1.4. Cases Where Crack Width Ranges Between 50 mm and 150 mm**

In cases where the crack width ranges between 50 mm and 150 mm, the cracks should be reinforced with stitching elements. To achieve this, the adjacent stones or infills of the crack should first be cleaned, and steel connectors capable of resisting tensile stresses should be installed (**Figure 6.2**). The masonry surface to be reinforced must

be fully exposed, and all displaced masonry units around the crack must be removed and cleaned. Joint material should be removed from both sides of the crack, 500 mm on each side, making a total length of 1 meter, to create space for the reinforcement bars. The cleaned joint gaps should be injected at low pressure (2–3 bar) with a mortar mix compatible with the original mortar of the structure. Ribbed or grooved steel bars with a minimum yield strength of 150 MPa and tensile strength of 400 MPa should be placed in the prepared gaps to ensure proper adhesion to the masonry units. After placing the steel bars, the gaps should be injected at low pressure (2–3 bar) with a mortar mix compatible with the original structure. Once all the steel bars are in place, the entire crack should be completely filled with injection mortar. For reinforcement purposes, it is recommended to reinforce the crack at intervals of at least 500 mm along its length.

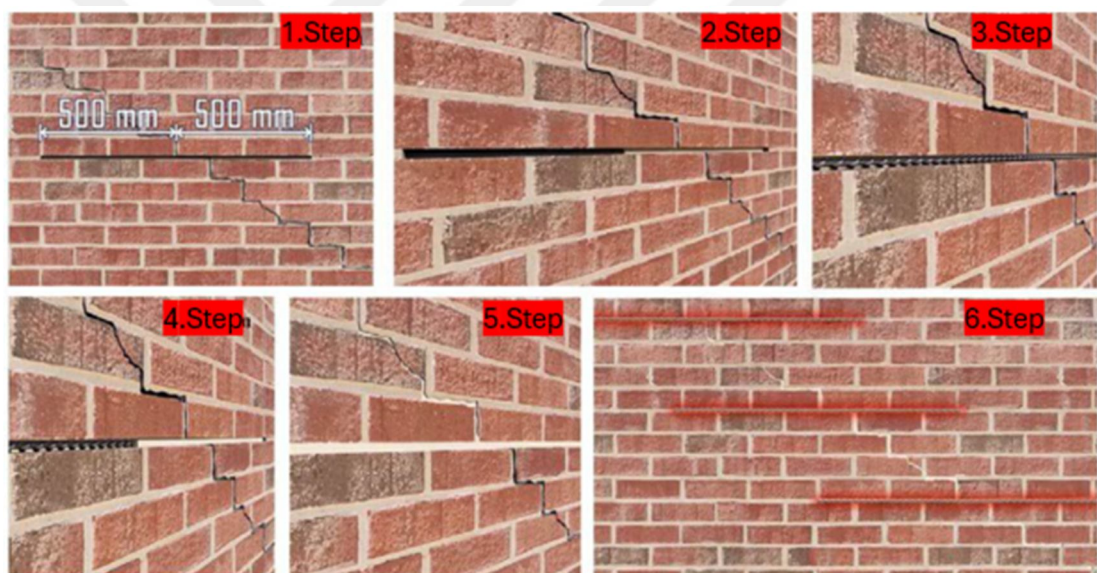


**Figure 6.2:** Reinforcement of Cracks Using Stitching Elements [27].

## 6.2. Repair of Section Losses

After the repair and reinforcement of cracks, it is recommended to identify and replace masonry elements on the surface that have lost their original texture, as well as to restore the areas with section losses. In regions requiring removal, the process should be carried out carefully to avoid damaging adjacent bricks, and the cleaned areas should be prepared to ensure the new elements fit perfectly into the existing surface. Repairs made to restore missing parts should be integrated harmoniously with the rest

of the structure. These repairs must also be distinguishable from the original state of the structure to prevent misrepresentation of its artistic and historical authenticity. Additionally, during the restoration of section losses, attention should be paid to the vertical load path, ensuring that the thickness of the masonry walls is consistent across all floors and properly aligned.



## 7. CONCLUSION

This study has highlighted the crucial role that Structural Health Monitoring (SHM) plays in the restoration and preservation of historical structures, with a particular focus on the Oshki Church in Erzurum, Turkey. Through the integration of advanced monitoring techniques and thorough structural assessments, valuable insights were gained into the current state of the church, including its vulnerabilities and areas requiring intervention.

The data collected from the SHM system provided a comprehensive understanding of the structural behaviour of the Oshki Church, revealing key issues such as material degradation, cracking, and settlement. Based on this data, tailored restoration and strengthening recommendations were made to ensure the building's long-term stability, seismic resilience, and preservation of its historical significance. These recommendations included the reinforcement of load-bearing walls, completion of missing sections, crack repair, foundation strengthening, and the enhancement of seismic resilience.

The findings underscore the importance of combining traditional restoration techniques with modern engineering practices, particularly in the context of historical structures that require both preservation and protection from the effects of time and environmental factors. By employing SHM technology, it becomes possible to make data-driven decisions, ensuring that interventions are both effective and minimally invasive to the building's heritage.

Ultimately, the Oshki Church case study demonstrates that SHM is not only an invaluable tool for assessing the health of historical structures but also a vital part of decision-making in their restoration and strengthening. As SHM systems continue to evolve, their role in the preservation of cultural heritage will undoubtedly grow, helping to safeguard these invaluable structures for future generations. The integration of SHM into restoration processes is a model that can be applied to other historical buildings, ensuring their continued survival and relevance in the modern world. In addition to the technical and structural benefits, the application of SHM in historical preservation also promotes a deeper understanding of the long-term behaviour of

cultural heritage buildings. This proactive approach allows for early detection of potential issues, minimizing the risk of unforeseen damage that could compromise the safety and longevity of the structure. By continuously monitoring key parameters such as deformations, vibrations, and material conditions, SHM provides a real-time picture of a building's health, allowing for timely and informed decisions about necessary repairs or reinforcements. Furthermore, the integration of SHM with restoration efforts fosters a more sustainable approach to conservation. Rather than relying solely on traditional restoration methods, which may not always account for the building's evolving condition, SHM empowers conservationists and engineers to make data-driven adjustments to the restoration plan, ensuring that interventions are both efficient and effective. This approach reduces the likelihood of over-repairing or under-repairing certain components, optimizing resource use and minimizing the environmental impact of the restoration process.

The restoration of the Oshki Church serves as a key example of how modern technology, such as SHM, can enhance traditional conservation practices, ensuring the preservation of historical and cultural heritage while addressing the practical challenges of maintaining the structural integrity of ancient buildings. As SHM systems continue to advance, they will provide even greater capabilities for assessing and protecting the health of historical structures worldwide. This will allow for the continued use and appreciation of these buildings by future generations, ensuring that they remain an integral part of cultural and architectural history.

In conclusion, the combination of advanced monitoring technologies and targeted restoration strategies provides a holistic framework for preserving the architectural and cultural heritage of historical buildings. The insights gained from this study can serve as a model for future restoration projects, highlighting the importance of incorporating SHM into the decision-making process for building preservation. This integrated approach not only protects the physical structure but also ensures the continued cultural relevance of these buildings, bridging the gap between the past and the future.

## REFERENCES

- [1] Z. Peng, J. Li, H. Hao, and Y. Zhong, “Smart structural health monitoring using computer vision and edge computing,” *Eng Struct*, vol. 319, p. 118809, Nov. 2024, doi: 10.1016/j.engstruct.2024.118809.
- [2] J. F. Waldner and A. Sadhu, “A systematic literature review of unmanned underwater vehicle-based structural health monitoring technologies,” *Journal of Infrastructure Intelligence and Resilience*, vol. 3, no. 4, p. 100112, Dec. 2024, doi: 10.1016/j.iintel.2024.100112.
- [3] E. Lydakis, H. Koss, R. Brincker, and S. D. R. Amador, “Data-driven sensor fault diagnosis for vibration-based structural health monitoring under ambient excitation,” *Measurement*, vol. 237, p. 115232, Sep. 2024, doi: 10.1016/j.measurement.2024.115232.
- [4] G. Kang, J. Jang, G. Cho, I. Y. Lee, and Y.-B. Park, “Real-time structural health monitoring of carbon fiber-reinforced plastic sandwich structures with carbon nanotube-dispersed core using electromechanical behavior data,” *Polym Test*, vol. 136, p. 108471, Jul. 2024, doi: 10.1016/j.polymertesting.2024.108471.
- [5] A. Entezami, H. Sarmadi, and B. Behkamal, “Removal of freezing effects from modal frequencies of civil structures for structural health monitoring,” *Eng Struct*, vol. 319, p. 118722, Nov. 2024, doi: 10.1016/j.engstruct.2024.118722.
- [6] A. Alsehami, M. Houada, A. Waqar, S. Hayat, F. Ahmed Waris, and O. Benjeddou, “Internet of things (IoT) driven structural health monitoring for enhanced seismic resilience: A rigorous functional analysis and implementation framework,” *Results in Engineering*, vol. 22, p. 102340, Jun. 2024, doi: 10.1016/j.rineng.2024.102340.
- [7] L. Neumann, P. Wittenberg, A. Mendler, and J. Gertheiss, “Confounder-adjusted Covariances of System Outputs and Applications to Structural Health Monitoring,” Sep. 2024, [Online]. Available: <http://arxiv.org/abs/2409.17735>
- [8] B. Zhang, C. Othmani, T. Khelfa, H. Zhang, C. Lü, and A. Njeh, “Acoustoelastic guided and surface waves in waveguides with focus on non-destructive testing and structural health monitoring applications — A review of recent studies,” *Int J Non Linear Mech*, vol. 167, p. 104912, Dec. 2024, doi: 10.1016/j.ijnonlinmec.2024.104912.
- [9] C. H. Chin, S. Abdullah, A. K. Ariffin, S. S. K. Singh, and A. Arifin, “A review of the wavelet transform for durability and structural health monitoring in automotive applications,” *Alexandria Engineering Journal*, vol. 99, pp. 204–216, Jul. 2024, doi: 10.1016/j.aej.2024.04.069.
- [10] M. M. Wharton, “Photogrammetry and mean intensity mapping as methods of low-cost structural health monitoring,” *Mech Syst Signal Process*, vol. 219, p. 111583, Oct. 2024, doi: 10.1016/j.ymsp.2024.111583.

- [11] F. Falchi, M. Girardi, G. Gurioli, N. Messina, C. Padovani, and D. Pellegrini, “Deep learning and structural health monitoring: Temporal Fusion Transformers for anomaly detection in masonry towers,” *Mech Syst Signal Process*, vol. 215, p. 111382, Jun. 2024, doi: 10.1016/j.ymsp.2024.111382.
- [12] D. Xu, X. Xu, M. C. Forde, and A. Caballero, “Concrete and steel bridge Structural Health Monitoring—Insight into choices for machine learning applications,” *Constr Build Mater*, vol. 402, p. 132596, Oct. 2023, doi: 10.1016/j.conbuildmat.2023.132596.
- [13] M. Sakr and A. Sadhu, “Visualization of structural health monitoring information using Internet-of-Things integrated with building information modeling,” *Journal of Infrastructure Intelligence and Resilience*, vol. 2, no. 3, p. 100053, Sep. 2023, doi: 10.1016/j.iintel.2023.100053.
- [14] A. Monaco, G. Bertagnoli, L. La Mendola, M. C. Oddo, and A. Pennisi, “Preliminary validation of an innovative stress sensor for the Structural Health Monitoring of masonry buildings,” *Procedia Structural Integrity*, vol. 44, pp. 806–813, 2023, doi: 10.1016/j.prostr.2023.01.105.
- [15] J. Etxaniz, G. Aranguren, J. M. Gil-García, J. Sánchez, G. Vivas, and J. González, “Ultrasound-based structural health monitoring methodology employing active and passive techniques,” *Eng Fail Anal*, vol. 146, p. 107077, Apr. 2023, doi: 10.1016/j.engfailanal.2023.107077.
- [16] I. Y. Lee, J. Jang, and Y.-B. Park, “Advanced structural health monitoring in carbon fiber-reinforced plastic using real-time self-sensing data and convolutional neural network architectures,” *Mater Des*, vol. 224, p. 111348, Dec. 2022, doi: 10.1016/j.matdes.2022.111348.
- [17] F. E. Gunawan, T. H. Nhan, M. Asrol, Y. Kanto, I. Kamil, and Sutikno, “A New Damage Index for Structural Health Monitoring: A Comparison of Time and Frequency Domains,” *Procedia Comput Sci*, vol. 179, pp. 930–935, 2021, doi: 10.1016/j.procs.2021.01.082.
- [18] P. Gardner, L. A. Bull, N. Dervilis, and K. Worden, “Overcoming the problem of repair in structural health monitoring: Metric-informed transfer learning,” *J Sound Vib*, vol. 510, p. 116245, Oct. 2021, doi: 10.1016/j.jsv.2021.116245.
- [19] A. J. Hughes, R. J. Barthorpe, N. Dervilis, C. R. Farrar, and K. Worden, “A probabilistic risk-based decision framework for structural health monitoring,” *Mech Syst Signal Process*, vol. 150, p. 107339, Mar. 2021, doi: 10.1016/j.ymsp.2020.107339.
- [20] P. Gardner, X. Liu, and K. Worden, “On the application of domain adaptation in structural health monitoring,” *Mech Syst Signal Process*, vol. 138, p. 106550, Apr. 2020, doi: 10.1016/j.ymsp.2019.106550.

[21] M. Sun, W. J. Staszewski, and R. N. Swamy, "Smart Sensing Technologies for Structural Health Monitoring of Civil Engineering Structures," *Advances in Civil Engineering*, vol. 2010, pp. 1–13, 2010, doi: 10.1155/2010/724962.

[22] F. Moreu, X. Li, S. Li, and D. Zhang, "Technical specifications of structural health monitoring for highwaridgy bes: New chinese structural health monitoring code," Feb. 16, 2018, *Frontiers Media S.A.* doi: 10.3389/fbuil.2018.00010.

[23] T. Yapılar, İ. Deprem, R. Y. Kılavuzu, and V. G. Müdürlüğü, *Guide for Earthquake Risk Management of Historical Structures*, Vakıflar Publishing House, Ankara, 2017.

[24] F. Çakir, "A simplified method for determining the seismic performance of historical structures: A case of Kaya Çelebi Mosque," *Journal of the Faculty of Engineering and Architecture of Gazi University*, vol. 36, no. 3, pp. 1643–1656, 2021, doi: 10.17341/gazimmfd.754183.

[25] T. KORKUT, "İşhan (İşhani) Manastır Kilisesi'nin Dünü ve Bugünü," *Journal of Academic Tourism Studies*, vol. Cilt:4 Sayı:2, no. Cilt:4 Sayı:2, pp. 19–41, 2023, doi: 10.29228/jatos.73204.

[26] Desoi GmbH, "Desoi catalog," [Online]. Available: <https://www.desoi.de/catalog/de/>. [Accessed: Jan. 27, 2025].

[27] Buildfix, "Buildfix official website," [Online]. Available: <https://www.buildfix.com.au>. [Accessed: Jan. 27, 2025].

## BIOGRAPHY

I graduated from the Civil Engineering Department (English Program) at Gaziantep University. Between July 2008 and August 2010, I worked as a site engineer for Tinsa Construction on the Adıyaman Burç Dam and Hydroelectric Power Plant (HPP) Project. During this period, I was involved in the construction of structures such as the Hydroelectric Power Plant Building, Penstocks, Energy Tunnel, Surge Tank, and Diversion Tunnel.

From March 2011 to February 2012, I worked as a control engineer on the Ataşehir Premium Sports Complex Project, contracted by Topyay A.Ş. for Doğa Yatırım A.Ş. Following two years of experience in building inspection, I served as a structural project designer at Feza Architecture-Engineering. Since 2017, I have been running my own business as a partner in the same firm.

I am a member of the Istanbul Branch of the Chamber of Civil Engineers (IMO). I am married and a father of three children.

## **PUBLICATIONS AND PRESENTATIONS FROM THE THESIS**

F. Akturk, A. C. Zulfikar, and F. Cakir, "Decision-making mechanism through structural health monitoring: The case of Oshki Church in Erzurum," in *Proc. 8th Int. Halich Congr. Multidiscip. Sci. Res.*, Istanbul, Turkey, Dec. 2024.

